Volume 6, Number 3, July 1963

ASLE TRANSACTIONS

A Publication of the American Society of Lubrication Engineers

ACADEMIC PRESS
NEW YORK and LONDON

NOTICES

Readers are invited to submit written discussions on any of the papers contained in this issue. Discussions received within two months from the publication date of this issue will be published in a following issue. Correspondence should be addressed to Society Headquarters.

ASLE is constantly looking for new and useful papers on every aspect of lubrication including research, design, application and maintenance. Authors having papers which they believe would be of interest to the readers of either *ASLE Transactions* or *Lubrication Engineering* are encouraged to submit them to the Society for publication consideration. If an author desires, he may request that a paper also be considered for presentation at one of the Society's meetings. Presentation before a meeting, however, is not a prerequisite for publication. An Author's Guide covering the preparation of papers for publication is available from Society Headquarters on request.

Lubrication Engineering is published monthly by the American Society of Lubrication Engineers, 5 N. Wabash Avenue, Chicago 2, Illinois.

ASLE Transactions is published quarterly by Academic Press for the American Society of Lubrication Engineers.

OFFICERS OF THE SOCIETY

E. E. Bisson, *President*
S. R. Calish, Jr., *Vice President at Large*
M. M. Gurgo, *Secretary*
J. H. Kahlke, *Treasurer*
L. B. Sargent, Jr., *Chairman, Presidential Council*
J. Le Sire, *Western Regional Vice President*
B. M. Dunham, *Atlantic Regional Vice President*
C. H. Elsley, *Canadian Regional Vice President*
G. W. Gergeceff, *Southern Regional Vice President*
B. T. Harding, *Midwest Regional Vice President*
T. Osters, *Central Regional Vice President*
R. J. Torrens, *Northeastern Regional Vice President*

C. A. Bailey, *Director*
R. C. Garretson, *Director*
E. J. Gesdorf, *Director*
R. K. Gould, *Director*
D. L. Hill, *Director*
R. L. Johnson, *Director*
C. S. Mercer, *Director*
A. A. Raimondi, *Director*
E. S. Reynolds, *Director*

INDUSTRIAL MEMBERS

Alemite Division, Stewart Warner Corp.
The Alpha Molykote Corp.
Aluminum Company of America
American Oil Co.
Bendix Prod. Div., Bendix Corp.
Bethlehem Steel Co.
Bowser Briggs Filtration Division
The Cincinnati Milling Machine Co.
Cities Service Petroleum, Inc.
Crane Packing Co.
Dravo Corp.
The Elco Lubricant Co.
The Farval Div., Eaton Mfg. Co.
Humble Oil & Refining Co.
Garlock Inc.
Gulf Oil Corp.
The Hodson Corp.
E. F. Houghton & Co.
Lincoln Engineering Division
The Lubri-Zol Corp.
National Cash Register Co.
C. A. Norgren Co.
Paz Oil Co., Ltd.
Quaker Chemical Corp.
Rocketdyne Div., North America Aviation, Inc.
Shell Oil Co.
Sinclair Refining Co.
Socony Mobil Oil Co., Inc.
Standard Oil Co. of California
Sun Oil Co.
Texaco, Inc.
Timken Roller Bearing Co.
Trabon Engineering Corp.
U.S. Steel Corp.
R. T. Vanderbilt Co., Inc.
Westinghouse Electric Corp.
Wynn Oil Co.
YPFB Oil Co.

A Publication of the American Society of Lubrication Engineers

ASLE TRANSACTIONS

Volume 6 Number 3

EDITOR

John Boyd

ASSOCIATE EDITORS

W. J. Anderson
A. Cameron
D. Godfrey
R. K. Gould
P. M. Ku
A. A. Raimondi
L. B. Sargent, Jr.
D. W. Sawyer
A. B. Two

EDITORIAL REVIEW COMMITTEE

C. M. Allen
F. R. Archibald
J. S. Ausman
D. C. Bardy
P. A. Bennett
E. W. Brennan
A. F. Brewer
R. A. Burton
H. Chalk
E. S. Cain
W. E. Campbell
C. W. Georgi
J. W. Givens
W. A. Gross
H. Hanau
D. F. Hays
L. E. Hoyer
J. Johnson
R. L. Johnson
B. W. Kelley
P. Lewis
A. W. Lindert
E. H. Loeser
F. Macks
H. E. Mahncke
J. R. McCoy
H. W. McCulloch, Jr.
R. McKay III
M. E. Merchant
F. Osterle
E. Rabinowicz
G. S. Reichenbach
B. G. Rightmire
B. R. Ruley
E. A. Ryder
E. A. Saibel
H. W. Scibbe
M. C. Shaw
L. B. Sibley
L. N. Tao
J. P. Wettach
L. L. Withrow
S. J. Supel, Editorial Assistant

CHAIRMAN PUBLICATIONS COMMITTEE
A. A. Raimondi

EXECUTIVE SECRETARY, ASLE
D. B. Sanberg

ACADEMIC PRESS
New York and London

COPYRIGHT ©, 1963, BY AMERICAN SOCIETY OF LUBRICATION ENGINEERS
CHICAGO, ILLINOIS
ALL RIGHTS RESERVED

ASLE Transactions is published quarterly by Academic Press Inc., 111 Fifth Avenue, New York 3, N. Y. Subscriptions to ASLE members are available through ASLE headquarters. Subscriptions to non-members are available from the Publishers. Price per volume: $18.00.

MADE IN THE UNITED STATES OF AMERICA

ASLE TRANSACTIONS 6, 161-177 (1963)

Friction Measurements on a Low Earth Satellite[1]

By J. B. RITTENHOUSE,[2] L. D. JAFFE,[3]
R. G. NAGLER,[4] and H. E. MARTENS[5]

The coefficient of sliding friction for a number of materials was measured during the flight of Ranger 1 spacecraft. Flat disks of materials of interest were rotated at a speed of 8–14 inches per minute while in contact with ⅛-inch diameter hemispherical riders. Because of the low orbit achieved by Ranger 1, the experiment was exposed to vacuum in the range of 3×10^{-6} to 8×10^{-9} mm Hg. For unlubricated metals sliding on metals, the friction coefficient averaged about 0.5; for some combinations of metals, it occasionally exceeded 1.0. Lower values were observed with lubricants of grease or gold-plate and for ceramics sliding against metals. The coefficient of friction was very low, averaging 0.04, for metallic pairs lubricated with molybdenum disulfide and for polytetrafluoroethylene sliding against metals and ceramics. Relatively low friction coefficients were found for metallic materials sliding against unlubricated metallic and ceramic materials when at least one member of the pair was of high hardness. The coefficients observed for unlubricated metal pairs were not inconsistent with the hypothesis that high friction tends to correlate with high mutual solid solubility. In general the coefficients in space and in a laboratory vacuum of 5×10^{-6} mm Hg were not systematically different. For unlubricated metallic materials, friction in vacuum was higher than in air at shorter running times.

Introduction

THE successful operation of spacecraft requires mechanical motions. Such devices as deployable solar panels, directional antennas, temperature control louvers, and aimed vidicons need moving parts. As spacecraft become more advanced, and sampling of lunar or planetary surfaces or operation of vehicles on the surfaces are required, many types of bearing and gear problems will have to be solved. It will not always be practical to have all bearings and gears completely sealed and pressurized. This means that there must be a clear understanding of the basic principles which govern friction, wear and lubrication in the environment of space.

Contributed by the ASLE Technical Committee on Lubrication Fundamentals and presented at the Annual Meeting of the American Society of Lubrication Engineers held in New York, April, 1963.

[1] This paper presents the results of one phase of research carried out at the Jet Propulsion Laboratory, California Institute of Technology, under Contract NAS7-100, sponsored by the National Aeronautics and Space Administration.

[2] Formerly Research Specialist, Jet Propulsion Laboratory, California Institute of Technology, Pasadena, California; now with Lockheed Missiles and Space Company, Palo Alto, California.

[3] Chief, Materials Research Section, Jet Propulsion Laboratory, California Institute of Technology, Pasadena, California.

[4] Research Engineer, Materials Research Section, Jet Propulsion Laboratory, California Institute of Technology, Pasadena, California.

[5] Assistant Chief, Materials Research Section, Jet Propulsion Laboratory, California Institute of Technology, Pasadena, California.

On Earth, exposed solid surfaces quickly adsorb films of oxygen and water vapor, which act as lubricants and reduce friction and wear. Surfaces which are free of adsorbed films of atmospheric gases tend to weld to each other and coefficients of friction are high (*1–3*). In the environment of deep space, removal of adsorbed films and cleaning of surfaces takes place in several ways. Gases in adsorbed films may be lost into the vacuum. Sputtering caused by protons hitting the surfaces may accelerate this loss. Adsorbed gases may diffuse into the material. Carbon dissolved in the material may diffuse to the surface and react with adsorbed oxygen or water to form carbon monoxide, which is less strongly adsorbed (*4*). Mechanical wear of moving surfaces provides another important cleaning mechanism. Once surfaces are clean of adsorbed films, they will tend to stay clean in the environment of deep space.

To simulate the vacuum of space, 10^{-12}–10^{-16} mm of mercury, in a laboratory chamber of practical experimental size and in the presence of materials of interest is beyond the present state of the art. The best that can now be done is approximately 10^{-9} mm of mercury. Calculations (*5*) indicate that such a vacuum is probably insufficient to remove adsorbed molecular layers from some materials.

Some information on friction and wear will be obtained from the operation or failure of various spacecraft, but such an approach is slow, not quantitative, unreliable, and risky in that it may mean jeopardizing a mission. It was decided, therefore, to design a flight friction experiment specifically to provide information on frictional behavior of materials in deep space. Such an experiment was flown

on Ranger 1 and Ranger 2 spacecraft in hope of obtaining engineering data for the design of future spacecraft as well as fundamental data on the behavior of rubbing surfaces in ultrahigh vacuum.

Experimental equipment

The flight friction experiment assembly was about 14 inches long, 7 inches wide, 6 inches high, weighed about 19 pounds including batteries, and was completely self-contained, requiring only attachment to the spacecraft structure and a connection to the spacecraft telemetry for data synchronization and read-out. A switch closure in the spacecraft command controller and sequencer activated a latching relay to start the assembly 367 minutes after launch.

Figure 1 shows an exterior view of a flight friction experiment assembly. The 28 volt, 150 ma, 8000 rpm DC gear motor was sealed in the rectangular housing shown

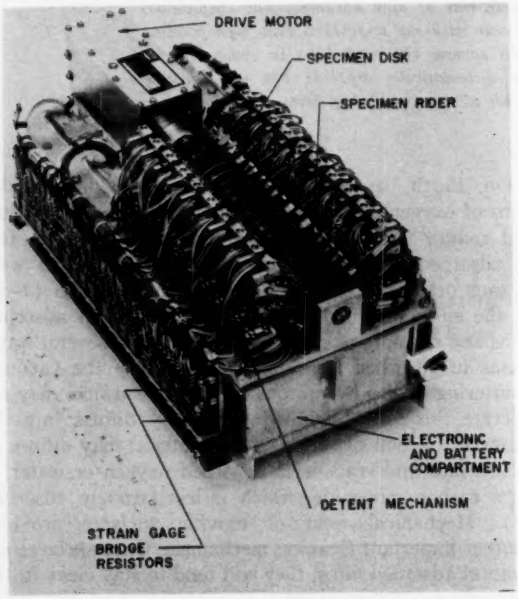

FIG. 1. Friction experiment assembly with temperature control surfaces removed.

at the top of this figure. This motor developed 0.3 oz inch of torque, but the gear reduction (2700:1) provided 300 oz inch of torque at 3 rpm to the output shaft which was coupled to the disk drive shaft. The support bearings for this drive shaft were doubled sealed 440C stainless steel ball bearings with retainers made of polytetrafluoroethylene reinforced with glass and lubricated with molybdenum disulfide. The races were coated with epoxy bonded molybdenum disulfide. The inboard bearing was sealed in the motor housing and the output shaft was brought through a double "O" ring stuffing box. The outboard bearing can be seen in its support bracket in the right center of Fig. 1.

The sealed motor housing and the electronic and battery compartment (Fig. 1) had a leak rate such that a pressure of at least $\frac{1}{2}$ an atmosphere ($\sim$ 7 psi) would be retained after the assembly had been exposed to vacuum conditions for 10 hours. The design specification for the friction assembly called for an operating life of at least 5 hours.

Twenty disk specimens were spaced along the drive shaft, and two $\frac{1}{8}$-inch diameter hemispherical rider specimens traced concentric paths on each side of each disk. A force of 0.3 lb was applied to each rider at 90° to the surface of the disks by a calibrated coil spring. The rider and coil spring were mounted in a housing which was inserted into a loop at one end of a cantilever spring (see Fig. 2). Two wire resistance strain gages cemented

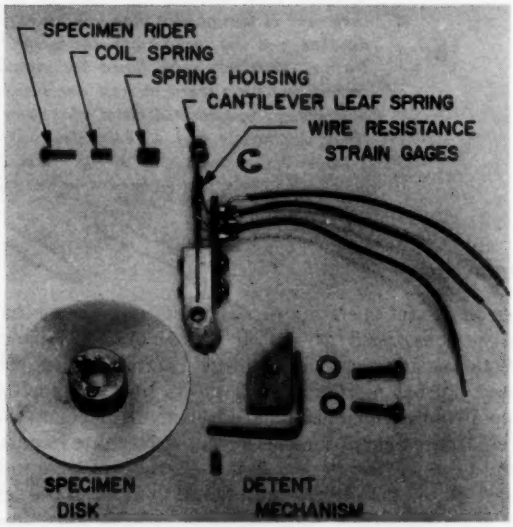

FIG. 2. Rider and disk assembly details

on opposite sides of the cantilever spring measured its deflection and thus indicated the friction force; this, divided by the fixed normal force, gave the friction coefficient. The cantilever spring was mounted on a block attached to a support post on the top deck of the flight friction assembly.

A detent mechanism was designed to move the cantilever spring and associated rider clear of a disk if the coefficient of friction became excessive, to obviate the possibility of the rider seizing to the disk and stopping the disk drive shaft. The detent mechanism (Figs. 1 and 2) consisted of a right angle leaf spring with a small set screw in one end, and bolted to a small bracket which was part of the support post. The set screw was perpendicular to the detent spring and operated against a detent in the block holding the cantilever spring. It was adjusted to hold the cantilever spring until the coefficient of friction approached a value of 2; above this value the screw moved out of the detent and removed the rider from the disk.

The two strain gages on each cantilever spring formed one half of an electrical bridge circuit. Each strain gage circuit also had associated with it one fixed resistor and two adjustable resistors for null and sensitivity adjustments. These resistors were mounted on a bracket which was attached to the top deck and the side of the electronic and battery compartment (Fig. 1). The wiring for the bridge circuits was combined into four cable harnesses and introduced into the sealed electronic and battery compartment through four sealed and potted bulkhead connectors. For all wiring outside of the electronic and battery compartment, polytetrafluoroethylene insulation was used to reduce the possibility of loss of polymer or plasticizer in the vacuum of deep space.

The friction assembly commutator, located in the electronic and battery compartment, connected in sequence each half-bridge circuit to the power supply and to two fixed precision resistors, common to all measurements, which completed the bridge. Every 10 seconds a switch closure in the spacecraft telemetry commutator activated a pulsing circuit in the friction assembly and caused a stepping motor to advance the friction assembly commutator. This closure was made 6 seconds before data read-out to allow time for transients to die out.

Circuits in the electronic compartment provided seven code voltages on commutator segments 1, 2, 3, 45, 46, 47, and 49 (0, 5, 0, 0, 0, 5, and 2.5 volts respectively), which permitted identification of the intervening commutator segments and calibration of the measuring circuits. Also provided were three thermistor bridge circuits, one for indicating the temperature inside the compartment and two indicating the temperature along the top deck of the assembly. One thermistor was attached to a bracket on the top deck between the 6th and 7th disks from the motor end of the drive shaft. Another thermistor was on a bracket between disks 14 and 15. These temperature measurements were on commutator segments 30, 60, and 90. The seven codes, three thermistors, and 80 strain gage bridges measuring coefficient of friction required a 90 segment friction assembly commutator.

The output of this commutator, consisting of successive 10-second samples of friction data, temperature data, and calibration codes, was fed through a DC amplifier in the electronic compartment which amplified it to the 0–5 volt DC signal required by the spacecraft telemetry. The system of commutation, data encoding, and decommutation used in the spacecraft and ground telemetry is described in Ref. (*6*). The encoded signal was an FM analog of the coefficient of friction. A spacecraft telemetry channel transmitted to Earth this encoded signal from the friction experiment for 1 second out of each 10-second period; during the other 9 seconds measurements of other spacecraft functions were transmitted on this channel.

The electronic and battery compartment of the friction assembly also contained the strain gage power supply and the 19 cell silver-zinc battery which supplied 28 volt DC power and was rated at 2.5 amp-hours at 0.25 amp. The start signal from the spacecraft command controller and sequencer to a pulsing circuit in the friction assembly closed and latched a relay in the electronic compartment, thus activating the experiment. The relay circuit was designed to unlatch when the battery voltage dropped below 24 volts. This was the lowest voltage at which the measuring circuit remained in calibration and was above the voltage at which cell reversal could occur in the battery. With the relay in the open position the entire assembly stopped.

Thermal control surfaces of polished aluminum were attached to the sides of the electronic and battery compartment. Across the drive motor housing was another thermal control surface of aluminized polyethylene terephthalate film reinforced with a polytetrafluoroethylene grid. A magnesium thermal control plate was attached to the spacecraft about 1 inch above the friction assembly. It shaded the entire assembly and equalized the temperature gradients that could have resulted from the sunlight and shadow stripes produced by the spacecraft structure in its planned sun-oriented attitude.

Study of the temperature conditions to be expected in flight indicated that the disks furthest from the drive motor should be the coldest parts of the assembly. Grease was applied to sides of the two furthest disks by cotton swabs against which these disks rubbed; the swabs were retained by clips. The coldest disks were chosen to avoid possible condensation on other parts of the system by constituents evaporating from the grease.

A view of the friction experiment assembly mounted on Ranger 1 spacecraft appears in Fig. 3. Additional information about the flight and ground support equipment is given in Ref. (*17*).

The vacuum system for laboratory vacuum tests was pumped with a 15 cfm rotary mechanical pump and a 7-inch oil-diffusion pump with a pumping speed of 1440 liters per second at 10^{-4} mm Hg. Between the oil-diffusion pump and the high-vacuum valve was a liquid-nitrogen-cooled chevron baffle designed to minimize vapor backstreaming and creep of pumping fluids. A stainless steel base plate and an 18-inch diameter glass bell jar, with a liquid-nitrogen-cooled annulus inside, were on top of the high-vacuum valve. Thermocouple gages in a tubulation in the base plate and at the rotary pump inlet monitored vacuum pressure to 10^{-3} mm Hg. A modified Baird-Alpert ionization gage in a tubulation in the base plate monitored the vacuum pressures to 10^{-8} mm Hg. The empty system was capable of achieving a vacuum of 2×10^{-8} mm Hg with the liquid-nitrogen annulus and baffle operating. With a friction assembly in the system a vacuum of about 5×10^{-6} mm Hg was achieved.

Materials used

A complete list and all of the available information on the materials used in this investigation are given in

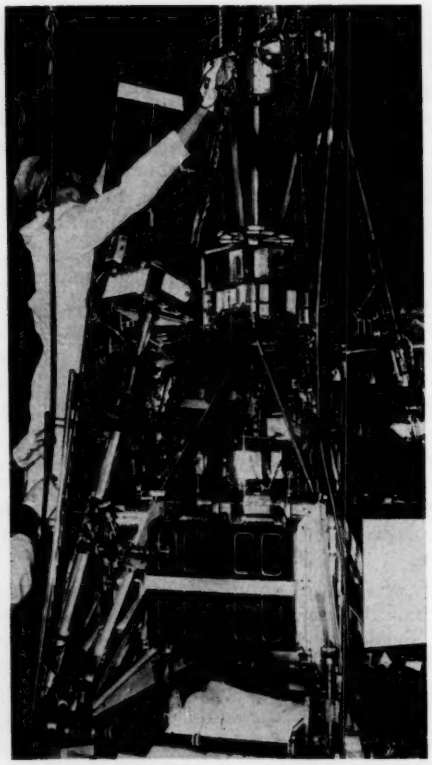

FIG. 3. Ranger 1 spacecraft. Friction experiment is on right side just above white rectangle of temperature-control paint. In flight, large solar cell panels are extended at right angles to main axis of spacecraft.

Table 1. Riders were machined from small ($\frac{1}{8}$–$\frac{1}{4}$ inch) diameter bar stock or from the $1\frac{3}{4}$-inch diameter bar stock used for the disks. For all metallic disks and riders contact surfaces were specified to have a 5-microinch finish.

After final machining all disks and riders were thoroughly cleaned in methyl ethyl ketone, dried, and placed in individual sealed polyethylene bags. All assembly operation involving the disks and riders were performed by operators using plastic gloves to reduce contamination of the contact surfaces.

The quantity of magnetic materials chosen for the flight friction experiments was limited because the magnetometer experiment on the Ranger spacecraft required that the magnetic field be kept below 0.5 γ at the magnetometer, which was about 7 feet from the friction assembly. Since many future spacecraft will carry magnetometers, the choice of materials for bearings, gears, and other moving parts may also be limited to nonmagnetic materials. By proper choice of materials of construction and components and by the use of magnetic shielding, the magnetic field of the flight friction assemblies was kept within specification.

Within the constraints on magnetic properties and on the number of disks and riders, and the need for adequate replication, materials and lubricants likely to be of some engineering interest were selected for test. Also selected were some unalloyed metals whose behavior might check the theory (*7*) that friction and seizure tendency between clean unlubricated surfaces will be high if the rubbing materials have high mutual solid solubility, and relatively low if they have low solid solubility in each other.

Laboratory tests and Ranger 1 and 2 flights

The friction experiment assemblies were subjected to a leak test which consisted of placement in a vacuum of 5×10^{-6} mm Hg for at least 5 hours and measuring the change in pressure in the sealed electronic and battery compartment. They were also subjected to a complete flight acceptance environmental test according to JPL specification 30201E (*8*). For friction tests in laboratory vacuum, the thermal control surfaces were removed from an assembly which was placed inside the vacuum system. The data output was obtained through the ground support equipment. During these tests the thermistors indicated the temperature of the assembly to be between 50 and 75 F.

Preliminary preflight systems tests of Ranger 1 spacecraft were conducted using the entire spacecraft system with associated system check-out equipment and data recording facilities. During these tests, a "stand-in" friction experiment assembly was used, which allowed the disks to be turned as well as the electronics operated. The final preflight systems test of the flight assembly, on which the disks and riders had not been previously run, was carried out in an air-conditioned room (75 F, 50% relative humidity) about 3 days prior to launch. The disk drive shaft was turned and all electronics operated so that data were obtained through the spacecraft telemetry system for two complete cycles of the commutator (30 minutes). This was done to check that the experimental equipment was operational in the spacecraft system and to obtain some in-air data through this system that could be compared with data from space. During this final preflight systems test, the thermistors indicated the temperature of the assembly to be 75 F. The launch shroud was then placed over the spacecraft and purged with dry nitrogen. During the period that the spacecraft was on the launch pad an air conditioning blanket surrounded the shroud and the dry nitrogen purge was maintained. The temperature was less than 80 F and relative humidity was around 10%.

On 8/23/61 at 1004 GMT (Greenwich Mean Time), Ranger 1 was launched. A malfunction of the second stage of the launch vehicle resulted in the spacecraft being injected into a low altitude orbit of apogee 504 km (313 miles) and perigee 170 km (106 miles), instead of the elliptical orbit of very high apogee originally planned. The vacuum (*9*) at the apogee attained was about

TABLE 1
Materials Tested

Material	Commercial designation	Diam. (in.)	Diamond pyramid hardness	Composition weight (%) C	Mn	P	S	Si	Cr	Ni	Mo	Fe	Al	Cu	Others
Iron-nickel chromium alloy (1)[a]	A286	1 3/4	327	0.06	1.65	0.024	0.01	0.57	15.60	25.61	1.26	Bal.	0.15	—	1.98 Ti, 0.004 B
		1/4	284	0.033	1.51	0.026	0.009	0.61	15.66	24.58	1.25	Bal.	0.20	—	2.22 Ti, 0.003 B
Alloy steel (2)	4340	1/4	423	0.40	0.73	0.007	0.018	0.30	0.78	1.78	0.25	Bal.	—	—	
Martensitic stainless steel (3)	440C	1 3/4	658	1.04	0.41	0.016	0.07	0.41	16.75	0.11	0.56	Bal.	—	—	
		1/4	618	0.96	0.34	0.016	0.013	0.44	17.57	0.25	0.51	Bal.	—	0.10	
Copper-base alloy	Aluminum bronze ASTM-B-169-55-F	1 3/4	187	—	—	0.01	—	0.09	—	—	—	0.66	7.98	Bal.	
Aluminum-base alloy (4)	2024T4 QQ-A-268-1	1 3/4	149	—	0.60	—	—	0.25	0.10	—	—	0.25	Bal.	4.35	1.50 Mg, 0.25 Zn
	AMS-4120-E	1/8	166	—	0.58	—	—	0.23	0.10	—	—	0.22	Bal.	4.38	1.52 Mg, 0.23 Zn
Nickel	"A"-Nickel	1/4	321	0.04	0.22	—	0.008	0.02	—	99.5	—	0.13	—	0.09	
Copper	Oxygen-free high conductivity	1 3/4	95	—	—	—	—	—	—	—	—	—	—	99.95	
Aluminum	Electrical grade	1 3/4	35	—	—	—	—	—	—	—	—	—	99.45		
Silver	Fine, Grade A	1 3/4	71	—	—	—	—	—	—	—	—	—	—	—	99.95 Ag
Tungsten	—	1/8	483	—	—	—	—	—	—	—	—	0.006	—	0.0024	99.9 + W, 0.0016 Mg, < 0.0004 Ca
Aluminum oxide	Synthetic-sapphire	1/8	2520	Polycrystalline rod											
Tungsten carbide	Flame plate	—	1440	Flame sprayed on A286. Specified thickness 0.005 inch.											
Polytetrafluoro-ethylene	AMS 3651	3/16	—	Commercial rod											
Polytetrafluoro-ethylene	AMS 3651	1 3/4	—	Reinforced with 15% glass fiber. Impregnated with 5% molybdenum disulfide.											
Gold plating	—	—	—	Plated on A286 in accordance with MIL-G-14548A to a minimum thickness of 0.0005 inch.											
Silver plating	—	—	—	Plated on A286 in accordance with QQ-S-365 Type II to a minimum thickness of 0.0005 inch.											
Molybdenum disulfide	No. 4306	—	—	Phenolic bonded on A286.											
Grease	ETR-H	—	—	Silicone oil with organic dye thickener.											

[a] Specified heat treatment: (1) 1800F, 1 hour, oil quench; 1325F, 16 hours, air cool. (2) 1550F, 1/2 hour, oil quench; 1000F, 1 hour, air cool. (3) 1850F, 1/2 hour, oil quench; 450F, 2 hours, air cool. (4) 920F, 1/2 hour, water quench; 375F, 9 hours, air cool.

7.8×10^{-9} mm Hg, at perigee about 2.1×10^{-6} mm Hg. Re-entry was sometime during 8/29 or 8/30/61.

Ranger 1 telemetry showed that the friction experiment was not on at 1522 GMT on 8/23. The spacecraft command controller and sequencer was scheduled to start the experiment at 1611 GMT on 8/23/61, 367 minutes after launch. Because of the nonstandard orbit, spacecraft telemetry was not being received by any of the tracking stations at this time. About 0531 GMT on 8/24 (13 hours 20 minutes after scheduled start), satisfactory data from the friction assembly were received. Additional data were received from succeeding orbits until 1401 GMT on 8/24/61 (21 hours 50 minutes after scheduled start). The experiment was off at 1536 GMT on 8/24/61. Therefore, it can be concluded that the friction experiment ran for approximately 22 hours and shut itself off at the predetermined low battery voltage. Table 2 summarizes the times, orbits, altitude and vacuum (*9*) at which friction experiment telemetry data were received. Data received during the Ranger 1 flight indicated that the temperature of the experiment was in the range of 100–144 F. It was concluded that this had no significant effect on the friction data.

TABLE 2
Summary of Ranger 1 Passes from Which Coefficient of Friction Data Were Obtained August 24, 1961

Greenwich Mean Time	Orbit number	Altitude (km)	Vacuum[a] (mg Hg)
0528	13	163	2.6×10^{-6}
0658	14	162	2.6×10^{-6}
0705	14	179	1.7×10^{-6}
0834	15	170	2.1×10^{-6}
0842	15	219	6.7×10^{-7}
0915	16	443	1.7×10^{-8}
1007	16	181	1.6×10^{-6}
1017	16	260	3.0×10^{-7}
1049	17	453	1.5×10^{-8}
1145	17	230	5.2×10^{-7}
1226	18	427	2.1×10^{-8}
1401	19	378	4.3×10^{-8}

[a] Ref. (*9*)

Acceptance, environmental, and preflight tests of the friction assembly for Ranger 2 were conducted in the same manner as those for Ranger 1. On 11/18/61 at 0812 GMT, Ranger 2 was launched. A malfunction of the second stage resulted in the spacecraft remaining in the low altitude orbit with apogee of 236 km (147 miles) and perigee 157 km (98 miles), instead of a highly elliptical orbit. The vacuum (*9*) at the apogee attained was about 4.7×10^{-7} mm Hg, at perigee about 3.0×10^{-6} mm Hg. Re-entry was on 11/19/61, about 20 hours after launch. During a period from 1322 to 1328 GMT telemetry was received from Ranger 2 and indicated that the friction experiment was not on. The spacecraft command controller and sequencer was scheduled to start the experiment at 1419 GMT, 367 minutes after launch. Because of the nonstandard orbit, spacecraft telemetry was not being received by the tracking stations at this time. During a period starting at 1456 GMT (37 minutes after scheduled start), 26 pieces of telemetered data were received. These were considered insufficient to permit meaningful discussion in this paper.

Reduction of data

The output data obtained from the friction experiment during the preflight systems test and during the flights were recorded in both analog and digital form. The analog data were recorded during the entire 1-second period that the friction experiment was connected to the spacecraft telemetry. (Some typical analog traces are shown in Appendix A.) The digital data were recorded 0.6 second after the analog data recording started.

Since the analog data record showed variations due to noise on the entire communication link as well as to frictional behavior, coefficient of friction values were determined taking a most probable value from the recorded analog trace. These were checked against values determined from the recorded digital data to assure that there was reasonable agreement. Besides the most probable value, a high and a low value were also taken from each recorded analog trace. In taking these values, obvious noise spikes were not considered.

These coefficient of friction data were plotted vs. time for each disk and rider. Figures 4 through 11 are plots for representative material combinations. Plots for remaining pairs are given in Ref. (*17*). Each combination of materials was used on several disks and riders; a separate curve is shown for each replicate. On each figure is a group of curves representing data on the assembly used for flight and for preflight measurements in air, and another group representing data from a nominally identical assembly used for laboratory vacuum tests. The data points are plotted at the most probable value of the friction coefficient, and a vertical line through the data point indicates the high and the low value of the coefficient observed during that period of data recording. Table 3 lists, for each material combination, the average of the most probable values for all replicates; these values are shown graphically in Figs. 12 and 13.

Many factors are known to affect the measurement of a coefficient of friction. There are also several sources of measurement error inherent in this experiment. A study of these errors has been made and is summarized in Appendix B. This study gave an estimated standard deviation of $\pm$ 0.035 for friction coefficient measurements near 0.2 and $\pm$ 0.05 for friction coefficients near 1.0.

Discussion of results

Comparisons of results in space, laboratory vacuum, and air are complicated by differences in running time. Many of the plots of friction coefficient in laboratory vacuum vs. time showed a trend at short times, which

TABLE 3
Coefficients of Friction

Rider	Disk	Lubricant	In air; preflight assembly No. 4; 15–30 min.[a]	In lab; vacuum assembly No. 4; 50–100 min.	In space; Ranger 1 assembly No. 4; 800–1300 min.	Literature data friction coefficient, in vacuum	Ref.
Nickel	Copper	None	0.20	0.67 (0.22 & 1.12)[b]	0.56 (0.42 & 1.0)[b]	1.50 after 10^1 to 10^2 turns	(7)
Aluminum	Copper	None	0.23	0.94	0.66		
Silver	Copper	None	0.38	0.22	0.70		
Tungsten	Copper	None	0.34	0.16	0.40	0.41 after 10^1 to 10^2 turns	(7)
Iron alloy A286	Iron alloy A286	None	0.26	0.50	0.62		
Copper alloy	Copper alloy	None	0.28	0.73	0.43	For brass: 0.60 to 0.75 after 10^3 strokes	(10)
Aluminum alloy 2024	Aluminum alloy 2024	None	0.56	0.67	0.33	0.32 to 0.57 after 10^3 strokes	(10)
Steel 440C	Steel 440C	None	0.07	0.18	0.10	0.44 after 10^5 turns	(11)
Iron alloy A286	Copper alloy	None	0.32	0.53	0.44		
Aluminum alloy 2024	Iron alloy A286	None	0.23	0.32	0.27		
Steel 4340	Iron alloy A286	None	0.33	0.38	0.60		
Steel 440C	Tungsten carbide	None	0.20	0.16	0.18		
Aluminum oxide	Steel 440C	None	0.11	0.16	0.07	0.36 after 10^5 turns	(12)
PTFE[d]	Iron alloy A286	None	0.02	0.04	0.02		
PTFE	Aluminum alloy 2024	None	0.02	0.06	0.08		
PTFE	Tungsten carbide	None	0.03	0.05	0.02		
Steel 440C	PTFE glass-fiber	Molybdenum disulfide	0.04	0.05	0.05		
Aluminum alloy 2024		impregnated in disk	0.01	0.07	0.01		
Iron alloy A286	Iron alloy A286	Phenolic	0.14	0.09	0.03	For 440C on 440C, phenolic-MoS_2: 0.025 after 10^5 turns	(11)
Steel 4340	Iron alloy A286	bonded molybdenum	0.17	0.08	0.07	For MoS_2 pellet on stainless: 0.06 to 0.10 after 4×10^3 turns	(13)
Aluminum alloy 2024	Iron alloy A286	disulfide	0.09	0.14	0.02		
Copper alloy	Iron alloy A286	on disk	0.15	0.09	0.01		
Iron alloy A286	Iron alloy A286	Silver plate on disk	0.25	0.17	0.46	For 440C: 0.06 after 10^5 turns	(11)
Iron alloy A286	Iron alloy A286	Gold plate on disk	0.12	0.17	0.13	For 440C: 0.10 after 10^5 turns	(11)
Iron alloy A286	Iron alloy A286	Grease	0.16[c]	0.20	0.24[c]		
Steel 4340	Iron alloy A286	Grease	0.08	0.24	0.05		
Copper alloy	Iron alloy A286	Grease	0.12[c]	0.17	0.14		
Aluminum alloy 2024	Iron alloy A286	Grease	0.15	0.11	0.11		

[a] At 3 rpm, nominal.
[b] Average for low-friction and high-friction modes, respectively.
[c] Data were discarded for one rider to which lubricant was apparently not properly applied.
[d] Polytetrafluoroethylene.

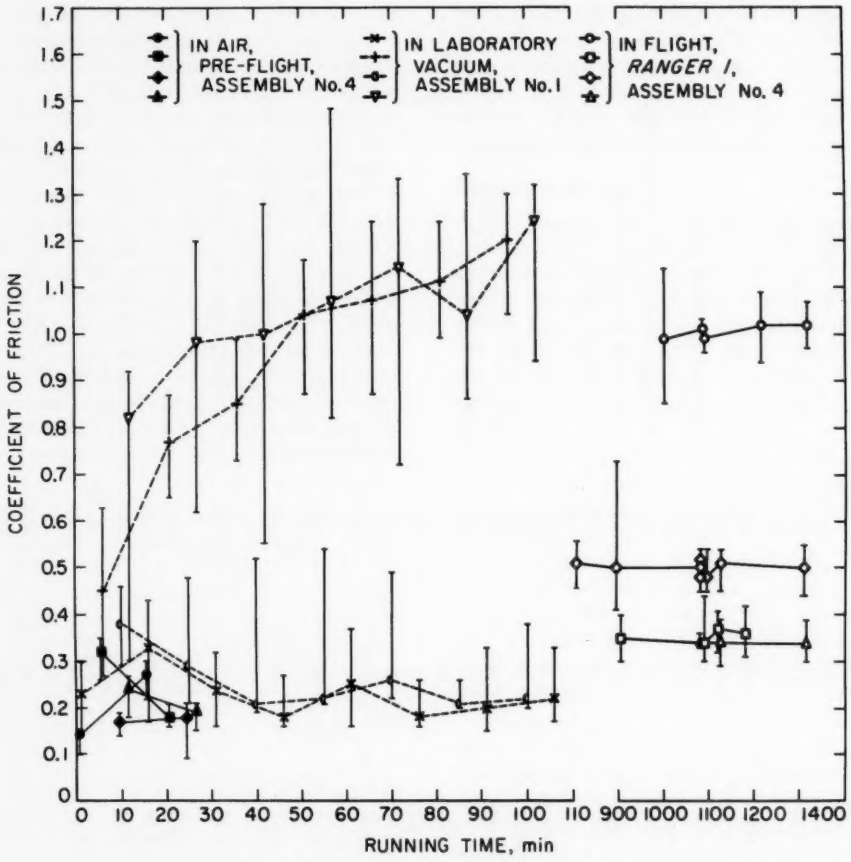
IN AIR, PRE-FLIGHT, ASSEMBLY No. 4
IN LABORATORY VACUUM, ASSEMBLY No. 1
IN FLIGHT, RANGER I, ASSEMBLY No. 4
COEFFICIENT OF FRICTION
RUNNING TIME, min

FIG. 4. Coefficient of friction vs. time for nickel on copper. Each symbol designates data from one rider-disk replicate; open and solid symbols of the same form designate data from this replicate in space and in air. Each symbol is shown at the most probable value. Vertical line through symbol indicates range during period of reading. Lines connecting symbols are only to help identify readings made on same replicate.

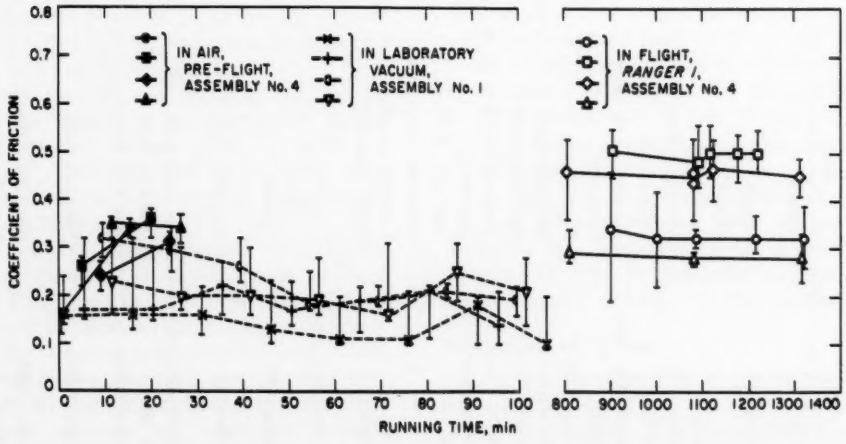
IN AIR, PRE-FLIGHT, ASSEMBLY No. 4
IN LABORATORY VACUUM, ASSEMBLY No. 1
IN FLIGHT, RANGER I, ASSEMBLY No. 4
COEFFICIENT OF FRICTION
RUNNING TIME, min

FIG. 5. Coefficient of friction vs. time for tungsten on copper

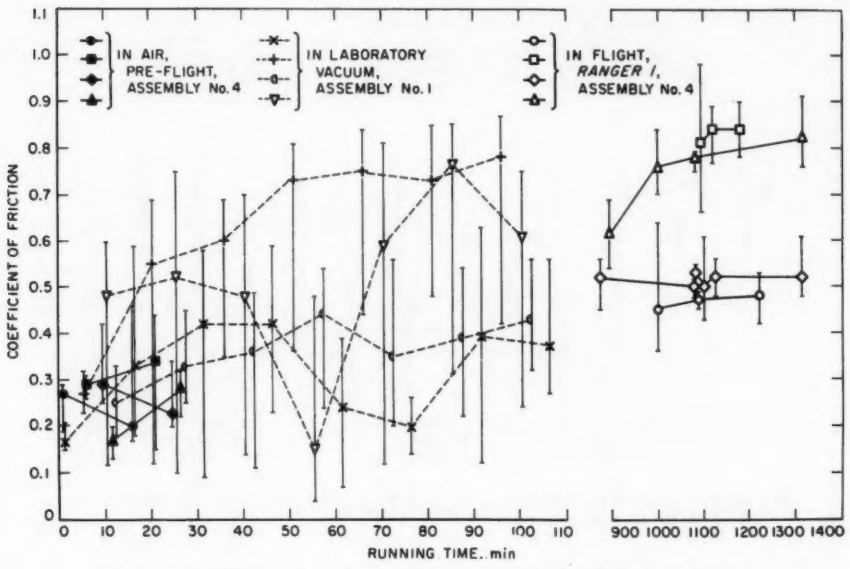
IN AIR, PRE-FLIGHT, ASSEMBLY No. 4
IN LABORATORY VACUUM, ASSEMBLY No. 1
IN FLIGHT, RANGER I, ASSEMBLY No. 4
COEFFICIENT OF FRICTION
RUNNING TIME, min

FIG. 6. Coefficient of friction vs. time for A286 iron-base alloy on A286

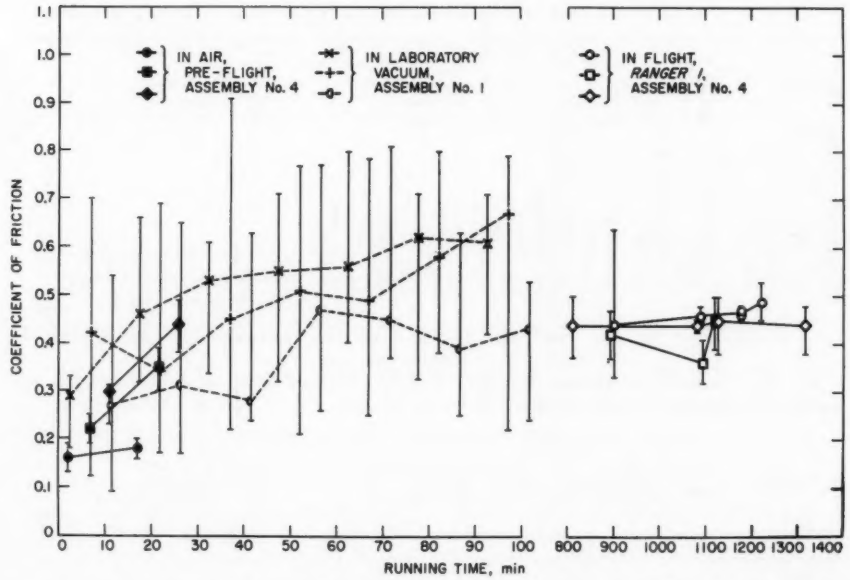
IN AIR, PRE-FLIGHT, ASSEMBLY No. 4
IN LABORATORY VACUUM, ASSEMBLY No. 1
IN FLIGHT, RANGER I, ASSEMBLY No. 4
COEFFICIENT OF FRICTION
RUNNING TIME, min

FIG. 7. Coefficient of friction vs. time for A286 iron-base alloy on copper-base alloy (aluminum bronze).

tended to level out at longer running times. It would clearly be desirable to compare the space data with measurements on identical assemblies and materials run in air and laboratory vacuum for the same times. Because of the nonstandard orbit of Ranger 1, the flight data were obtained after considerably longer running times than the anticipated 30–300 minutes. Ground data for comparison at the observed times are not available; it is planned to make such measurements and report them subsequently. In this paper, accordingly, comparisons of space data with air data will be minimized.

In discussing the results, a few typical plots will be considered in detail, but the comments and conclusions stated are based on examination of all of the data, not just on the tabulated averages given in Table 3.

Figure 4 shows the data obtained for a nickel rider on a copper disk. In the laboratory vacuum, two of the rider-disk replicates gave a low coefficient of friction

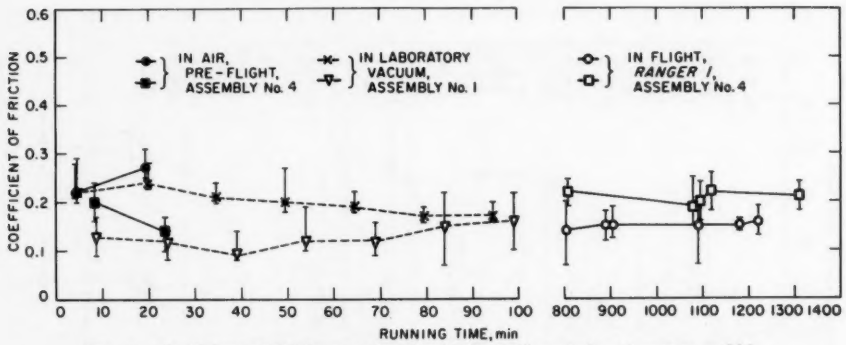
COEFFICIENT OF FRICTION
IN AIR, PRE-FLIGHT, ASSEMBLY No. 4
IN LABORATORY VACUUM, ASSEMBLY No. 1
IN FLIGHT, RANGER I, ASSEMBLY No. 4
RUNNING TIME, min

FIG. 8. Coefficient of friction vs. time for 440C stainless steel on tungsten carbide

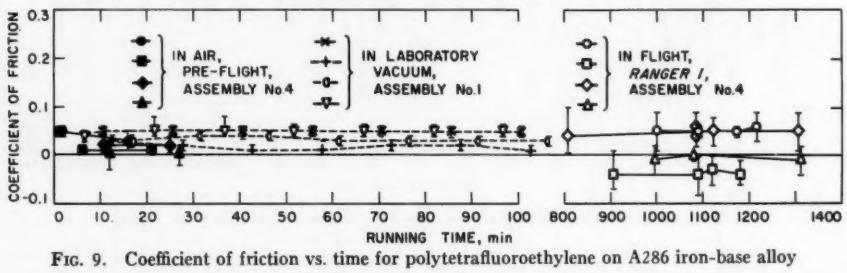
COEFFICIENT OF FRICTION
IN AIR, PRE-FLIGHT, ASSEMBLY No.4
IN LABORATORY VACUUM, ASSEMBLY No.1
IN FLIGHT, RANGER I, ASSEMBLY No.4
RUNNING TIME, min

FIG. 9. Coefficient of friction vs. time for polytetrafluoroethylene on A286 iron-base alloy

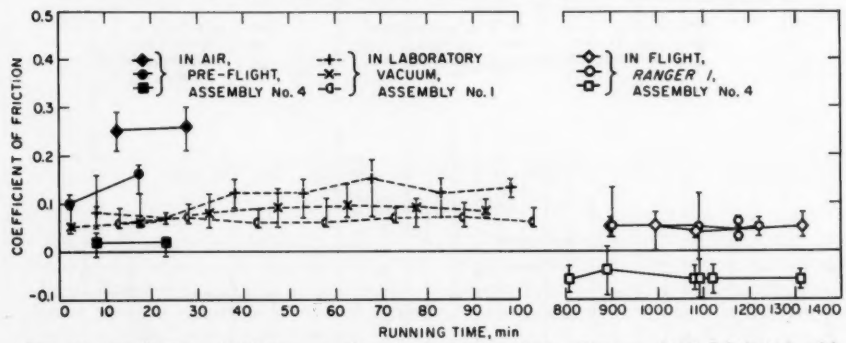
COEFFICIENT OF FRICTION
IN AIR, PRE-FLIGHT, ASSEMBLY No. 4
IN LABORATORY VACUUM, ASSEMBLY No. 1
IN FLIGHT, RANGER I, ASSEMBLY No. 4
RUNNING TIME, min

FIG. 10. Coefficient of friction vs. time for A286 iron-base alloy on A286 lubricated with phenolic-bonded molybdenum disulfide.

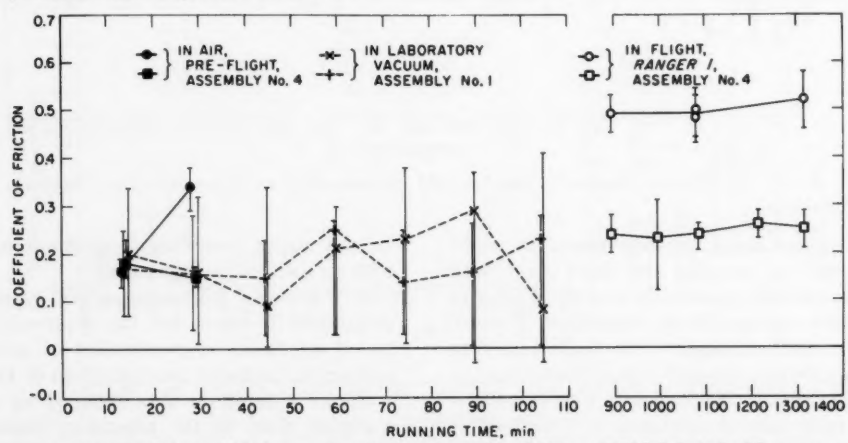
COEFFICIENT OF FRICTION
IN AIR, PRE-FLIGHT, ASSEMBLY No. 4
IN LABORATORY VACUUM, ASSEMBLY No. 1
IN FLIGHT, RANGER I, ASSEMBLY No. 4
RUNNING TIME, min

FIG. 11. Coefficient of friction vs. time for iron-base alloy A286 on A286 lubricated with grease

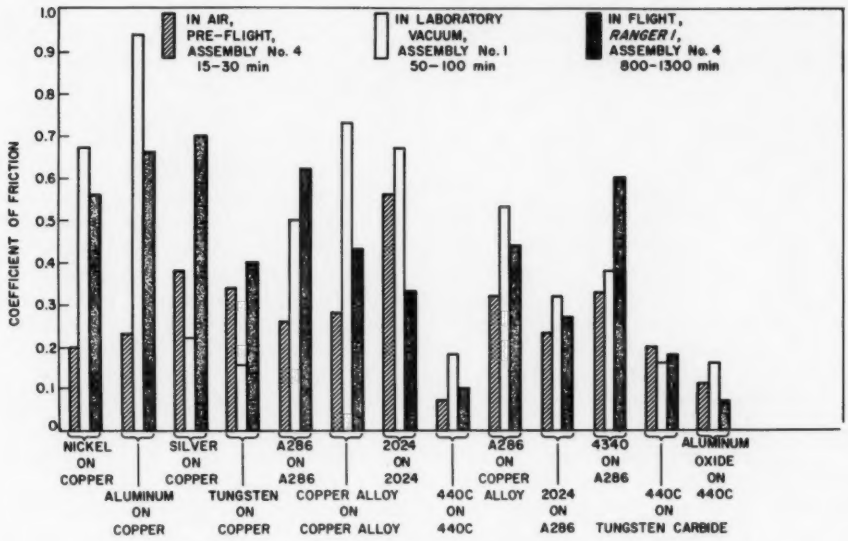

FIG. 12. Coefficients of friction for unlubricated metallic and ceramic material

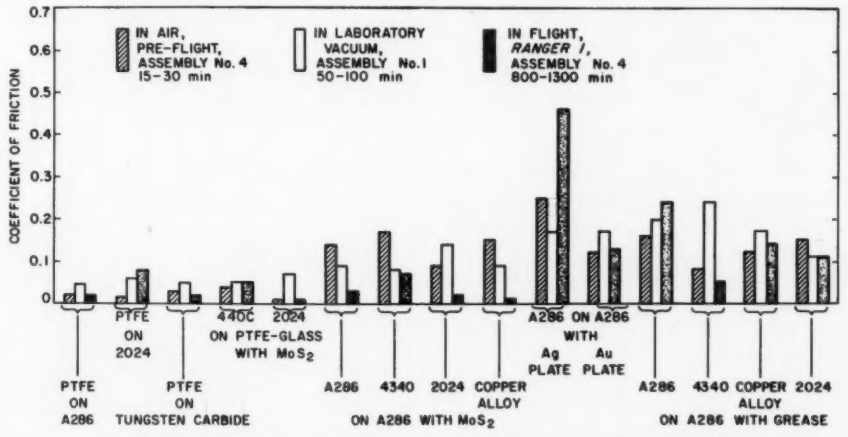

FIG. 13. Coefficients of friction for lubricated and polymeric materials

(0.18–0.26) and two combinations gave a high value (1.04–1.20). In flight measurements three replicates showed a low coefficient (0.34–0.51) and one showed a high value (about 1.0). This may merely mean that some replicates gave incorrect results. If high-friction and low-friction modes really occurred, a cause may be an oxide layer on the copper disk or the nickel rider, which may sometimes be removed by the vacuum or mechanical rubbing. Coffin (*7*) has reported a coefficient of friction for nickel and copper in vacuum somewhat greater than the higher values observed here.

For aluminum vs. copper, the coefficients of friction measured in laboratory vacuum were high. 0.70–1.34 for times over 50 minutes. In space, one rider gave very high coefficients (1.4–1.5); these single rider values need confirmation. Results may be complicated by the presence of aluminum oxide films. For silver vs. copper, the coefficients measured in space were much higher than in laboratory vacuum. Coefficients as high as some obtained for nickel-copper and aluminum-copper did not occur, however. Figure 5 shows the data for tungsten vs. copper. The coefficients obtained were the lowest of any pair using copper as one component; the average in space was the same as that reported for laboratory measurements by Coffin (*7*).

For the iron-base alloy A286 against A286, unlubricated (Figure. 6), for the copper-base alloy (aluminum bronze) against copper-base alloy, and for the aluminum-base alloy 2024 against 2024, moderate coefficients of friction, averaging about 0.55 in vacuum, were obtained. These and other metal-on-metal pair showed some suggestion of high-and-low-friction modes,

but the data did not permit a definite decision on this point. The measured values for copper- and aluminum-base alloys agree with those taken in laboratory vacuum by Hansen *et al.* (*10*).

The stainless steel 440C, running against 440C, displayed relatively low friction (0.10 in space). As the replicates, on separate disks, agreed very well, this is not likely to be an erroneous measurement; it may be associated with the high hardness of this material or with lack of removal of absorbed gases or of an oxide layer in the vacuum encountered. Buckley *et al.* (*11*) reported a higher value in laboratory vacuum.

Data for an iron-base alloy rider (A286) on a copper-base alloy disk (aluminum bronze) are shown in Fig. 7. Moderate friction coefficients were observed. This was true also for an aluminum-base alloy rider (2024) and a ferritic steel rider (4340) on an austenitic iron-alloy disk (A286). These unlubricated combinations averaged 0.42 friction coefficient in vacuum.

For combinations using metals and ceramics, such as 440C stainless steel on tungsten carbide (Fig. 8) and aluminum oxide on 440C, there was little difference between the space, laboratory vacuum, and air data. The friction coefficients were relatively low, never exceeding 0.27. These materials were all hard.

Figure 9 gives the data for a polytetrafluoroethylene rider on an A286 iron alloy disk. The coefficients of friction were very low, never exceeding 0.07. The small negative values sometimes obtained are attributed to scatter. Similar results were obtained for polytetrafluoroethylene on 2024 aluminum alloy and on tungsten carbide, and for 440C steel and 2024 on polytetrafluoroethylene reinforced with glass and impregnated with molybdenum disulfide. There were some variations in the recorded data which may have been due to the nonhomogeneous surface caused by the exposure of the reinforcing fiber. These were not of sufficient magnitude to affect the over-all coefficient of friction. The materials pairs with polytetrafluoroethylene as one element showed friction coefficients averaging 0.01–0.08; these are comparable to the 0.10 reported for polytetrafluoroethylene on polytetrafluoroethylene in a laboratory vacuum (*15*).

Data in Fig. 10 are for an A286 iron alloy rider on an A286 disk coated with phenolic-bonded molybdenum disulfide. The low values of friction coefficient (0.01–0.07 in space) are typical of those obtained for riders of 4340 steel, 2024 aluminum alloy, and copper alloy (aluminum bronze) on a disk of A286 lubricated with a coating of phenolic-bonded molybdenum disulfide. They are also in general agreement with literature results (*11*, *13*) for molybdenum disulfide lubrication in vacuum. The values in space were a little lower than those in laboratory vacuum, which were in turn generally lower than those in air. This may be due to a difference in running time, the friction decreasing with time. It is known that "running-in" is important with this lubricant (*13*, *16*).

For A286 on A286 iron alloy lubricated with silver plate, the space data gave a much higher coefficient (0.46 average). This could have been due to wear of the silver plate, which may have been thinner than the 0.0005-inch minimum thickness specified. With gold plate, friction was fairly low (0.13 in space) and agreed with laboratory measurements by Buckley *et al.* (*11*).

Figure 11 shows the results for an A286 rider on an A286 iron alloy disk with a grease lubricant. A study of the flight and preflight data led to the conclusion that for one of the rider and disk replicates the lubricant was not being properly applied and thus an unrealistically high value for the friction coefficient was obtained. Discarding the data for this rider, the coefficient averaged 0.24. Other materials combinations run with a grease lubricant, such as 4340 steel, copper alloy (aluminum bronze), and 2024 aluminum alloy on A286 iron alloy, generally showed somewhat lower friction.

It is possible that during the time in the flight environment some of the grease could have migrated to disks where it was not desired and thus affected the coefficients of friction, even though care was used to restrict the grease to those combinations which were to be lubricated and to the disks expected to be coldest, and the arrangement of the disks was such that each could not "see" any but the adjacent disks. Examination of the available data did not indicate an effect attributable to grease migration.

General comparisons

Table 4 summarizes the results obtained for the various classes of materials. For metals running against metals, unlubricated, the friction coefficient averaged over all pairs was the same in space, 0.5, as in laboratory

TABLE 4
Summary of Results

Materials combination and lubricant	Average coefficient of friction		
	In air, preflight 15–30 min.[a]	In lab, vacuum 50–100 min.	In space, Ranger 1 800–1300 min.
Metal vs. metal, unlubricated	0.29	0.48	0.48
Ceramic vs. metal, unlubricated	0.16	0.16	0.12
Polytetrafluoroethylene vs. metal or ceramic	0.02	0.05	0.04
Metal vs. metal, molybdenum disulfide lubricant	0.14	0.10	0.04
Metal vs. metal, metal film lubricant	0.18	0.17	0.30
Metal vs. metal, grease lubricant	0.13	0.18	0.14

[a] Running time at 3 rpm.

vacuum; this compared with 0.3 in air. Some of the difference may be due to the longer running times in vacuum.

Though the average in vacuum was 0.5, some individual values of friction coefficient above 1.0 were observed. All of these involved copper-base alloys: nickel and aluminum vs. copper in space, and aluminum bronze vs. aluminum bronze in laboratory vacuum. Four additional combinations showed occasional values above 0.8 in either space or laboratory vacuum: silver vs. copper, 4340 steel and A286 vs. A286 iron-base alloy, and 2024 vs. aluminum-base alloy.

Figure 14 is a plot of the friction coefficient in vacuum vs. hardness of the harder material, for unlubricated metallic pairs. A definite trend towards low friction coefficient at high hardness is evident. At low hardnesses the figure shows a wide range in friction coefficient.

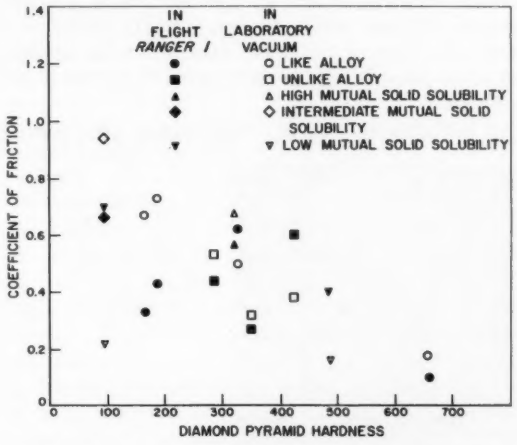

FIG. 14. Average friction coefficient in vacuum vs. hardness lubricated metallic pairs.

The hypothesis that high friction coefficient in vacuum is related to high mutual solid solubility (*7*) has been mentioned; the copper disks and their unalloyed riders were selected to check this hypothesis. Nickel and copper show complete mutual solid solubility. Aluminum is moderately soluble in copper, but copper has low solid solubility in aluminum, and intermetallic compounds exist (*14*). Silver and copper show only slight mutual solid solubility (less than 1% at 200 C) (*14*). Tungsten and copper are essentially insoluble in each other. The average friction coefficients in vacuum were 0.62 for nickel-copper, 0.80 for aluminum-copper, 0.46 for silver-copper, and 0.28 for tungsten-copper. The first two pairs were the only ones in the entire experiment to show friction coefficient values above 1.0, and the third pair showed some values above 0.8. Thus, there may be a trend in the expected direction, though it is not clean-cut.

The solubility hypothesis is somewhat difficult to apply to multiphase engineering materials. It is generally accepted, however, that like materials sliding on each other tend to show higher friction than unlike materials. In this work, the like alloy pairs averaged 0.44 friction coefficient in vacuum and the unlike 0.42—not a significant difference. On the other hand, of the four pairs of like materials, one showed friction coefficient values above 1.0 and two others above 0.8. Of the three unlike alloy pairs, none had values above 1.0 and one (4340 steel vs. A286 iron-base alloy) had values above 0.8.

One of the pairs of like alloy (440C steel) was much harder than the other alloys tested. If this material is excluded the average friction coefficient for like alloy pairs in vacuum was 0.54, slightly higher than for unlike pairs. This suggests examining like and unlike alloys, as well as metals of high and low mutual solid solubility, at comparable hardness levels. In Fig. 14 the points are identified as like or unlike, and solubilities are indicated. No very obvious trends with "likeness" or solubility are noted: the various types scatter over the triangular distribution of friction coefficient vs. hardness.

Returning to Table 4, the ceramic vs. metal combinations showed fairly low coefficients of friction, averaging 0.12 in space. The harder member of each pair was, in these cases, extremely hard. Combinations of metal vs. metal with molybdenum disulfide lubricant and of polytetrafluoroethylene vs. metal or ceramic gave the lowest coefficient, averaging 0.04 in space. Metal vs. metal combinations with grease lubricant had somewhat higher friction. Metal vs. metal with metal film lubricants averaged still higher friction; this may have been influenced by wearing away of the film. In all of the lubricated materials, the method of applying lubricant undoubtedly has an important effect (*16*).

The coefficients in space were not systematically different from those in laboratory vacuum (Table 4). It is possible that the pressure difference between the space and laboratory vacuums achieved was too small to bring out a difference in friction behavior. It is also possible that a difference in behavior was masked by differences between experiment assemblies. (The same assembly was not used in laboratory vacuums as in space because it was desired to fly unworn disks and riders.)

Agreement of the measurements with data in the literature for other laboratory vacuum tests is somewhat spotty (Table 3). Some of the differences may be due to differences in vacuum; others must be attributed to differences in the exact materials used, in surface preparation, in speeds, loads, and other factors. The time, track length, or number of turns or strokes may be important also; for the Ranger 1 space data, the running time of 800–1300 minutes corresponded to 2400–3900 turns of the disks.

Conclusions

1. An experiment for measuring the coefficient of sliding friction for a number of material combinations was designed and fabricated to meet all flight acceptance

tests required for Rangers 1 and 2 and was flown on these spacecraft. The apparatus functioned in space as designed, on both flights. Although the orbits attained were different than planned, meaningful data were obtained from Ranger 1.

2. Under the conditions of the experiment (including vacuums of 8×10^{-9} to 3×10^{-6} mm Hg), polytetrafluoroethylene sliding against metals and ceramics, as well as metals sliding on metals with a molybdenum disulfide lubricant, appeared to have very low coefficients of friction, averaging 0.04. Ceramics sliding against metals, unlubricated, and metals sliding on metals with grease or gold-plate lubrication, showed intermediate values, averaging 0.13. Unlubricated metals sliding on metals showed moderately high coefficients, averaging about 0.5; with some pairs values above 1.0 were observed.

3. For unlubricated metals sliding against metals or ceramics, the friction coefficient tended to be low when at least one member of each pair was of high hardness.

4. The data were not inconsistent with the hypothesis that high coefficients of sliding friction between metals in vacuum can be correlated with high mutual solubility of the materials.

5. The friction coefficients measured in space, with exposure to vacuums of 8×10^{-9}–3×10^{-6} mm Hg, were not, in general, systematically different from those measured in the laboratory at a vacuum of 5×10^{-6}–1×10^{-5} mm Hg. For unlubricated metallic materials, the friction coefficients observed in vacuum were generally higher than those measured in air at shorter running times.

Appendix A

Sample Data Traces from Telemetered Records

Figure 15 shows about 45 seconds of a telemetry record taken with the receiving antenna properly locked on the spacecraft. The portions of the record pertinent to the friction experiment are marked on the figure. These particular signals were received about 1080 minutes after the friction experiment started. Figure 16 shows the same signals taken at the identical time but by a different receiving antenna, which was not properly locked on the spacecraft. Most of the flight data had noise similar to that represented in Fig. 16, with some variations in noise amplitude.

Air and laboratory vacuum data showed little telemetry

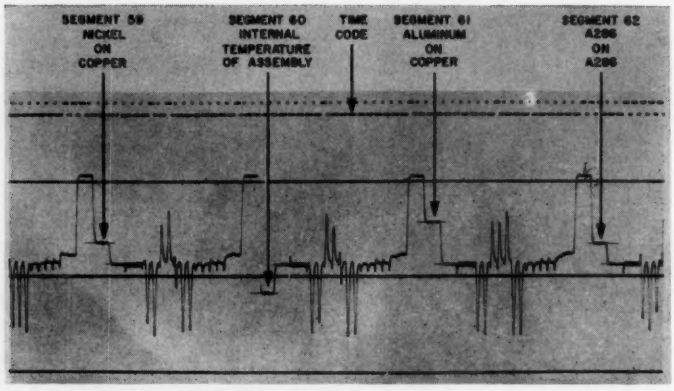

FIG. 15. Flight telemetry record. Antenna properly locked on spacecraft

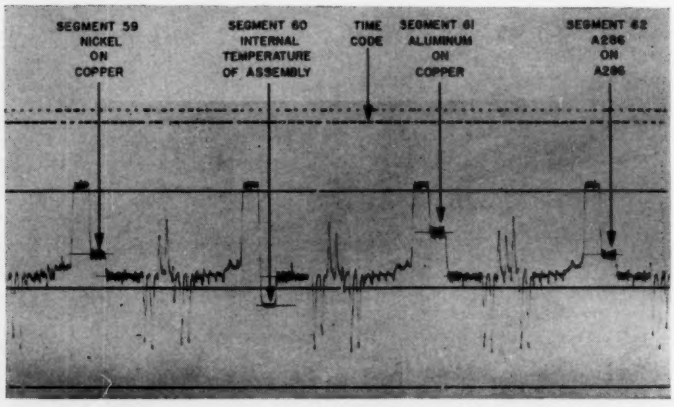

FIG. 16. Flight telemetry record. Antenna not properly locked on spacecraft

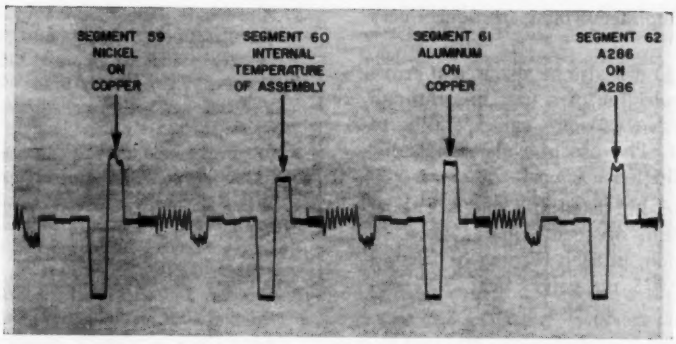

FIG. 17. Preflight telemetry record

or recording noise. Some mechanical noise was observed. Figure 17 shows data taken in air approximately 25 minutes after experiment start for the same materials combinations shown in Figs. 15 and 16.

Appendix B

ERROR ANALYSIS

Certain mechanical errors for this experiment arise from the dynamic system used to transmit an analog of the friction coefficient. Closely controlled assembly techniques held the disk wobble and the position of the coil spring holder to ± 0.001 inch each, corresponding to errors in the normal force and thus in the coefficient of friction of 1.6%. Torsion forces on the leaf spring strain gage sub-assembly were found to lower friction coefficient readings by 1.3%. These sub-assemblies are also subject to mechanical hysteresis. Hysteresis measurements on a complete rider arm assembly showed for full scale deflection a maximum hysteresis error of ± 0.06 volts, corresponding to ± 0.02 in coefficient of friction for coefficients near 0.2 and ± 0.03 for coefficients near 1; it is unlikely that such large deflections actually occurred.

Wear will flatten the contact points on the $\frac{1}{8}$-inch hemispherical riders. Both this and disk wear cause normal motion in the coil spring, changing the normal force by 1.6% for every 0.001 inch of wear. Because of the hemispherical rider shape most of the combinations wear back quite rapidly until the normal force has been lowered about 2%. From then on, though, normal wear, as observed in ground tests, proceeds very slowly except in the case of extremely soft materials such as pure aluminum.

Another error could arise from the geometry of the system used. Asperities on the rider will have some tendency to move around as well as over asperities on the disk. Because of the position of the leaf spring mounting, the spring will tend to deflect a little more than it would otherwise do; the friction coefficient will accordingly read slightly high. The magnitude of this error is difficult to estimate; the width of disk wear path observed on ground tests indicates that it must have been less than 10% and was probably much less.

The graphical calibration charts of leaf spring load vs. output voltage could only be read to values corresponding to ± 0.02 in friction coefficient.

Electronic errors include those in the package itself and those in the telemetry and data recording systems. The electronic components used in the friction experiment assemblies were chosen for maximum time and temperature stability. Permissible changes in temperature and in battery voltage would change the output voltage of the strain gage bridge circuit by 0.4%, corresponding to 0.001–0.005 in friction coefficient. Because friction measurements were calibrated against the 0, 2.5, and 5 volt marker code signals which came through the same

TABLE 5
Error Summary

Nature of error	Error, Δf, in friction coefficient		$(\Delta f)^2 \times 10^4$	
	At $f = 0.2$	$f = 1$	$f = 0.2$	$f = 1$
Disc wobble and rider tilt	± 0.0032	± 0.016	.1	2.5
Torsion on leaf spring	— 0.0026	— 0.013	.06	1.7
Mechanical hysteresis	< ± 0.02	< ± 0.03	< 4	< 9
Wear	— 0.004	— 0.02	.16	4
Reading calibration curves	± 0.02	± 0.02	4	4
Asperity evasion	+ 0.002?	+ 0.01?	.04?	1?
Reading analog record	± 0.015	± 0.02	2.5	4
Battery voltage and temperature effects	± 0.001	± 0.005	.01	.25
Telemetry noise	± 0.02	± 0.02	4	4
Sum			10–14	21–30
Standard deviation, estimated $(\sqrt{\Sigma(\Delta f)^2}$	± 0.03–0.04	± 0.04–0.06		

amplifier, drift in the amplifier would introduce very little error.

Telemetry noise (Fig. 16) can also be a source of error. Uncertainties due to the selection of a best line through a noisy signal were about ± 0.05 volts, corresponding to 0.02 in friction coefficient. The use of code signals for calibration kept the recording error low.

The above error estimates are listed in Table 5. Taking the square root of the sum of their squares gave an estimated standard deviation, in each reading of friction coefficient, of about ± 0.035 for values near 0.20 and ± 0.05 for values near 1.

ACKNOWLEDGMENTS

The authors wish to thank, for their assistance in various phases of the experimental work, John Casani, Linwood Douglass, Max Goble, Charles Kirsten, Stanley Peterson, Raymond Piereson, William Takai, and Norman Williams. Preliminary design of equipment for the flight friction experiment was by the Jet Propulsion Laboratory; final design and construction by United Electrodynamics Corporation of Pasadena, California.

REFERENCES

1. BOWDEN, F. P., and YOUNG, J. E., "Friction and Adhesion of Clean Metals," *Nature* **164**, 1089-1090 (1949).
2. BOWDEN, F. P., and YOUNG, J. E., "Friction of Clean Metals and the Influence of Adsorbed Films," *Proc. Roy. Soc. (London)* **A208**, 311-325 (1951).
3. ROWE, G. W., "Vapor Lubrication and the Friction of Clean Surfaces," *Proc. Conf. Lubrication Wear, London*, 1957 333-338.
4. HAM, J. L., "Mechanisms of Surface Removal from Metals in Space," *Aerospace Eng.* **20**, 20-21, 49-52, 54 (1961).
5. DUSHMAN, S., "Scientific Foundation of Vacuum Technique." Wiley, New York, 1949.
6. "Spacecraft Design Specification for Ranger A1 and A2." Jet Propulsion Laboratory, California Institute of Technology, Pasadena, California, 1961.
7. COFFIN, F. L., JR., "A Study of the Sliding of Metals with Particular Reference to Atmosphere," *Lubrication Eng.* **12**, 50-59 (1956).
8. "Environmental Test Specification for Ranger." JPL Specification 30201E, Jet Propulsion Laboratory, California Institute of Technology, Pasadena, California, 1961.
9. SISSENWINE, N., DUBIN, M., and WEXLER, H., "The United States Standard Atmosphere, 1962," *J. Geophys. Res.* **67**, 3627-3630 (1962).
10. HANSEN, S., JONES, W., and STEPHENSON, A., "High Vacuum Friction," Litton Industries of California, Report to U. S. Air Force Office of Scientific Research, AFOSR Report TR 59-97, Beverly Hills, California, 1959.
11. BUCKLEY, D. H., SWIKERT, M., and JOHNSON, R. L., "Friction, Wear, and Evaporation Rates of Various Materials in Vacuum to 10^{-7} mm Hg," *ASLE Trans.* **5**, 8-23 (1962).
12. BUCKLEY, D. H., and JOHNSON, R. L., "Gallium Rich Films as Boundary Lubricants in Air and in Vacuum to 10^{-9} mm Hg," presented at ASLE-ASME Lubrication Conference, Pittsburgh, Pennsylvania, October, 1962.
13. JOHNSON, V. G., and VAUGHN, G. W., "Investigation of the Mechanisms of MoS_2 Lubrication in Vacuum," *J. App. Phys.* **27**, 1173-1179 (1956).
14. HANSEN, M., "Constitution of Binary Alloys," 2nd ed., McGraw-Hill, New York, 1958.
15. KING, R. F., and TABOR, D., "Effect of Temperature on the Mechnical Properties and the Friction of Plastics," *Proc. Roy. Soc.* **B66**, 728-736 (1953).
16. CLAUSS, F. J., "Lubricants and Self-Lubricating Mechanisms for Spacecraft Mechanisms," Lockheed Missiles and Space Division Tech. Report 894812, Sunnyvale, California, 1961.
17. RITTENHOUSE, J. B., JAFFE, L. D., NAGLER, R. G., and MARTENS, H. E., "Friction Measurements on a Low Earth Satellite," Technical Report No. 32-402, Jet Propulsion Laboratory, Pasadena, California.

DISCUSSION

P. M. KU (*Southwest Research Institute, 8500 Culebra Road San Antonio 6, Texas*):

The authors are to be commended for publishing this very interesting and informative paper. The paper is significant in three respects. First, it describes the successful development of a compact and rugged device for conducting friction measurements in a spacecraft in flight. This is an accomplishment of no small order. Secondly, it shows that laboratory vacuum tests, conducted properly, correlate quite well with flight tests. Thirdly, it demonstrates that at moderate temperatures, effective lubrication can be maintained over a considerable length of time in a vacuum environment of 10^{-6}–10^{-8} torr, using conventional solid lubricants and without resorting to elaborate lubricating techniques.

In recent years, the effects of the rigors of outer space on bearing friction and life have been matters of grave concern. There is little doubt that bearings operating in high vacuum will eventually lose their lubricant and be stripped of oxide and other surface films. The question is really how long a lubricated bearing can operate in high vacuum, before such adverse effects take place. In the Ranger 1 tests, the lubricated pairs maintained constant, low friction for at least 22 hours of test duration, and this was limited by the life of the power supply. It would have been most interesting if the test duration could have been extended to provide some information on the useful life of the sliding pairs.

In tests conducted in our own laboratory, at comparable temperatures and at a pressure approximately one decade lower, many unlubricated sliders and ball bearings (without initial outgassing and bakeout) operated for more than 10 days without experiencing a rise in friction. Sliders and bearings lubricated with MoS_2-based lubricants and PTFE have maintained constant, low friction for periods up to and some exceeding 6 months. These results seem to indicate that reasonably long life is obtainable with rather conventional solid lubricants, without resorting to trick designs, in a vacuum of 10^{-7}–10^{-9} torr at moderate temperatures. For still higher vacuums, it would seem that reasonable life can also be realized if the bearing is shielded so as to retard lubricant loss.

The authors are obviously keenly aware of the problems associated with friction measurements in vacuum environment. They have taken great pains to minimize cross-contamination of the test specimens and have carefully considered the sources and probable magnitudes of measurement errors. There is no intention to question the authors' results. Although it is difficult to believe that cross-contamination from, say, the volatile constituents of the grease could have been completely eliminated, nevertheless, the

friction values for most unlubricated pairs are, in general, in qualitative agreement with our laboratory vacuum results under comparable test conditions. The very low friction observed by the authors for PTFE on metal and for metals lubricated with a bonded MoS_2 film is most intriguing. In our laboratory tests referred to, the coefficient of friction for such sliding pairs was of the order of 0.15–0.25, depending upon the metals used. Referring to Figs. 14 and 15, a coefficient of friction of —0.05 is shown. It does not appear that a *negative* coefficient of friction can be the result of scatter. Could it possibly be due to some malfunctioning of, say, the strain gage circuit used in friction measurement? Errors of this type could show up more noticeably when the friction is low but would hardly be noticeable when the friction is high.

ROBERT L. JOHNSON (*NASA, Lewis Research Center, 21000 Brookpark Road, Cleveland, Ohio*):

The paper describes the results of a significant and stimulating effort in friction research. Preparing this experiment alone is a difficult task that deserves special commendation.

Deficiencies in planning and conducting the experiments are a result of the authors' succumbing to the temptation to obtain too much data on too varied types of materials. The low friction obtained with 440-C is a very strong indication of surface contamination. Most probably the contamination was from condensation of the volatile constituents of the grease that was used in a concurrent run. Additional contamination could also have its origin from the polytetrafluoroethylene used in other experimental couples or in insulating the maze of electric wires surrounding the experiment. Condensation material obtained from such fluorinated polymers has been shown to have lubricating capabilities. Although the low friction values obtained with 440-C make it most suspect of contamination, it is likely other couples were also affected.

The use of average friction coefficients in discussion to compare data in air and in vacuum is meaningless. There is no reason to expect any consistent influence of the different environments within the wide group of materials. This is particularly true for noble metals grouped with metals that have very stable and tenacious oxide films.

AUTHORS' CLOSURE:

The authors thank Mr. Ku for his interesting discussion of our paper. We were indeed fortunate that the device operated for 22 hours in space. The actual design lifetime was 10 hours. We recognize that longer term data on friction of sliding pairs in space is required. The successful operation of moving parts for long periods on such satellites as Tiros and the Venus interplanetary probe, Mariner II, show that properly selected materials in contacting pairs with low vapor pressure lubricants have given a reasonable solution to the problem of friction and lubrication is space. There is no doubt, however, that more work is needed to assure the reliability of more complex mechanisms contemplated for future manned and unmanned spacecraft.

We are gratified to learn that some of our measurements agree with those made in Mr. Ku's laboratory. With regard to the negative values of the coefficients of friction obtained for some of the PTFE specimens, we believe that these result from scatter ("noise") arising in the electronic portion of the experimental apparatus and in the telemetry system. For example, a demodulated telemetry subcarrier frequency of 583 cycles per second corresponded nominally to a friction coefficient of 0.00, and 581 cycles per second to a coefficient of 0.04. With a true coefficient of 0.04, an electrical scatter of 3 cycles per second could cause an observed frequency of 584 cycles per second; this would be read as a negative coefficient. Errors of this sort were reduced but not eliminated by in-flight calibration; they are included in the estimate of over-all measurement error given in the paper.

We thank Mr. Johnson for his analytical discussion of our paper. We would like to comment, however, that the number and variety of materials incorporated into the experimental assembly were chosen with the thought in mind that only a limited number of spacecraft flights were available for this type of experiment, so it was therefore considered expedient to obtain a maximum amount of data from the minimum number of tests. It is true that contamination of the friction surfaces may have occurred by condensation of organics from other portions of the experimental equipment. We think it is unlikely that this occurred to an extent sufficient to affect the experimental results. The high stability of polytetrafluoroethylene in vacuum is well established (*C1–C6*). Moreover, when this polymer does decompose, the product is essentially 100% monomer, which would not condense at the temperature and pressure of the experiment. In the flight experiment replicates were run on several disks and riders. The greased disks were not visible from the 440C riders or disks. The indirect paths, via mutually visible surfaces, along which condensation and resublimation would have to occur, were different for the different replicates. It seems, therefore, most unlikely that transfer of grease constituents took place reproducibly to the 440C disks and riders and did not take place to the intervening or adjacent disks and riders of other materials.

The usefulness of average friction coefficients in comparing data is a matter of opinion. We see no reason to rule out, a priori, the possibility that metals, as a class, will behave differently than polymers, or that lubricated surfaces will behave differently than unlubricated.

REFERENCES

C1. FLORIN, R. E., WALL, L. A., BROWN, D. W., HYMO, L. A., and MICHAELSEN, J. D. Factors Affecting the Thermal Stability of Polytetrafluoroethylene," *J. Res. Natl. Bur. Std.* **53**, 121-130 (1954).

C2. MADORSKY, S. L., HART, V. E., STRAUS, S., and SEDLAK, V. A., "Thermal Degradation of Tetrafluoroethylene and Hydrofluoroethylene Polymers in a Vacuum," *J. Res. Natl. Bur. Std.* **51**, 327-333 (1953).

C3. MADORSKY, S. L., and STRAUS, S., "Thermal Degradation of Polytetrafluoroethylene as a First-Order Reaction," *J. Res. Natl. Bur. Std.* **64A**, 513-514 (1960).

C4. WRIGHT, W. W., "Thermal Degradation of Fluorine-Containing Polymers, Polyphenylene Oxide and Polyphenylenes, High Temperature Resistance and Thermal Degradation of Polymers," pp. 248-269, Society of Chemical Industry Monograph No. 13, London, 1961.

C5. SIEGLE, J. C., and MUUS, L. T., "Pyrolysis of Polytetrafluoroethylene," presented to American Chemical Society, September, 1956. (Abstract No. 16, p. 8S, in Abstracts of Papers of 130th Meeting.)

C6. SIEGLE, J. C., MUUS, L. T., LIN, T. P., and LARSEN, H. A., "Molecular Structure of Perfluorocarbon Polymers. II. Pyrolysis of Polytetrafluoroethylene (submitted to *J. Am. Chem. Soc.*).

ASLE TRANSACTIONS 6, 178-191 (1963)

Lubrication of Ball Bearings for Space Applications

By W. C. YOUNG,[1] F. J. CLAUSS,[2] and S. P. DRAKE[3]

The operation of equipment on satellites and space probes has placed new demands on lubricants. To evaluate lubricants for these uses, the authors have conducted a program of testing lubricants and instrument-size ball bearings in pressures of 10^{-7}–10^{-9} torr.

Four classes of lubricants have been tested. Bearings with the best oil and grease lubricants have operated for over 1 year. The most promising tests with special retainers have lasted from 3 to 6 months. Tests with dry-film lubricants have shown poor reproducibility and short lifetimes, e.g., the maximum was 3 months.

Introduction

THE operation of equipment in space has placed new demands on lubricants. Lubricants must now operate in a new environment. They must provide long term lubrication for unattended equipment of which high reliability is required. They must do this in a system when minimum weight and complexity is required.

The parts of space environment that affect lubrication are: (1) zero gravity, (2) radiation, and (3) ultrahigh vacuum.

Zero gravity eliminates the use of gravity feed systems and some pressurization systems, i.e., reservoirs cannot be directly gas pressurized so the pressure must be applied through a bladder or piston. Hence, it is desirable to use lubricants which can function satisfactorily without replenishment. This is also desirable from a weight and complexity standpoint.

Radiation sources are the Van Allen belts, solar radiation, and in-flight reactors. All organic and semiorganic materials are adversely affected by radiation, so this factor must be evaluated both in the choice of lubricants and in the choice of bearing materials when plastics are involved. The effects vary with the material as is shown in Table 1.

The amount of annual radiation on the surface of a vehicle in polar orbit at a 2300-mile altitude is 2×10^9 ergs per gram (carbon) (*3*). The annual dosage inside a 0.10-inch aluminum skin is 6×10^6 ergs per gram (C). The annual radiation includes the Van Allen belt, and solar and cosmic radiation.

TABLE 1

Effect of Radiation on Materials

Material	Radiation dosage required for threshold damage (ergs/gm (C)[a] (*1, 2*)
Polyphenyl ethers	1×10^{11}
Mineral oils	5×10^{10}
Dimethyl silicones	1×10^{8}
Methyl phenyl silicones	1×10^{10}
Chlorinated silicones	5×10^{9}
Dibasic acid esters	5×10^{10}
Silicate and disiloxane esters	1×10^{10}
Phenolic (filled)	3×10^{10}
Polyester	9×10^{9}
Polytetrafluoroethylene	2×10^{6}

[a] Ergs per gram (carbon) refers to the energy absorbed by the carbon-walled, CO_2-filled ion chamber selected as the standard. It is indirectly a measure of the field and not a measure of the energy absorbed by the sample.

The above table is for static irradiation in air.

Most lubricants function satisfactorily in this environment. With the use of in-flight reactors, the radiation will be dependent upon the reactor, the shielding, and the location of the lubricated part. Testing is required for lubricants operating in this area.

The high vacuum of space (e.g., the pressure at 500 miles altitude is between 10^{-9} and 10^{-10} torr) results in the following: (1) increased rates of vaporization of volatile lubricants, (2) creepage of oil along surfaces, and (3) cold welding of metals due to loss of surface films.

This paper reports on the authors' evaluation of lubricants that must function in space for 1 or more years. In the first evaluation of materials in this environment, bearings were operated at 10^{-7}–10^{-9} torr without replenishment of the lubricant. Tests are being prepared in which the lubricant will be evaluated while operating under vacuum and radiation.

Contributed by the ASLE Technical Committee on Bearings and Bearing Lubrication and presented at the Annual Meeting of the American Society of Lubrication Engineers held in St. Louis, Missouri, May, 1962.

[1] Senior Scientist, Lockheed Missiles & Space Company, Palo Alto, California.

[2] Staff Scientist, LMSC, Palo Alto, California.

[3] Research Laboratory Analyst, LMSC, Palo Alto, California.

Equipment and pretest preparation

Lubricants and Bearings

The following types of lubricants are being evaluated: (1) oil lubricants, (2) grease lubricants, (3) molybdenum disulfide based lubricants, and (4) special retainer materials.

Table 2 lists the seven types of R-3 size ($\frac{3}{16}$-inch bore, $\frac{1}{2}$-inch outside diameter) ball bearings that were used; their use was dependent upon the lubricant to be tested.

Table 2
Types of Test Bearings

Type	Lubricant	Bearing material	Bearing description
1	Oil and grease	440C	Deep groove, ribbon retainers, double shielded
2	Oil and grease	52100	Same as above
3	Oil	440C	Deep grove, paper base phenolic retainers, double shielded
4	Oil	52100	Same as above
5	MoS_2	440C	Deep groove, ribbon retainers, unshielded
6	Special retainer	440C	Angular contact, double shielded
7	Special retainer	440C	Angular contact, unshielded

Run-in Procedure

Before applying the oil or grease lubricants to bearings with ribbon retainers, the bearings were given an initial run-in with a light oil at 8000 rpm for 24 hours and then ultrasonically cleaned. The amount of lubricant applied varied from 25 to 50 mg for oils and 50–100 mg for greases.

Bearings with phenolic retainers were not run-in before lubrication. The retainer was vacuum impregnated with the test oil at room temperature and approximately 50 mg of oil was used although the weight ranged from 20 to 90 mg.

In testing the molybdenum disulfide films, unassembled bearings were supplied to the lubricant manufacturer for application of the film, and the bearings were then assembled by the bearing manufacturer. The bearing to which the lubricant was applied was operated back and forth slowly by hand and blown out with clean, dry gas prior to testing; this procedure was repeated several times. The bearings were then operated at 4 rpm for approximately 10 minutes, stopped, blown out and run at 4 rpm in the opposite direction for 10 minutes; this operation was repeated until the bearings had run from 30 to 60 minutes. The same run, blow out, reverse procedure was followed at 8000 rpm for 20–30 minutes.

Bearings with special retainer materials were not given a run-in.

The bearings were installed on small induction motors and these units were mounted in vacuum chambers. Both bearings on any one motor received the same lubricant.

Test Motors

Figure 1 shows a disassembled motor of the type originally used. The motor shaft was machined to $\frac{3}{16}$-inch diameter; the bearing housings were opened to expose the bearings to the vacuum. The exposed stator windings

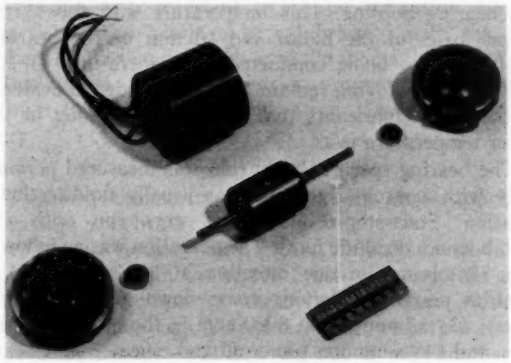

Fig. 1. Test motor of original type

can be seen in the photograph. In the absence of convection cooling, the motors overheated when operated above 100 volts in vacuum. Overheating caused excessive outgassing and breakdown of the varnish insulation which, in turn, short circuited the stator windings. Thereafter, the motor voltage was kept in the range of 70–90 volts during operation in vacuum. This motor was not used for elevated temperature testing.

Figure 2 shows the motor now being used as well as the motor just described. It has a "canned" stator to

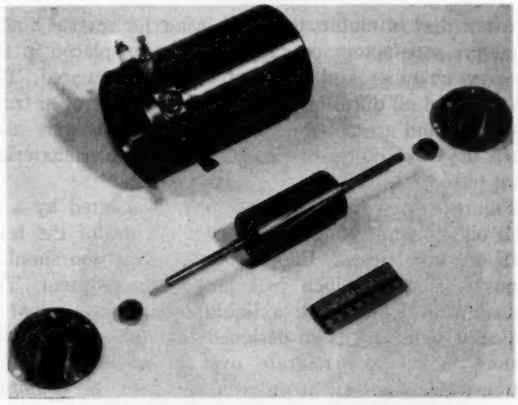

Fig. 2. Test motor of latest design

prevent outgassing and employs polytetrafluoroethylene (PTFE) insulation to allow higher temperature use. It was successfully operated in vacuum at 300 F for over 2000 hours.

The radial load on the bearings was that of the rotor. The original motor had a radial loading of 155–165 gm (5.6 oz) while the newer motor ranged from 270 to 280 gm (9.7 oz). No axial load was used except in some tests with the special retainers. The bearings for testing the special retainers were angular contact type bearings, and axial loads of ¼ and 1 lb were used with them.

The temperature in most tests was 160–200 F, as measured by iron-constantan thermocouples attached to the bearing housing. This temperature was due to the power losses of the motor and friction of the bearing. Tests are also being conducted at temperatures of 225 and 300 F employing radiant heating in order to evaluate further those lubricants that appeared promising in the lower temperature tests.

The bearing speed of 8000 rpm was measured periodically with a strobe light and was usually unidirectional rotation. Start-stop-reverse tests were run with the molybdenum disulfide films. The operation was as follows: (1) 52 minutes in one direction at 8000 rpm, (2) 8 minutes power off (giving coast down and some stop time), (3) 52 minutes at 8000 rpm in the opposite direction, and (4) 8 minutes power off and repeat.

Evaluation Criteria for Lubricants

The two criteria used to evaluate bearing lubricants were the coast time and the lifetime. The coast time was the time required to slow down from 8000 rpm to a full stop when the power to the motor was cut off. This was an indication of the running torque of the pair of bearings and was determined about once a week. Coast times are given in the data tables (1) when there was a change in the weekly determination, (2) at approximately every 500 hours for short tests, or (3) at every 1000-hour period for the longer ones.

Vacuum Systems

After a set of motors operated in air for several hours, to assure satisfactory operation, they were placed in the vacuum chamber and the system was evacuated. The system used oil diffusion pumps and liquid nitrogen traps when oils and greases were tested; ion pumps were used when dry film lubricants and special retainer materials were tested.

Figure 3 shows a typical chamber evacuated by a 6-inch oil diffusion pump and used for some of the tests with oils and greases. Eight motors can be run simultaneously in the 18-inch bell jar of this system. The system is provided with a liquid nitrogen trap that is optically tight and is so designed that oil from the diffusion pump must migrate over a surface at liquid nitrogen temperature in order to get into the chamber. Pressure is measured with a modified Bayerd-Alpert ionization gauge that is connected to the baseplate by ⅝-inch ID tubulation. This particular unit normally sustains a pressure of 2 to 3×10^{-8} torr with the eight motors all in operation; for short periods, it has operated at 9×10^{-9} torr.

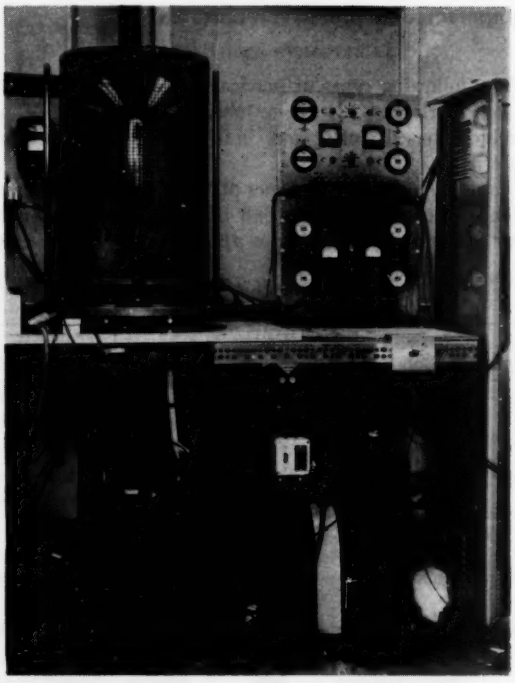

FIG. 3. Test set-up with oil diffusion pump

Also used are several systems that are evacuated by oil diffusion pumps and maintain pressures during testing of 1×10^{-9} torr (6-inch DP, stainless steel chamber) to 2×10^{-7} torr (4-inch DP, glass bell jar, high-temperature tests with greases). The lowest pressure we have maintained for periods of several hours or more has been 6×10^{-10} torr.

Figure 4 shows a typical chamber evacuated by an ion pump. Several sizes of chambers and pumps have been used, ranging from 6-inch ID by 10 inches long to 14-inch ID by 20 inches long stainless steel chambers and 90–360 liters per second pump speeds.

Lifetime

The lifetime was the operation time until the increase in bearing torque was sufficient either to stall the motor or to prevent its being restarted (following measurement of the coast time). Stalling doubled the motor current and blew the circuit fuse, thereby cutting off power to the motor and its timer.

Lubricant evaluation

Tests with Oils

Table 3 gives results for four oils tested in air and in vacuum. All oil lubricated bearings are still operating in air after almost 15 months, whereas only two have approached this time in vacuum.

Table 4 summarizes the results of testing oil lubricants to 1 February 1962.

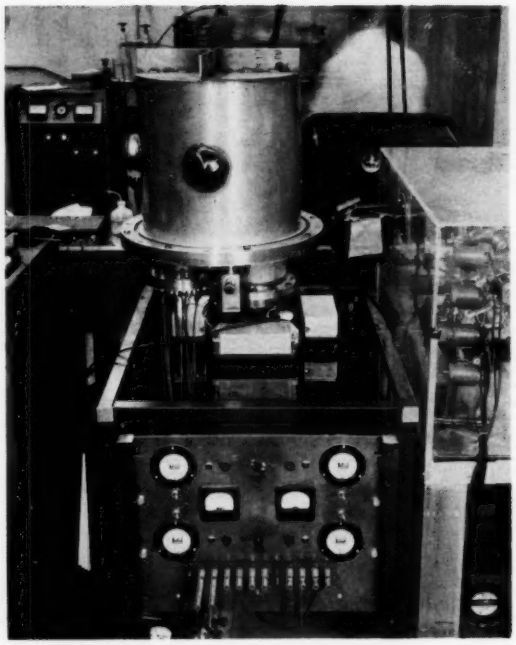

FIG. 4. Test set-up with ion pump

Tests were run with chlorophenyl methyl polysiloxane "as received" and after removal of the 50% more volatile fraction by distillation. These tests were run to determine whether removal of the more volatile material would improve the operation lifetime in vacuum. The unstripped material gave better times and is still operating after 7428 hours; the stripped material failed at 3335 hours. Tests are being conducted to determine if this failure was due to the higher running temperature produced by the more viscous, stripped material or due to the bearing material (the stripped material was run in a 440C stainless steel bearing; the unstripped in a 52100 chrome steel bearing). The long operation time of over 10,665 hours in air indicates that the lubricating properties were not affected by distillation.

Bearings with machined retainers of paper base phenolic had longer operating times than those with steel ribbon retainers. For example, chlorophenyl methyl polysiloxane failed after 4574 hours in bearings with ribbon retainers but was still operating after 7428 hours in bearings with the phenolic retainers.

The predominant method of failure was the loss of lubricant with resultant wear and formation of wear particles. The bearings were lubricated with the polyphenyl ether and failed at 2476 hours; the lubricant decomposed, the decomposition products depositing between the shield and the outer race, leaving the bearing dry.

TABLE 3

Lifetimes of Selected Oil Lubricants

Oil	Lifetime[a] Air (hr)	Lifetime[a] Vacuum (hr)
Chlorophenyl methyl polysiloxane, 50% more volatile fraction removed by distillation	10,665[b]	3355
Chlorophenyl methyl polysiloxane, as received	—	7428[b]
Petroleum oil used for mechanical vacuum pumps	10,701[b]	9847[b]
Diphenylbis-*n*-dodecyl silane	10,679[b]	1367
Mixed isomeric five ring polyphenyl ether	10,700[b]	2476

[a] One year = 8760 hours.
[b] Still running.

TESTS WITH GREASES

Table 5 summarizes the tests with grease lubricated bearings to February, 1962.

The best results with a grease lubricant occurred in a test lasting 9613 hours at 175 F before failure; the grease used was chlorophenyl methyl polysiloxane thickened with a lithium soap. Additional tests with this material are being conducted at 225 and 300 F with another test at 160 F for comparison and are still running after 1400 hours.

Next in performance was a synthetic wide-temperature range grease, methyl phenyl polysiloxane with a dye thickener, which is still operating after 4568 hours.

The predominant cause of failure was the loss of the oil, resulting in clogging of the bearing by the thickener. A typical failure of a grease lubricated bearing is shown in Fig. 5; the grease was the lithium soap thickened polysiloxane and the failure time was 9612 hours. The darkened and hardened condition of the grease, which is apparent, causes the bearing to freeze or require a greatly increased driving torque.

TESTS WITH MOLYBDENUM DISULFIDE FILMS

Table 6 summarizes the results of testing bearings lubricated with bonded films of molybdenum disulfide.

FIG. 5. Failed grease lubricated bearing

TABLE 4
Tests with Oil Lubricants

Lubricant	Brg. type[a]	Initial wt. lub. (mg)	Rotor wt. (gm)	Brg. housing temp. (°F)	Press. (torr)	Coast time (min)	(sec)	(hr)	Results
Chlorophenyl methyl polysiloxane	2	26	156	160–190	6×10^{-6} to 4×10^{-7}				Failed at 4574 hr. Bearings had almost complete loss of lubricant.
Same as above	4	28.3 20.6	162	144–180	2×10^{-7} to 2×10^{-8}	2	54 after	108	Still running after 7428 hr.
						3	14	916	
						3	10	2452	
						3	52	3773	
						4	23	4741	
						5	25	5711	
						4	55	6881	
						5	8	7428	
2/3 chlorophenyl methyl polysiloxane, 1/3 molybdenum disulfide	1	51.9 53.8	156	170–212	760 to 2×10^{-6}	0	50	47	Failed at 177 hr. Both bearings dry.
						0	40	98	
Chlorophenyl methyl polysiloxane, 50% more volatile, fraction removed by distillation	3	61.7 62.0	157	170–200	4×10^{-7} to 3×10^{-8}	1	56	759	Failed at 3335 hr.
						1	6	1342	
						9	14	1577	
						9	19	2256	
						9	17	3150	
Same as above	3	54.4 52.9	159	102–140	760	0	49	1565	Still running after 10,665 hr.
						2	27	3051	
						4	3	4661	
						4	7	6176	
						4	10	8749	
						3	24	9826	
						3	40	10,665	
Diphenylbis-*n*-dodecylsilane	3	31.0 33.0	158	106–140	760	1	42 after	1601	Still running after 10,679 hr.
						1	34	2610	
						1	34	3877	
						4	20	5011	
						4	5	6000	
						4	18	7054	
						5	57	7992	
						6	21	9123	
						5	48	9840	
						6	14	10,679	
Same as above	3	30.9	157	166–175	4×10^{-7} to 6×10^{-8}	2	10	885	Failed at 1367 hr. Both bearings dry; one had black debris.

[a] Description of bearing types is given in Table 2.

[a] Description of bearing types is given in Table 2.

TABLE 4, *continued*

Lubricant	Brg. type[a]	Initial wt. lub. (mg)	Rotor wt. (gm)	Brg. housing temp. (°F)	Press. (torr)	Coast time (min)	Coast time (sec)	Coast time (hr)	Results
Hexa butoxy disiloxane	1	25.4 23.1	162	130–215	6×10^{-6} to 5×10^{-7}	2 3 6	27 4 45	3235 3883 4052	Failed at 4244 hr.
Same as above	3	18.4 11.9	158	135–175	8×10^{-7} to 3×10^{-8}	2 6 10 12 2 3 4	24 34 26 39 53 6 1	19 212 1323 2209 3412 4534 5172	Failed at 5309 hr. Both bearings filled with black dust.
85% hexa butoxy disiloxane, 15% dioctyl sebacate	3	28.2 19.2	156	175–180	2×10^{-6} to 5×10^{-7}	0 1	58 1 after	131 298	Failed at 468 hr. Both bearings showed loss of lubricant and had wear particles.
Silicone oil used for diffusion pumps	4	24.8 24.8	157	163–190	2×10^{-7} to 4×10^{-8}	10 4 9 7 7 5 4 3	5 after 48 2 37 55 0 2 35 after	107 268 461 1248 2070 2237 2382 2527	Failed at 2603 hr. Almost complete loss of lubricant; both bearings filled with wear particles.
Tri aryl phosphate	2	42.7 29.1	162	184–190	8×10^{-6} to 2×10^{-6}	1	47 at start		Failed at 164 hr. One bearing had balls badly worn; other was almost frozen. Both had almost complete loss of lubricant.
Same as above	3	30.3 27.9	166	158–176	2×10^{-6} to 2×10^{-7}	0	55 after	167	Failed at 763 hr. Both bearings filled with wear debris; both had almost complete loss of lubricant.
Mixed isomeric five ring polyphenyl ether	3	72.4 69.0	162	151–170	4×10^{-6} to 6×10^{-8}	1 1 6 4 1	34 42 17 31 38 after	1336 1815 1983 2152 2344	Failed at 2476 hr. Both bearings discolored and had complete loss of lubricant. One bearing packed with wear debris.

TABLE 4, *continued*

Lubricant	Brg. type[a]	Initial wt. lub. (mg)	Rotor wt. (gm)	Brg. housing temp. (°F)	Press. (torr)	Coast time (min)	Coast time (sec)	Coast time (hr)	Results
Mixed isomeric five ring polyphenyl ether	3	62.6 59.8	157	110–140	760	0	34	after 1601	Still running after 10,700 hr.
						0	33	2610	
						0	31	3710	
						0	23	5032	
						0	29	6021	
						0	27	7075	
						0	25	9144	
						0	28	9861	
						0	55	10,700	
Petroleum oil used for mechanical vacuum pumps	3	49.5 58.2	159	167–200	5×10^{-6} to 1.5×10^{-8}	0	16	1313	Still running after 9847 hr.
						0	18	2130	
						0	18	3042	
						0	16	4003	
						0	15	4990	
						0	14	5976	
						0	13	7083	
						0	16	7914	
						0	18	9300	
						0	15	9847	
Above petroleum oil dissolved in 20% xylene	1	46.0 42.8	166	164–197	7×10^{-6} to 8×10^{-8}	0	43	470	Still running after 4263 hr.
						0	43	869	
						0	40	2079	
						0	24	3423	
						0	34	4263	
Petroleum oil used for mechanical vacuum pumps (same oil as above)	3	49.2 51.7	157	106–135	760	0	8	1601	Still running after 10,701 hr.
						0	8	2249	
						0	26	3421	
						0	29	4529	
						0	27	5852	
						0	39	7075	
						0	36	8013	
						0	33	9145	
						0	33	9862	
						0	32	after 10,701	

TABLE 5
Tests with Grease Lubricants

Lubricant	Brg. type[a]	Initial wt. lub. (mg)	Rotor wt. (gm)	Brg. housing temp. (°F)	Press. (torr)	Coast time (min)	(sec)	(hr)	Results
Chlorophenyl methyl polysiloxane thickened with lithium base soap	1	91.4 100.6	160 and 158	132–220	2×10^{-6} to 2×10^{-8}	1	53 after	2233	Failed at 9612.5 hr. One bearing still operable with low torque, turnable but grease had turned brown; other bearing was almost frozen and grease was hard and black.
Same as above	1	55.0 64.7	276	155–165	2×10^{-6} to 4×10^{-7}	3 2 4	31 57 8	153 893 1411	Still running after 1411 hr.
Same as above	1	67.3 56.0	273	221–225	2×10^{-6} to 4×10^{-7}	2 2 5	44 18 2	153 885 1403	Still running after 1403 hr.
Same as above	1	54.4 56.4	277	285–300	2×10^{-6} to 4×10^{-7}	3 2 2	2 24 10	153 893 1412	Still running after 1412 hr.
Phenyl methyl polysiloxane with dye thickener	1	110.9 96.1	157	160–180	9×10^{-8}	0 2 2 1 3 5 4	34 10 36 55 3 12 44 after	2 599 953 2013 2912 3896 4369	Still running after 4568 hr.
MIL-G-3278 grease	1	96.8 110.9	159	140–190	3×10^{-7} to 4×10^{-8}	0 0 1 4 5	49 after 37 10 28 27 after	2 309 863 1580 2420	Still running after 2420 hr.

[a] Description of bearing types is given in Table 2.

The best performance results were obtained in a test with a film of molybdenum disulfide bonded with sodium silicate to the races and retainers. This test reached 2213 hours before failure.

Poor reproducibility was characteristic of tests with molybdenum disulfide films. A test with a sodium silicate bonded MoS_2 film ran 1862 hours, while a second test with the same material and the same pretreatment ran 28 hours. Only one bearing failed in either case. In other tests with sodium silicate bonded films, failure times of 1796 and 25 hours were recorded for the same film with the same pretreatment.

In most tests, the lubricant was applied to only the races and retainers, while in others it was applied to the races, retainers, and balls. Tests were continued in an effort to evaluate which was the better application; insufficient conclusive data are available at this time.

The predominant cause of failure was wear-through of the film resulting in wear of the retainer and enlargement of the ball pocket. The retainers broke in some instances while in others a few of the balls came out of the retainers. The typical failure shown in Fig. 6 is of a bearing lubricated with a film applied to the races, retainers, and balls. The failure occurred after 1533 hours. One bearing retainer was split and the balls and races were shiny, indicating loss of lubricant. The other bearing was in satisfactory condition and could have continued operating.

In start-stop-reverse tests, the best results were also obtained with films bonded with sodium silicate. Bearings so lubricated ran 772 hours with 771 reversals, or approximately one-third of their life of 2213 hours for unidirectional operation. On the other hand, an epoxy bonded film that operated 308 and 467 hours unidirectionally operated for 771 hours with 771 reversals, under start-stop-reverse conditions.

Tests with Special Retainer Materials

Table 7 gives the results of testing bearings with special retainer materials. These materials are plastics

TABLE 6
Tests with MoS_2 Based Lubricants

Lubricant	Brg. type[a]	Rotor wt. (gm)	Brg. housing temp. (°F)	Press. (torr)	Coast time (min)	Coast time (sec)		Coast time (hr)	Results
Sodium silicate bonded molybdenum disulfide, applied to races and retainers only	5	159	160–180	8×10^{-6} to 9×10^{-8}	1	7	after	5.6	Failed at 2213 hr.
					6	17		771	Both bearings contained black wear particles. Balls and retainers worn; ball pockets badly worn
					4	49		1419	
					5	56		2021	
					4	31		2181	
Same as above	5	159	140–185	2×10^{-6} to 2×10^{-7}	6	53		82	Failed at 772 hr. Debris in raceways caused high torque. Start-stop-reverse test with 771 reversals.
					5	18		223	
					2	41		391	
					3	0		726	
Sodium silicate bonded molybdenum disulfide applied to races and retainers after special pretreatment	5	157	160–170	8×10^{-6} to 8×10^{-7}	5	14		5.6	Failed at 1862 hr. One bearing still satisfactory.
					3	39		753	
					4	21		1232	
					3	56		1761	
Same as above	5	158	RT–140	760 to 2×10^{-7}					Failed at 28 hr. One bearing frozen, other in fair condition.
Sodium silicate bonded molybdenum disulfide applied to races and retainers after grit blasting and special surface pretreatment	5	157	150–158	8×10^{-6} to 8×10^{-7}	4	14		5.6	Failed at 1796 hr.
					6	50		656	
					4	30	after	1664	
Same as above	5	157	RT–150	760 to 2×10^{-7}					Failed at 25 hr. One bearing frozen; other in fair condition.
Epoxy bonded molybdenum disulfide applied to races and retainers	5	162	90–160	5×10^{-6} to 1×10^{-7}					Stopped at 467 hr. One bearing failed at 308 hr; it had orange discoloration over surface. Second bearing failed at 467 hr; retainer was badly worn.
Same as above	5	160	140–170	5×10^{-6} to 2×10^{-7}	7	24	after	82	Failed at 771 hours. One bearing in fair shape; other was almost frozen and retainer badly worn. Stop-start-reverse test with 771 reversals.
					5	56		725	
Same as above	5	275	RT–140	760 to 2×10^{-6}	1	1		66	Failed at 88 hr. One bearing still in fair condition, other was frozen with balls chewed up.
Molybdenum disulfide bonded to races and retainers with proprietary coating	5	275	150–170	6×10^{-7} to 2×10^{-7}	15	50		144	Failed at 457 hr.
Molybdenum disulfide bonded to races, retainers and balls with proprietary coating	5	275	160–184	6×10^{-7} to 4×10^{-8}	30	27		144	Failed at 1533 hr.
					7	42		693	
					8	20		1366	
					2	50	after	1533	

[a] Description of bearing types is given in Table 2.

TABLE 7
Tests with Special Retainers

Lubricant	Brg. type[a]	Rotor wt. (gm)	Axial load (lb)	Brg. housing temp. (°F)	Press. (torr)	Coast time (min)	Coast time (sec)		Coast time (hr)	Results
Retainers of reinforced polytetrafluoroethylene	7	275	No load for first 518 hr; 1 lb for remainder of test (2662 hr)	145–170	4×10^{-6} to 6×10^{-8}	18	35	after	279	Failed at 3180 hr. Both retainers badly worn.
						21	30		446	
						8	42		547	
						3	1		835	
						8	44		1355	
						11	28		2311	
						8	42		2863	
						2	18		3150	
Retainers of 60% polytetrafluoroethylene and 40% glass fibers with molybdenum filler	7	275	1	RT–140	760 to 4×10^{-6}					Failed at 27.5 hr. Retainer material flaked off and caused balls to jam.
Retainer of 60% polytetrafluoroethylene, 40% glass fibers with molybdenum disulfide filler	7	275	¼	165–190	3×10^{-7} to 6×10^{-8}	1	25		255	Still running after 4353 hr.
						0	49		923	
						1	29		1882	
						1	49		2961	
						1	59		3512	
						2	18		4353	
Same as above	7	275	¼	165–190	3×10^{-7} to 6×10^{-8}	1	25		255	Still running after 3681 hr.
						0	49		923	
						1	29		1882	
						1	49		2961	
						1	59	after	3512	
Retainer of sintered nylon with molybdenum disulfide	6	275	1	RT–135	760 to 4×10^{-6}					Failed at 27 hr. Both retainers were broken and flakes from retainers had jammed between races and balls.
Retainer of sintered nylon with molybdenum disulfide	6	275	¼	RT	760 to 4×10^{-7}					Failed at 43 hr. One retainer was broken. Both had flakes causing jamming of balls and races.
Porous sintered nylon vacuum impregnated with silicone oil	6	275	1	RT–190	760 to 4×10^{-6}	0	30	after	28.5	Failed at 160 hr. One bearing half destroyed. Both fell apart when torque measurements were made after the test.
Same as above	6	275	¼	175–180	3×10^{-7} to 9×10^{-8}	1	0		255	Failed at 331 hr. One retainer completely destroyed, other in fair shape.
Retainer of pressed graphite impregnated with silver	6	275	¼	RT–184	76 to 2.5×10^{-7}	2	43		71.4	Failed at 140.6 hr.
Retainer of 55% sintered bronze, 27% polytetrafluoroethylene and 18% molybdenum disulfide	6	275	¼	170–200	1×10^{-7} to 5×10^{-8}	1	43		71	Still running after 1984 hr.
						5	44		593	
						5	35		1143	
						5	4		1984	
Retainer of 50% bronze, 50% molybdenum disulfide	6	275	¼	170–190	1×10^{-7} to 5×10^{-8}	4	31		72	Still running after 1984 hr.
						4	17		592	
						4	12		1143	
						5	0		1984	

[a] Description of bearing types is given in Table 2.

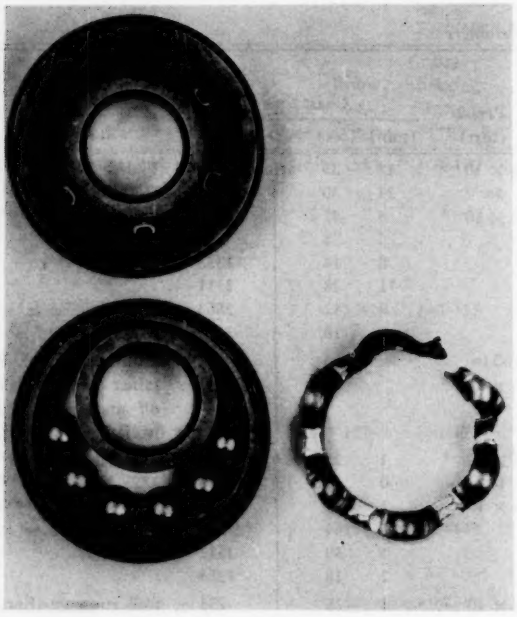

FIG. 6. Failed molybdenum disulfide lubricated bearings

or soft metals which are completely or partially self-lubricating; in addition, some contain liquid or solid lubricants.

The best results have been with two reinforced PTFE compositions, one of which contained molybdenum disulfide. The best of the two was a 60% PTFE-40% glass fiber composition, containing MoS_2, which is still running after 4353 hours (with an axial loading of ¼ lb). Poor times have resulted with the oil-impregnated materials as indicated by a 331-hour operation with an oil impregnated porous nylon.

Special retainer materials are sensitive to axial loading. As an example, another test with the 60% PTFE-40% glass fiber composition, containing MoS_2, lasted only 27.5 hours with a 1-lb load. The best results with a 1-lb load were obtained with a reinforced PTFE retainer. This material ran 3180 hours before failure; the first 518 hours were with no load, the remainder was with a 1-lb loading. This was the second best result with a reinforced PTFE material.

The cause of failure was wear of the ball pocket. In some cases, only enlargement of the pocket resulted; in others, the material flaked and jammed between the ball and retainer; in a few cases, the retainers broke or crumpled.

The failure shown in Fig. 7 was the reinforced PTFE retainer which failed after 3180 hours. The enlargement of the pocket and a crack between two pockets can be seen. Another failure shown in Fig. 8 is that of a sintered nylon containing molybdenum disulfide which failed after only 27 hours. The retainers of both bearings were broken.

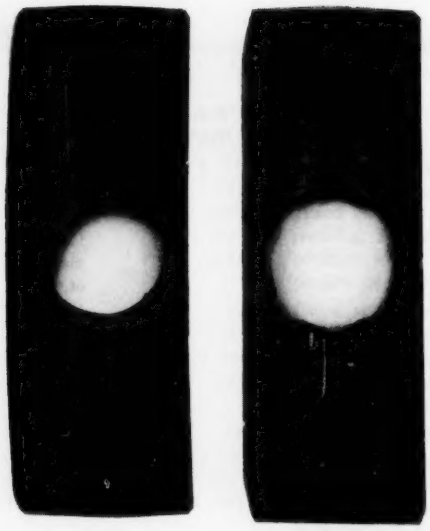

FIG. 7. Failed bearings with reinforced polytetrafluoroethylene retainers.

FIG. 8. Failed bearings with porous nylon retainers

Conclusion

Lightly loaded ball bearings using oil and grease lubricants have been operated for over 1 year in a pressure of 10^{-8} torr. Over 6 months of successful operation has been achieved with special retainer materials. Tests with molybdenum disulfide films have given shorter life times and poor reproducibility of results. Tests are continuing as part of an effort to lengthen the lifetimes of these lubricants and to examine the effects of temperature, radiation and load.

Appendix

The validity of testing the oil and grease lubricated bearings in chambers evacuated by oil diffusion pumps

and of testing more than one lubricant in the same chamber may be questioned. The authors believe that the test results are valid under these conditions. Backstreaming is reduced by baffling and by use of liquid nitrogen traps. Any backstreaming or cross contamination would be expected to deposit on the cold walls of the chamber rather than to pass around a shield and onto the bearing surfaces (which are hotter than the chamber). A test of an unshielded, unlubricated bearing, run in a vacuum chamber evacuated by a diffusion pump, failed at 25 hours. A test using vacuum pump oil in a double shielded bearing ran only 2600 hours in vacuum in comparison with the almost 10,000 hours of operation in vacuum achieved with a petroleum base oil. Greater uniformity and length of lifetimes would have resulted if the vacuum pump oil had been lubricating the bearings. As noted, the lifetimes varied from 164 hours with a phosphate ester to the near 10,000 hours of operation with the above-mentioned petroleum oil.

ACKNOWLEDGMENTS

The authors wish to acknowledge the support of Lt. Col. A. P. Bush, III of Space Systems Division, United States Air Force; W. L. Finch, Reliability Manager, Lockheed Missiles & Space Company; and of C. F. MacLean, Supervisor of Materials and Process Section, Space Systems Division, LMSC. The work of A. M. Hirotsu in performing many of the tests is also gratefully acknowledged.

REFERENCES

1. "The Effects of Nuclear Radiation on Lubricants and Hydraulic Fluids," Report No. 4, 30 April 1958; Addendum, 31 March 1959; Second Addendum, 15 March 1960, The Radiation Effects Information Center, Battelle Memorial Institute, Columbus, Ohio.
2. "The Effect of Nuclear Radiation on Elastomeric and Plastic Materials," Report No. 3, 31 May 1958; Addendum, 30 April 1960, The Radiation Effects Information Center, Battelle Memorial Institute, Columbus, Ohio.
3. "Space Material Handbook." (C. G. Goetzel and J. B. Singletary, eds.). *LMSC* 3-34-61-1 and *DDC* (*ASTIA*) 284547.

DISCUSSION

DOUGLAS GODFREY and NEAL W. FURBY (*California Research Corporation, Richmond, California*):

The testing of lubricants is important to the advancement of space vehicle technology. The authors are to be commended for their approach to the problem and the valuable results obtained.

We should like to speculate on the significance of coast time reported in the paper. For most of the oils and greases used, coast time increased with running time. For solid lubricants, the coast time decreased or was ill-defined. The synthetic fluids used, some of which are thickened with high molecular weight materials, show marked increase in coast time with running. We believe that a permanent reduction of viscosity could account for the increase in coast times observed. Peeler and Kovacich (*A1*) have reported a permanent reduction of viscosity of fluids which were exposed to high shear rates in a sonic oscillator test.

It is important to understand the difference between temporary and permanent reduction of viscosity. Furby and Stirton (*A2*) have elucidated this point. Reduction of viscosity may be temporary and reversible and only observed during high shear rate testing. This temporary reduction in viscosity is a result of "lining up" of long-chain molecules in the direction of flow. Lewis and Murray (*A3*), experimenting with similar bearings lubricated with oils and run in air, concluded that the increase in coast times they observed was a result of a temporary reduction of viscosity due to the high shear rates. Lewis and Murrays' data on thickened and unthickened oils appear to verify that the apparent reduction of viscosity they observed was temporary. Permanent loss of viscosity occurs when conditions such as rough surfaces and cavitation break down long-chain polymer molecules. In the paper under discussion, permanent loss in viscosity no doubt occurred because coast times did increase after long exposures to 8000 rpm.

In some of the tests there is an abrupt decrease in coast time. Perhaps at that point the fluid viscosity became too low to maintain hydrodynamic lubrication, and boundary lubrication occurred. A second possible reason is loss of fluid by evaporation. This point could well be the beginning of the bearing failure. The one petroleum oil evaluated, which was apparently very viscous, did not show any increase in coast time. These data are consistent with the observation of greater shear stability of unthickened hydrocarbons compared to some synthetic fluids containing additives of high molecular weight (*A3*).

REFERENCES

A1. PEELER, R. L., and KOVACICH, S. A., "Development and Testing of Aircraft Hydraulic Fluids," Symposium on Hydraulic Fluids, *ASTM Spec. Tech. Publ.* No. 267, 91-102 (1960).
A2. FURBY, N. W., and STIRTON, R. I., "Viscosity Stability of Hydraulic Fluids," *Appl. Hydraulics Pneumatics*, **12**, 84-88 (1959).
A3. LEWIS, P., and MURRAY, S. F., "Effect of Lubricant Properties on the Coastdown Characteristics of Instrument Bearings," *Lubrication Eng.* **18**, 10-16 (1962).

EARL G. JACKSON (*United Shoe Machinery Corp., Research Department, Balch Street, Beverly, Massachusetts*):

This paper presents data on what must be one of the longest running programs in this technical area, and one of very few that can show bearing lives extending well beyond 1 year. The quantity and extent of these data provide opportunity for much more study than this discussor has been able to apply to them, but the following comments and questions arose out of careful reading:

(1) In considering the effect of radiation on lubricants, including solids, it should be noted that this factor is often markedly different in air than it is in vacuum. For instance, it has been determined experimentally that PTFE is quite stable in vacuum under radiation fluxes that cause appreciable deterioration in air. Any evaluation of performance for space applications, therefore, must include concurrent exposure to the various space features rather than tests of one factor at a time. Otherwise good bearings may be erroneously disqualified, or perhaps because of some other mechanisms, deficiencies may not be detected.

(2) Was the variation in amount of oil absorbed by synthane retainers due to viscosities of the oils, porosity of the synthane, technique of impregnation, or other reasons? A brief examination of the tabulated data shows that there is no linear relationship

between life and amount of oil, but of course there were other simultaneous variations such as bearing steel, temperature of operation, and pressure range. Have the authors made a more exhaustive study of this factor?

(3) In comparing the two versions of F50 oil, the authors point out that the 440C vs. 52100 factor may be involved. This is worth checking in view of one argument that the chrome carbides in 440C make it a more abrasive material when running under marginal lubricating conditions. This discussor doesn't consider that argument proven, however, since he has observed dry tests in which 440C bearings lasted longer than 52100.

(4) The fact that synthane retainers gave better life than ribbon retainers is not surprising in view of general experience that the cage is the weakest part of a ball bearing, and that dry or marginal operation calls for the best possible rubbing material combinations for cage and balls. And incidentally, this discussor has found that motors with lower available torque are useful in tests such as these because they stall at an earlier stage of the failure progression, and so more readily reveal the responsible mechanisms. Hysteresis type motors, for instance, provide a very constant torque and speed, and in similar tests have stalled before the cage was ruptured or the rotor could rub heavily on the stator.

(5) Have the authors made any analysis of the oiled tests with respect to oil properties such as relative volatility, creep, lubricity, or requirements for oxygen in order to lubricate? Would they conclude that lowest vapor pressure is the principal requirement?

(6) Have they noticed whether one end of the motor tends to fail bearings more than the other?

(7) The long lives, i.e., thousands of hours, obtained with some solid films must be gratifying to many designers responsible for equipment using this range of sizes and speeds. It might be advisable, however, to point out that Buckley *et al.* (*B1*) showed that the coefficient of friction for 52100 on 52100 was at a minimum in the 10^{1}–10^{-6} torr range and rose sharply thereafter. Results obtained at pressures in the high 10^{-7} torr range and above may not, therefore, give results typical of higher space vacua. It will depend somewhat on whether the lubricating films are effective only so long as they are intact, or whether they can prolong life appreciably even with a certain amount of metal to metal contact.

In conclusion, the industry must be grateful for the large amount of test data made available here, and the authors are to be congratulated on being able to run such an extensive and informative program.

REFERENCE

B1. BUCKLEY, D. H., SWIKERT, M., and JOHNSON, R. L., "Friction, Wear, and Evaporation Rates of Various Materials in Vacuum to 10^{-7} mm Hg," *ASLE Trans.* **5**, 8-23 (1962).

ROBERT L. JOHNSON (*NASA Lewis Research Center, 21000 Brookpark Rd., Cleveland 35, Ohio*):

For several years the authors group has continued a very active program on vacuum lubrication. Reporting such an effort in the open literature is a significant contribution.

Certain aspects of the paper should be amplified by the authors in regard to their testing methods. First, is the probability that their vacuum chamber was contaminated (a) by back migration of diffusion pump oil, (b) by oil vapors from the eight different motors (using various lubricants) that were run concurrently, and (c) by degassing of motor and electric wire insulation; such circumstances would very likely influence the data obtained. Was any effort made to determine the extent of contamination in the system or the role that contamination would play in the results? Has an attempt been made to run clean, unshielded bearings without lubrication in the chamber?

(2) The type of ionization gauge used for pressure measurement and its location should be described. Is the pressure reported for the petroleum oil used for mechanical vacuum pumps in Table 4 (1.5×10^{-8} mm Hg) correct? What is the vapor pressure for thin oil? The value reported appears inconsistent with other data given and some consistency of values should be expected with eight motors running in the same chamber.

(3) The contribution of bearing friction to bearing temperature levels was apparently considered to be insignificant since bearing temperatures were reported to be "due to the power losses of the motor." Was any attempt made to calculate bearing friction losses from deceleration rates?

(4) In regard to termination of endurance runs by fuse failures, did a significant number of the failures occur during restart after measuring coast time? Were the motors allowed to cool significantly prior to attempting restart? It would seem that a different criterion of failure might be used during restart when power requirement is normally greater. Were precision fuses used; also, would the authors indicate the range of sensitivity for the fuses? Also, substantial differences in failure point (torque) could occur with operating voltage varying from 70 to 90 volts. All these factors may have contributed to the substantial data scatter.

(5) The authors report data on the chlorophenyl, methyl polysiloxane as received and after removing the 50% more volatile fraction. The original silicone performed the best and the authors suggest that either the higher viscosity (which presumably resulted in higher bearing temperatures) or the use of 440-C bearings (52100 bearings were used with the original silicone) might account for the reduced life with the stripped fluid. Several other factors might also merit the authors attention. First, is the possibility that stripping of the oil may have removed a disproportionate amount of the chlorinated molecules which are particularly important in lubricating ferrous alloys with a silicone. Second, the differences in cage material should be more critical to lubrication than the change in race and ball materials. Silicone lubricants function better with nonferrous surfaces than with steel such as that used for the ribbon retainers. Third, viscosity and average molecular weight are important in lubrication; these factors could have been maintained essentially constant while reducing evaporation rate by using a more narrow cut rather than a stripped fraction.

(6) If, as indicated in the paper, "the predominant method of failure" was ". . . the loss of lubricant . . ." a correlation should exist between fluid evaporation rates and life. Have the authors attempted such a correlation? Also, has any attempt been made to measure the effectiveness of bearing shielding in reducing evaporation rates? Were the shields identical in all the shielded bearings tested? What influence does the absorptive cage material (synthane) have on evaporation rates? Does the grease thickener (e.g., lithium soap in silicone grease) influence the evaporation rate of the fluid constituent in the grease? Would the authors care to extrapolate the life data (on the basis of evaporation rates) to the lower pressures (e.g., 10^{-13}–10^{-9} mm Hg) that are more representative of space.

(7) The most notable result of the dry film studies has been the inconsistency of such data. While there is no question of the promise that MoS_2 coatings have substantial improvements in coating, formulations and application techniques appear to be needed. In the interest of consistent results, we have found it

advantageous to have research personnel coat our parts. Have the authors obtained any data to show the relative merit of coating the retainer alone, the retainer and the races, or all the component parts of the bearings?

(8) Do the authors have any data on the relative performance of loaded and unloaded bearings? It would seem that the increased probability of ball skidding with unloaded or very lightly loaded bearings could be troublesome. What considerations determined the use and amount of axial preload with several of the composite retainer materials?

AUTHOR'S CLOSURE

D. GODFREY and N. W. FURBY:

I appreciate these comments and the work is being reviewed with these in mind. I have no further comment.

E. G. JACKSON:

(1) The tests were run originally in vacuum due to the expense of combined vacuum and radiation testing. We are presently running tests in a vacuum chamber placed near a Cobalt-60 source to give us this combined environment. By testing first in vacuum, we hope to narrow the testing in vacuum and radiation to the most promising materials.

(2) We have attempted the correlations suggested by the discussor and likewise have found no correlation. We will continue to do so as we obtain more data.

(3) We hope to look into this further but have no results to report now.

(4) No comment.

(5) We have attempted correlations such as that suggested but have as yet been unable to obtain sufficient data nor develop it ourselves. Any comments on suggested correlations from other readers of this paper would be greatly appreciated.

We would not conclude that low vapor pressure is the principal requirement.

Tables D1 and D2 show some correlations that we have attempted. Based on this, we, at least presently, think that successful lubrication in vacuum requires extremely low vapor pressure or ability of the lubricating oil to be adsorbed or somehow react with the surface to be lubricated, or a combination of these two factors.

Table D1 gives the vapor pressure and operating time in vacuum of four highly refined petroleum oils of the same type

TABLE D1
Vapor Pressure and Operating Lifetime in Vacuum of a Class of Petroleum Oils

Oil	Vapor Pressure (Torr)	Lifetime in Vacuum (Hours)
B	1×10^{-7} (77 F)	790
C	1×10^{-8} (77 F)	1713
J	10^{-8} approx (77 F) 10^{-3} (482 F)	6000*
K	10^{-8} to 10^{-9} (77 F)	16775*

* Still running.

and from the same manufacturer. It can be assumed that the ability of these oils to react or be adsorbed on the surface to be lubricated is small and similar for all four oils. The lifetimes are seen to be inversely proportional to the vapor pressure.

Table D2 gives the results of tests with several silicone oils. Longer lifetimes result with increased polarity of the oil.

(6) Failures are random as to which end of the motor.

(7) We are continuously trying to improve our equipment to reach lower pressures, and with one chamber have gone into the 10^{-10} torr range for brief periods.

TABLE D2
Performance of Selected Silicone Oils

Oil	Operating Lifetime in Vacuum (Hours)
Dimethyl Polysiloxane	347
Methyl Phenyl Polysiloxane	6066
Chlorophenyl Methyl Polysiloxane	12760*
Fluorosilicone Oil	8500*

* Still running.

R. L. JOHNSON:

Comments (1)–(3) I attempted to cover in rewriting the paper for publication.

(4) A significant number of failures did not occur during restart and the motors were not allowed to cool before restarting. The motor and bearings are examined after a failure to determine if the failure is something other than bearing failure. The use of fuses has undoubtedly added somewhat to the scatter but would not effect the basic results.

(5) The stripped chlorophenyl methyl polysiloxane has given long term performance in air as shown in the data section, so we do not believe stripping had any effect on the lubricating properties of the oil. The tests were run using phenolic retainers so there was no difference in retainer material.

(6) In light of the testing we have performed since this paper was originally prepared, we would like to revise our statement on failures of oil and grease lubricants. The failures appear to be caused by a partial loss of lubricant and decomposition of the remaining material. These decomposition products appear to be similar to those encountered in air. Whether these decomposition products are due to thermal decomposition of the thin film remaining, a result of catalytic action of a clean metal surface, or what, we cannot say. We plan to look into what causes this decomposition ourselves and also hope that one of the oil or chemical companies may be induced by this paper to look into this further. The comments in (5) above apply here also.

We have not examined the effect of shielding or the use of grease thickeners on evaporation rates. Dr. Freundlich has done work in this area. We used the same retainers for all tests. The effect of the use of phenolic retainers is discussed in the text; we have not performed a detailed analysis to obtain something like a fixed percentage improvement. We doubt that performance at lower pressures would be much different since we are now operating at a level where mean-free path is significantly long. We are interested in testing at lower pressures as equipment becomes available.

(7) Our dry film lubricants were applied by the manufacturers since we believe that they could do the best with their own coating. We have tried coating the races and retainers versus coating the races, retainers, and balls, and the results are erratic with neither method clearly better.

(8) The loads are the loads indicated in the paper. As we narrow the field down with these screening tests we plan to run tests at various loads and temperatures. A thrust load was used with the special retainer materials because these bearings were angular contact. Various loads were used to determine the effect and at what load we should test.

We greatly appreciate the time and courtesy given us by the discussors in reading and commenting on this paper and welcome any further comments from them or others.

ASLE TRANSACTIONS 6, 192-200 (1963)

Friction-Wear Characteristics of Self-Lubricating Composites Developed for Vacuum Service

By D. J. BOES (ASLE)[1] and P. H. BOWEN (ASLE)[2]

The friction-wear characteristics in air and in vacuum are reported for a group of composites that have recently been developed for ultra high vacuum service. They have demonstrated their ability to carry loads of 1400 psi with low self-wear and negligible wear of the surfaces against which they slide. These composites, made up of polytetrafluoroethylene (PTFE) and a solid lubricant distributed throughout a metal matrix, have been utilized as self-lubricating components in ball bearings operating in environments that conventional lubricants cannot tolerate. These environments include high vacuum (10^{-8} torr) and temperatures from —180 to 400 F.

Introduction

CONSIDERABLE work has been done in recent years to develop lubricating materials for use in bearings and gears that enable them to operate without conventional lubricants, such as oils or greases. The effort became necessary because more and more frequently bearing lubricant systems were being called upon to operate in environments that conventional lubricants could not tolerate. These environments include high temperature, cryogenic temperatures, and high vacuum. In some very rigorous applications the lubricant must be capable of operating in more than one of these environments.

This paper discusses the results of a research program designed to develop a composite material capable of functioning as a load bearing surface with no lubrication other than that contained within itself. The products derived from this investigation were to be utilized as self-lubricating components for ball bearings and gears operating under a high load-low speed condition. It was necessary that the composites function satisfactorily in a vacuum of 10^{-6}–10^{-9} torr and over a temperature range from cryogenic to 400 F.

The composites investigated in this program were three component systems composed of various proportions of a resinous film former, a solid lubricant, and a metal binder. Fabrication of these components into machinable composites was accomplished by compacting the ingredients (in a powdered form) by a combination of heat and pressure. Before compaction, the powdered resin, solid lubricant, and metal were thoroughly blended to insure a homogenous distribution of these components in the composite.

In developing a combination of materials that delivers, when combined under the proper conditions, optimum performance in respect to friction and wear, a total of five variables must be considered: (1) solid lubricant ($MoSe_2$, WSe_2, $NbSe_2$, etc.), (2) binder (copper, silver, etc.), (3) film-former (PTFE or other suitable resin), (4) film-former–lubricant ratio, and (5) binder concentration.

The first composite composition investigated was that of PTFE, molybdenum diselenide, and copper. Adjustments were made in the copper concentration and the PTFE: $MoSe_2$ ratio and the effect of these adjustments determined by measuring the friction and wear of the composites under sliding conditions.

Experimental

The friction-wear characteristics of the composites was measured on the instrument shown in Fig. 1. A cylindrical specimen of the experimental composite (½-inch diameter × ⅝-inch long) equipped with a central relief is held in the chuck of a standard drill press that provides specimen drive. The rotating composite is loaded against a flat 440-C stainless steel disc locked in a specimen head and base that is equipped with a pneumatically floated spherical seat. This seat provides an essentially frictionless, self-aligning support and permits direct measurements to be made of the frictional forces generated between the rotating composite and the restrained disc. A thermocouple is located in the central relief of the composite providing a means for determining temperature rise due to frictional heating. Wear of the composite is measured by determining the amount of debris collected on the stainless disc during a 20-minute run. The weight of the clean, polished disc is measured (to 1×10^{-4} gm) before each run. The disc is then mounted in the instrument and the test composite ro-

Contributed by the ASLE Technical Committee on Bearings and Bearing Lubrication and presented at the Annual Meeting of the American Society of Lubrication Engineers held in New York, April, 1963.

[1] Research Engineer, Westinghouse Research Laboratories, Beulah Road, Churchill Borough, Pittsburgh 35, Pennsylvania.

[2] Senior Research Engineer, Westinghouse Research Laboratories, Beulah Road, Churchill Borough, Pittsburgh 35, Pennsylvania.

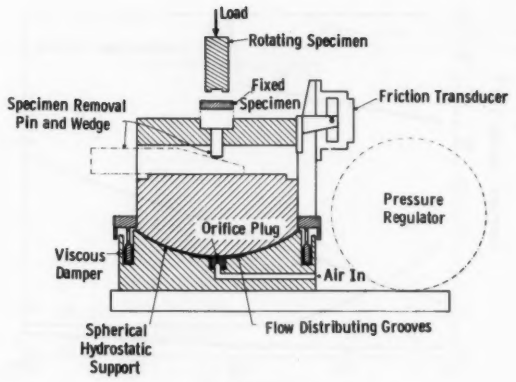

FIG. 1. Friction-wear tester

tated against it under load for a 20-minute period. Following test termination, the disc, containing the film deposited by the composite as well as any wear debris worn from the composite, is again weighed. The difference in weight is considered the amount of composite wear.

In order to check the reproducibility of these measurements, an experiment was performed in which a composite of a given composition was rotated against the disc under a 1000 psi load for various time intervals, and the friction and wear of the composite measured. After each test the disc was removed from the instrument, weighed, repolished, and finally returned to the instrument for the next test. The results of these tests are given in Table 1. It will be noted that coefficient of friction measurements deviated less than $\pm 3\%$ from the three run average. Although wear data did not agree as closely as did the friction data, sufficient justification existed for extrapolating wear data from a 20-minute run to a period of 1 hour.

TABLE 1
Reproducibility Data for Friction-Wear Tester

Composite Composition (vol %) PTFE	$MoSe_2$	Cu	Test duration (min)	Wear (gm/hr)	Coeff. of frict.
30	10	60	15	.0004	.185
30	10	60	20	.0002	.178
30	10	60	120	.0002	.175

All data contained in this report were measured on a specimen rotating in air against a 440-C stainless steel disc. A surface speed of 47 fpm was used at loads of 530, 725, and 940 psi. On those material combinations showing good wear performance, tests were made at 1400 psi as well.

Holding the copper concentration at 20%, the PTFE: $MoSe_2$ ratio was adjusted over a 1:3 to 4:0 range. The ratio delivering maximum wear resistance in this series was then held constant in a second series of preparations where metal concentration was adjusted from 0 to 70% by volume. A third and final series of tests was then made on composites in which the optimum metal concentration determined in series No. 2 was held constant and the PTFE:$MoSe_2$ ratio again adjusted over a 1:1 to 6:1 range. In this manner a combination of materials was determined that possessed the lowest wear characteristic for the materials group: PTFE-$MoSe_2$-Cu under high load-low speed sliding conditions. This technique was also employed for determining the optimum material combination for the PTFE-$MoSe_2$-Ag group. It was found to be very similar in ratio and metal concentration to that of the copper system. Due to this similarity, fewer experiments were required to finally determine the effect of lubricant substitution (WSe_2, $MoTe_2$, $NbSe_2$) on the friction-wear characteristics of the PTFE-Cu and PTFE-Ag systems.

Results and discussion

FRICTION AND WEAR

The wear data measured on the PTFE-$MoSe_2$-Cu composites are presented in Figs. 2–4 as curves plotting

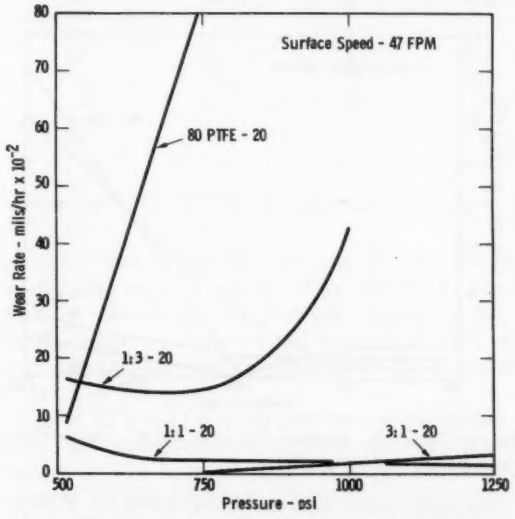

FIG. 2. Composite wear vs. pressure for 20% copper materials of various PTFE to $MoSe_2$ ratios.

wear rate in mils per hour (.001″ per hour) versus bearing pressure. In Fig. 2 are plotted the wear data for those composites in which the copper content was held at 20% (vol %) and the PTFE to solid lubricant ratio adjusted. It is of interest to note the substantial reduction in composite wear upon the addition of solid lubricant. From these tests the 3:1 ratio was selected as the series optimum and was in turn held constant during the second group of tests in which the friction-wear properties of composites containing various amounts of

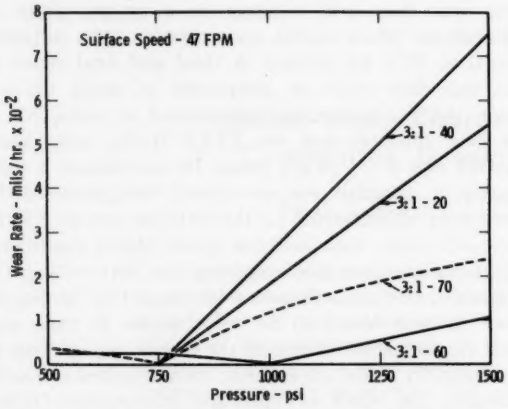

FIG. 3. Wear vs. pressure for 3:1 PTFE to $MoSe_2$ ratio with various copper concentration.

copper were measured. Figure 3 presents the results of these tests and shows that the composite of a 3:1 ratio that exhibits the lowest wear contained 60% metal. Increasing the copper content to 70% resulted in erratic composite performance and wear of the metal disc against which it ran. The final series of tests (Fig. 4) was made

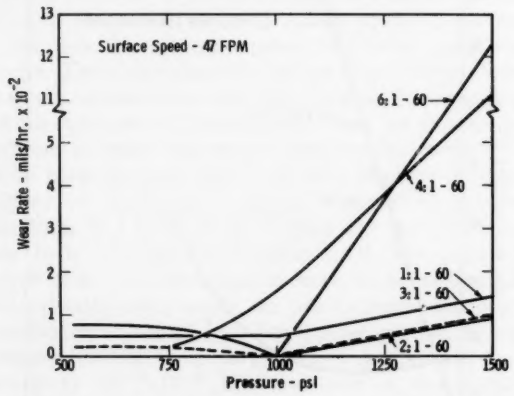

FIG. 4. Wear vs. pressure for 60% copper composition of various PTFE to $MoSe_2$ ratios.

to determine more accurately the effect of PTFE to solid lubricant ratio on the 60% copper composite. The data indicate that the differences in the wear characteristics between the 2:1 and 3:1 ratio of this composite were insignificant, while raising the ratio to 4 or 6 to 1 caused a sharp increase in composite wear rate.

The effect of metal substitution was next determined by replacing the copper binder with silver in the composite while retaining the optimum 3:1 PTFE to solid lubricant ratio. In Fig. 5 the results of this substitution are again presented as curves plotting wear rate of the composite v. bearing pressure. Although silver substitution does not significantly alter the optimum PTFE to solid lubricant ratio found with copper, it does result

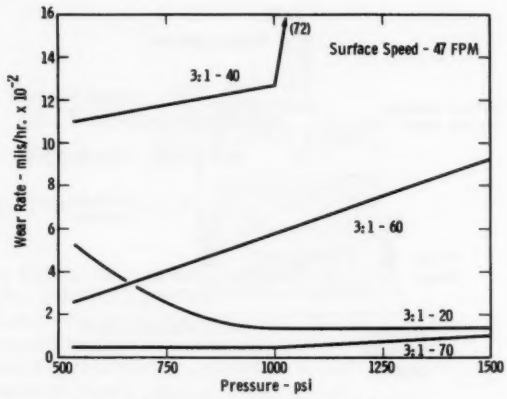

FIG. 5. Wear vs. pressure for 3:1 PTFE to $MoSe_2$ ratio of various silver concentrations.

in the ability to incorporate 10% (vol %) more metal in the specimen (70%) with no loss in wear resistance. As will be discussed later, silver substitution also causes a sharp reduction in the friction coefficient and frictional heating, a characteristic which may be very useful in the ultrahigh vacuum application proposed for these materials.

From the work described above, two material combinations of the PTFE-$MoSe_2$-metal composites were found which provided low wear characteristics and moderate to good friction properties. These are:

Parts by volume		Volume %
PTFE	Solid lubricant	Binder
2	1	60 Cu or 70 Ag
3	1	

Lubricant substitution

This section describes the results of a study to determine the effect of solid lubricant substitution on the friction-wear characteristics of the 60% copper and 70% Ag composites. In addition to molybdenum diselenide, other lubricants evaluated were tungsten diselenide, molybdenum ditelluride, niobium diselenide, molybdenum disulfide, and graphite. All composites were of the 2:1 PTFE to solid lubricant ratio. In the case of tungsten diselenide, both 2:1 and 3:1 ratios were tested with copper as the binder.

The wear and friction of composites containing these various lubricants is plotted against bearing pressure in Fig. 6 for 60% copper composites and in Fig. 7 for 70% silver composites. The data were taken from Tables 2 and 3. None of the composites exhibited differences in wear rates that were significantly greater than those one would expect from experimental error. It must be stated, therefore, that lubricant substitution does not affect the composite performance in respect to wear regardless of whether copper or silver is used as the binder.

TABLE 2
Wear Data on PTFE-Solid Lubricant-Copper Composites

Composite composition (vol %)			PTFE/Lube ratio	Composite wear (mils/hr × 10^{-2})			
PTFE	Solid lubricant	Copper		530	750	940	1400
60	20 $MoSe_2$	20	3:1	0[a]	0	1.9	3.8
40	20 $MoSe_2$	40	2:1	.9	0	1.3	2.9
26–2/3	13–1/3 $MoSe_2$	60	2:1	.26	0	0	1.0
30	10 $MoSe_2$	60	3:1	.26	.26	0	1.0
30	10 WSe_2	60	3:1	0	.38	0	.58
26–2/3	13–1/3 WSe_2	60	2:1	0	.55	.73	3.3
26–2/3	13–1/3 $NbSe_2$	60	2:1	0	.20	.38	.38
26–2/3	13–1/3 $MoTe_2$	60	2:1	.95	—	.20	1.5
26–2/3	13–1/3 MoS_2	60	2:1	0	.20	.20	2.0
26–2/3	13–1/2 Graphite	60	2:1	27	33	excessive wear	

[a] Wear rates of 0 indicates a wear of < .2 mils per hour × 10^{-2}.

TABLE 3
Wear Data on PTFE-Solid Lubricant-Silver Composites

Composite composition (vol %)			PTFE/Lube ratio	Composite wear (mils/hr × 10^{-2})			
PTFE	Solid lubricant	Silver		530	750	940	1400
60	20 $MoSe_2$	20	3:1	5.3	2.5	1.4	1.1
30	10 $MoSe_2$	60	3:1	2.5	4.5	5.5	9.3
22–1/2	7–1/2 $MoSe_2$	70	3:1	.45	.45	.45	1.0
20	10 $MoSe_2$	70	2:1	.40	—	.60	.75
20	10 WSe_2	70	2:1	1.6	1.1	1.1	1.1
20	10 $NbSe_2$	70	2:1	2.7	—	2.8	1.9
20	10 $MoTe_2$	70	2:1	0[a]	—	.3	.44

[a] Denotes wear of < .2 mil per hour × 10^{-2}.

On the other hand, coefficient of friction data measured on these composites indicate reductions in running friction of 25% (depending on load carried by composite) can be achieved by the proper choice of solid lubricant. For example, substitution of $NbSe_2$ for $MoSe_2$ in the 2:1-70 Ag composite provided a 19% reduction in the friction coefficient at the same load.

This fact, coupled with the lower friction coefficient and frictional heating (Fig. 8) exhibited by the silver composites, becomes an important consideration in the selection of binders and solid lubricants for composites to be used for high vacuum service. Removal of frictional heat poses a serious problem in high vacuum applications. It is advantageous, therefore, to choose that composite composition which affords the lowest friction coefficients with the material against which it slides so as to hold frictional heating of bearing surfaces to a minimum.

Figure 9 contains curves plotting the temperature rise discussed above against time for various loads studied. These data are included to demonstrate the manner in which the frictional heating occurs. They are of interest in that the rise is not gradual as one might expect but extremely rapid during the first few seconds. The time required to reach a steady state condition depends primarily upon load and normally occurs within 20 minutes. Data are included for both copper and silver composites and illustrate the lower operating temperature of the silver composite.

Figures 10 and 11 contain photographs comparing the macro- and microstructures of silver and copper matrix composites. The large particle size of PTFE compared to that of the dry lubricant ($MoSe_2$) is readily apparent in Fig. 10. Because of the relatively low temperatures used in fabrication, it is likely that bonding between metal particles is achieved through cold welding rather than sintering. It is apparent, however, that the metal is the continuous phase in both composites.

A comparison of the performance of both the silver and the copper composites with two commercially available materials was next undertaken. The results are given in Fig. 12. Material "A" was a PTFE matrix material that contained a filler and the solid lubricant MoS_2. Material "B" consisted of a sintered bronze matrix containing a combination of PTFE and solid lubricant. While the operation of the filled PTFE com-

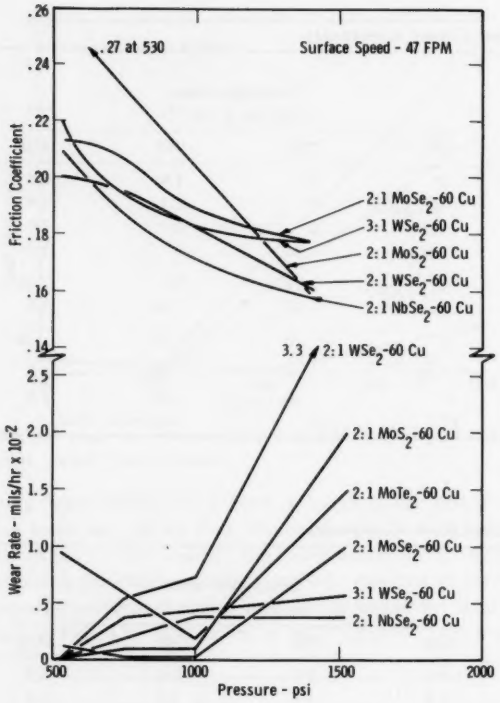

FIG. 6. Friction and wear-pressure relationship for 60% Cu using various lubricants composites.

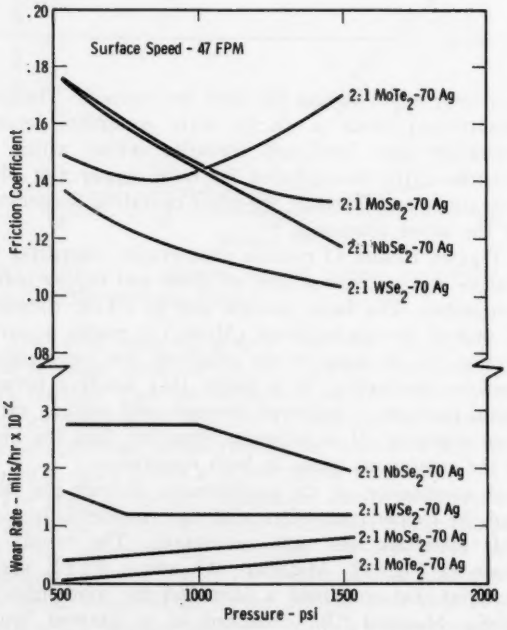

FIG. 7. Friction and wear-pressure relationship for 70% Ag composition using various lubricants.

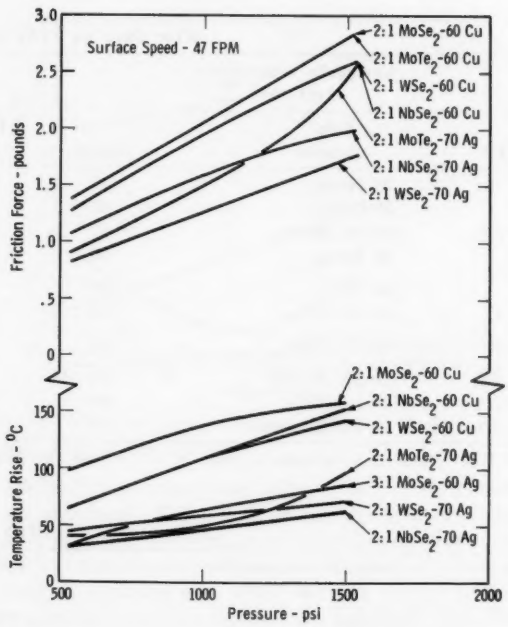

FIG. 8. Temperature rise and frictional force-pressure relationship for various lubricants in 2:1 ratio.

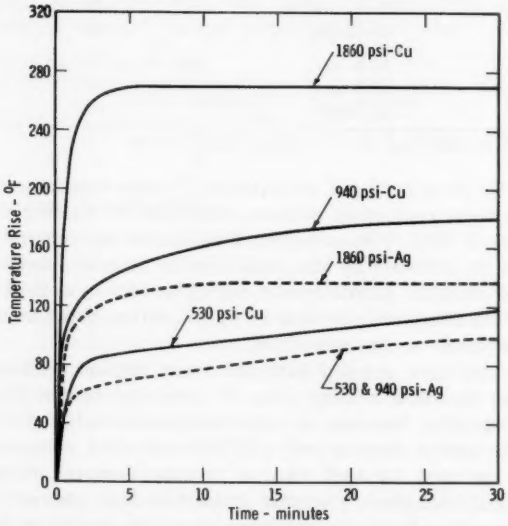

FIG. 9. Temperature rise-pressure relationship for copper and silver composites of 3:1-60 ratio.

posite was accompanied by low coefficients of friction over the load range studied (.21 and .11 at 530 and 1400 psi, respectively), it did not exhibit good wear resistance. The filled, sintered bronze material's wear rate was quite high even at the lowest load used and caused excessive wear of the 440-C stainless disc.

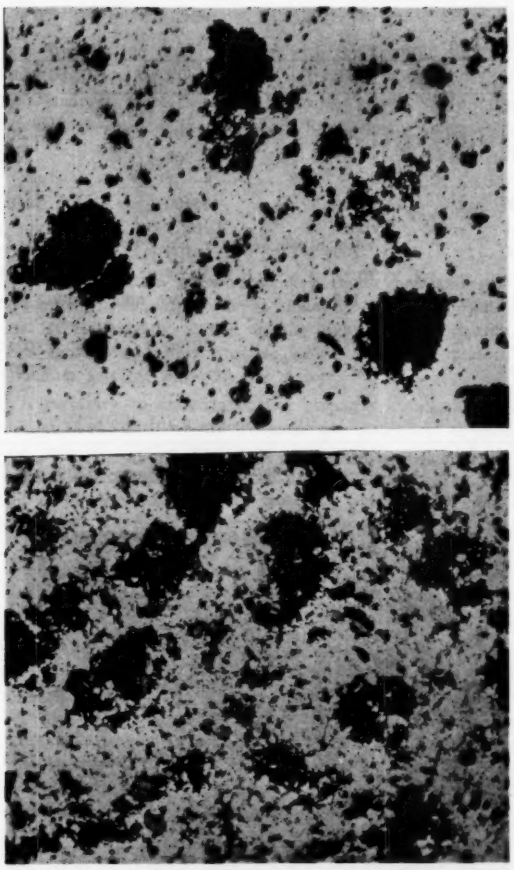

FIG. 10. Typical microstructure of hot pressed self-lubricating composites. Large dark areas are PTFE particles. Gray particles are $MoSe_2$; white areas are sintered copper or silver matrix. Top: 22½% PTFE:7½% $MoSe_2$-70% Silver, 100×; bottom: 30% PTFE:10% $MoSe_2$-60% copper, 100×.

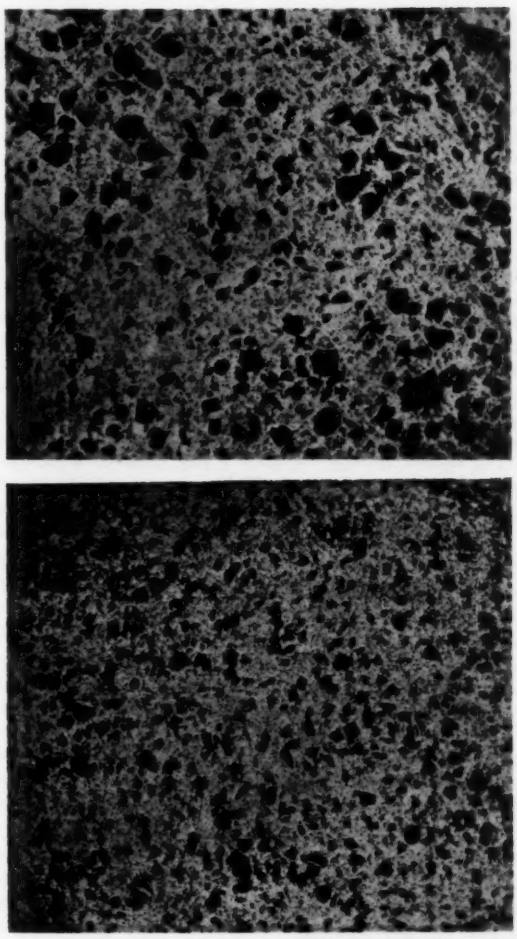

FIG. 11. Typical macrostructures of hot pressed self-lubricating composites. Top: 22½% PTFE-7½% $MoSe_2$-70% silver; bottom: 30% PTFE-10% $MoSe_2$-60% copper.

High vacuum tests

Upon determining the optimum compositions for the copper and silver composites, it was then desirable to evaluate their performance as bearing components under a reduced pressure of 10^{-7} torr. Composites of 2:1 WSe_2-70 Ag and 3:1 WSe_2-60 Cu were made and used as one piece inner land riding retainers in modified 20 and 30 mm bore ball bearings. The impact strength of the retainers was increased with the use of a .032" metal shroud on the O.D. of the retainer. Figure 13 is a photograph of one of these bearings showing the retainer and the various components of the bearing. The high vacuum tests were conducted in equipment described in a previous paper (*1*) and in the Aerospace Facility Research Chamber at AEDC. The bearing tester in which tests 1 and 2 were conducted is shown in Fig. 14. Briefly, the tester can be described as one which permits the operation, at speeds from 200 to 15000 rpm, of a single ball or sleeve bearing. Temperature, type of atmosphere, and pressure may be controlled and the bearing's running torque monitored continuously.

The bearings, equipped with retainers of the composites mentioned above and containing no other lubricant, were operated at various speeds and loads at a pressure of 10^{-7}–10^{-8} torr. Bearing performance was evaluated at temperatures up to 400 F and subjected to cold starts at —180 F. Results of some of these tests are given in Table 4.

Conclusions

A group of self-lubricating materials have been developed that have demonstrated their ability to carry bearing loads of 1400 psi with little self-wear and no wear of the 440-C stainless steel surfaces against which they are sliding at speeds of 47 fpm. These materials employ

TABLE 4
Vacuum Bearing Test Data

Test number:	1	2	3	4	5	6
Speed-rpm	11000	1800	35	35	35	35
Bearing size	204	204	305	305	305	305
Radial load (lb)	1.8	75	255	255	260	260
Axial load (lb)	—	5	—	—	—	—
Bearing mat'l	M-10	M-10	52100	52100	52100	52100
Retainer mat'l	Type 1	Type 1	Type 2	Type 2	Type 1	Type 1
Test time (hrs)	50	100	100	100	100	100
Avg. pressure (torr)	1×10^{-6}	2×10^{-7}	2×10^{-7}	2×10^{-7}	2×10^{-8}	2×10^{-8}
Bearing temp (°F)	75	400	115	115	see note below	
Coeff. of frict.	—	.001	—	—	—	—
Retainer wear (gm)	—	.0938	.0094	.0087	.0180	.0210
Bearing wt. loss (gm)	—	.0046	—.0084	—.0053	—.0048	—.0072

Type 1, 2:1 WSe_2-70 Ag
Type 2, 2:1 WSe_2-60 Cu

Note: Bearing rotation started at —180 F; test ran 40 hours at —150 F, followed by a 20-hour heating cycle to 300 F, with 40 hours accumulated at 300 F.

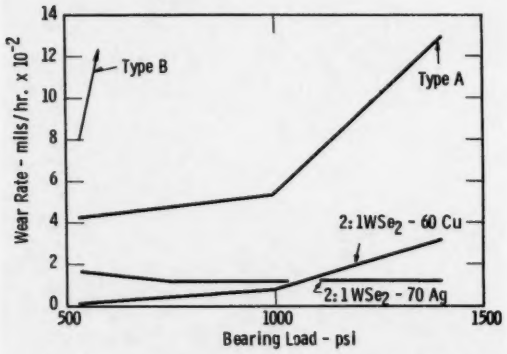

FIG. 12. Comparison of composite performance with commercially available materials.

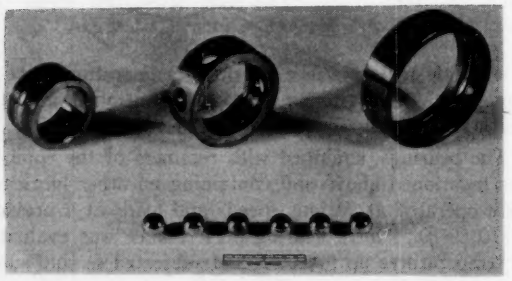

FIG. 13. 204 M-10 ball bearing with self-lubricating composite as retainer.

newly developed solid lubricants that are blended with a film former and bonded through heat and pressure with metal. Pertinent information describing their performance in an air atmosphere is listed below.

(1) Wear rates as low as $.5 \times 10^{-2}$ mils per hour

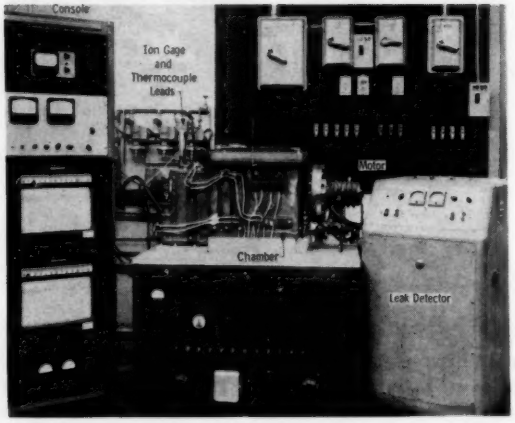

FIG. 14. Ultrahigh vacuum bearing and lubricant test apparatus.

can be achieved with these materials at loads up to 1400 psi.

(2) Friction coefficients for the PTFE-solid lubricant-copper composites range from .16 to .22, depending upon load and solid lubricant used.

(3) Friction coefficients for PTFE-solid lubricant-silver composites range from .10 to .16 and give much less frictional heating than the copper composites.

(4) As high as 70% by volume of metal binder can be employed in these composites with no impairment to their friction-wear properties.

The authors believe these composites hold potential as self-lubricating materials for application as sleeve bearings, gears, or ball bearing components in environments that conventional lubricants cannot tolerate. They have been evaluated as components in ball bearings with good success at cryogenic temperatures, 400 F, and 1×10^{-7} torr.

ACKNOWLEDGMENT

This investigation was conducted with the financial support of the United States Air Force under Contract AF 40(600)-915. The project engineers were Captain J. Pinson, Captain K. Jones, and Lieutenant C. Dean of the Aerospace Environment Office, Arnold Engineering Development Center, Air Force Systems Command, Arnold Air Force Station, Tennessee.

REFERENCE

1. Bowen, P. H., "Dry Lubricated Bearings for Operation in a Vacuum," *ASLE Trans.* **5**, 315-326 (1962).

DISCUSSION

L. J. Bonis (*Ilikon Corp., Natick, Massachusetts*):

The subject of the paper is a very timely one and one in which much more work will be done in the not too distant future. It is certainly a step in the right direction, although in this report the lowest pressure where tests were performed for vacuum services was only 10^{-8} torr.

It is necessary to understand that pressures of ultrahigh vacuum, at least of 10^{-9}–10^{-10} torr, are necessary to gather usable data on friction and wear characteristics, since the surface condition greatly differs above these pressure ranges. At pressures of 10^{-7}–10^{-8} torr, materials surfaces are quickly contaminated by foreign molecules and produce surface effects of different character than would be expected for the clean surfaces that result from the desorption and evaporation of materials exposed to ultrahigh vacuum environment.

The level of present experience concerning the effects of ultraclean surfaces and the properties and behavior of engineering materials, such as sliding surfaces for bearings and gears, has not been extensive enough to allow for realistic hypotheses regarding the fundamental understanding and subsequent extrapolations of these behaviors. This experience has, however, demonstrated that many effects not now understood occur and must be taken into account by the materials engineer when selecting and developing materials for service use in interplanetary space environment.

This paper, along with some other papers recently published, has certainly laid down the groundwork for further investigations on anti-friction materials of this nature.

We have found, however, from some earlier investigations, that in some alloy compositions it is not necessary to use a film former. Some of the layer structure dry lubricants readily form continuous films on the materials surface without the PTFE film forming action.

If I may make a few suggestions and pose several questions, I would like to point out that in the text there are references to the fact that frictional heating occurs in an extremely rapid fashion during the first few seconds of the test. One would expect this phenomenon in using dry lubricant materials that are embedded in the matrix, because these few seconds are required to form the lubricating film on the surface of material; and then the friction coefficient, and consequently the frictional heat, will not rise further—on the contrary, it will decrease in some instances.

Secondly, there are references made that the silver substitution causes a sharp reduction in the friction coefficient and frictional heating. This could be explained if one considers that the shear strength of the silver is orders of magnitude lower than, for instance, the copper. As a matter of fact, silver has been used and is being used itself as a soft film lubricant.

It would be interesting, and definitely would be instructive, to plot a ternary diagram in terms of friction coefficient of the various systems in order to determine the usable ranges of material. Each ternary would be an isothermal plane and the testing conditions (fixture, sample size, speed, etc.) would be identical for all points in the plane. In this way the lines in the ternary would indicate almost immediately which direction or which composition range (of PTFE; $MoSe_2$; Cu, for example) would be the optimum for performance, wear, and friction.

Also, I think it would be interesting to determine the organometallic decomposition products of the hot-coining of PTFE with copper or silver and a selenide. This could lead to some other application areas whereby presumably the organo-metallic product might be used as a single source dry lubricant or would assist in the lubrication process.

Table 4, in the summary of the vacuum tests which have been tabulated, shows various useful data. It would be advantageous to see, however, what the coefficient of friction is in each case.

Furthermore, it has been indicated in the literature that composite materials utilizing similar design technology would give better performance characteristics under ultrahigh vacuum conditions if the base matrix material is of a harder nature. In connection with the described composite wear measurement, I would like to suggest that, if weight measurement is used to determine the wear rate, weighing of the composite part (pin, cleaned of debris) would be more meaningful than the technique of measuring the weight gain of the stainless steel disk.

Finally, I believe that it would be helpful to compare a metal matrix dry lubricant combination composite material with (a) pure PTFE, and (b) with a PTFE-glass fiber-molybdenum disulfide composite. A comparative curve performed in ultrahigh vacuum for sliding friction has been plotted in Fig. A1, and it shows that the metal matrix composite (nickel alloy-MoS_2 composite) gives a considerably lower friction coefficient in ultrahigh vacuum than either the pure PTFE or the PTFE-glass fiber MoS_2 composite.

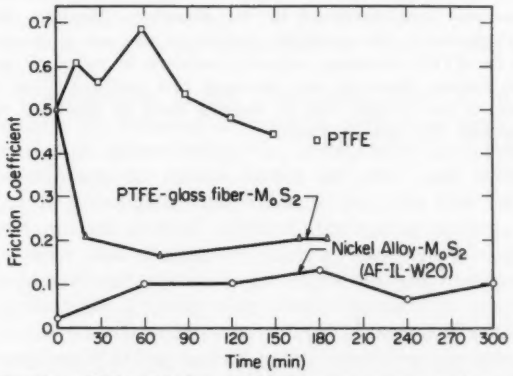

Fig. A1. Sliding friction coefficient measurements against polished 52100 tool steel in ultrahigh vacuum.

S. F. MURRAY (*Mechanical Technology Inc., 968 Albany-Shaker Road, Latham, New York*):

The material development work which is summarized in this paper represents a significant contribution toward the solution to the problem of operating bearings in a spatial environment. However, there are some minor points which this discussor would like to have clarified:

1. Does the author believe that enough data have been accumulated to show that solid lubricants such as the selenides represent a significant improvement over MoS_2?

2. Did the author evaluate a compress of solid lubricant and metal powder without the addition of PTFE as a film former? The work reported by Johnson, Swikert and Bisson in *NACA TN* 2027, February 1950, indicated that 10% MoS_2, 85% Ag, and 5% Cu was a very effective combination, although the friction values which they reported were slightly higher (0.18–0.24). The use of PTFE may be beneficial in improving the sliding characteristics but will decrease the useful temperature and radiation stability of these composites.

3. In Figs. 2 and 4, the differences in wear between the 1:1 and 3:1 proportions of PTFE:$MoSe_2$ seem rather small to make a selection of an optimum ratio, particularly in view of the wear reproducibility data shown in Table 1. Are there other reasons why the author feels that he can pin down an optimum concentration so closely?

AUTHORS' CLOSURE:

The authors wish to thank Dr. Bonis for his interesting and very useful comments.

It is agreed that wear and friction data measured in vacuums at pressures of 10^{-7}–10^{-8} torr are not necessarily indicative of materials performance at 10^{-11} torr and beyond. Plans to evaluate this type of composite material in an ultrahigh vacuum are now essentially complete and data should be available in the near future. This will reveal any differences that may exist because of contamination or desorption of materials in an ultrahigh vacuum.

A desirable method of measuring wear would be the weight loss of the test specimen as suggested by Dr. Bonis. However, not all composites exhibited optimum results, and some of the earlier specimens cracked or chipped during the wear test. With our better specimens, we are now measuring weight loss as suggested.

Composites that do not employ PTFE, or a similar material, have also been developed in our laboratory. However, their performance in this particular application was not as desirable as the PTFE-containing composite materials in regard to wear and friction. Materials were developed that exhibited either low wear or low friction, but no material could be developed that exhibited both characteristics.

The final point pertains to the comparison of the friction of unfilled PTFE, the PTFE-glass-MoS_2 composite, and the metal matrix PTFE-copper-$MoSe_2$ composite. With the exception of the unfilled PTFE material, we find the exact opposite friction characteristics in a positive pressure atmosphere and at vacuums of 10^{-7}–10^{-8} torr that Dr. Bonis did under higher vacuum tests. Substituting silver for copper in the composite brought the friction coefficient into the range of values obtained for the glass-filled material.

A direct comparison of the friction characteristics of the AF-1L-W20 composite with that of the Ag-PTFE-WSe_2 composite would be interesting in an ultrahigh vacuum.

In answer to Mr. Murray's first question, we believe there is justification for stating that the selenides offer significant advantages over MoS_2 in regards to friction coefficients and wear characteristics. Figure 6 illustrates this improvement in both parameters. For equivalent compositions, composite friction coefficients using MoS_2 as the solid lubricant ranged from 0.27 to 0.16, while substitution of tungsten diselenide for molybdenum diselenide reduces these coefficients to 0.21–0.16. In addition, recent work on the friction coefficients of the pure compounds supports these data (see Table C1).

TABLE C1
Friction Coefficient at 80 psi; Air; 25 C

Surface speed (fpm)	MoS_2	WSe_2
5	.23	.17
22	.21	.13
45	.17	.10

Regarding the selection of an optimum ratio of PTFE to solid lubricant, it is quite true that based on wear data alone the differences between the 1:1 and 3:1 ratios were not sufficient to permit the selection of 3:1 as the optimum ratio. Other factors, such as porosity and machinability, controlled the final selection of the 3:1 ratio.

Finally, the performance of composites of solid lubricant and metal powder without PTFE additions as a film former were evaluated. Their performance, however, did not compare favorably with the PTFE-containing composites at the high loads required for this work, particularly in regards to wear resistance. The use of PTFE in the composite reduced its wear rate by at least two orders of magnitude. The authors readily acknowledge the fact that the use of PTFE will limit the upper temperature limit and radiation resistance of the composite. However, other resins, that are more stable—oxidatively and thermally—than PTFE and whose radiation resistance is substantially greater are available and have been employed successfully in these composites. These materials are as yet in the experimental stage and therefore were not included in this paper.

ASLE TRANSACTIONS 6, 201-208 (1963)

Wear and Friction of Mechanical Carbons in Liquid Oxygen as Influenced by Transfer Films

By WILLIAM F. HADY (ASLE),[1] GORDON P. ALLEN (ASLE),[1] and ROBERT L. JOHNSON (ASLE)[2]

Experimental wear and friction studies were conducted with a series of mechanical carbons sliding against metal surfaces in liquid oxygen (—298 F) at sliding velocities to 6500 feet per minute and a load of 1000 gm. The data reported shows that dense highly graphitic carbons have potential use as seal and bearing materials for liquid oxygen applications.

High density graphitic carbons with a greater oxidation resistance and a greater capability of forming a transfer film gave the lowest wear and friction. Metals that form the most stable oxide films promote greater adherence of the graphite to the mating surface. Impregnated carbons must be selected with caution because frictional heating generated during sliding can initiate hazardous reactions between oxygen and certain unstable organic compounds.

Introduction

MECHANICAL carbons are being used in seals and bearings to operate over a wide range of temperatures and environments. One area employing carbons is in liquid oxygen applications; however, the basis for selecting particular types of carbon for use in oxygen is inadequately defined. The stringent compatibility requirement imposed by the liquid oxygen environment limits the selection of impregnated carbons to be used to those of known stability in oxygen. Any unstable organic compound in the carbon could react violently with the oxygen when sufficient heat is generated during sliding. Earlier friction and wear investigations have shown that mechanical carbons can be used as self-lubricating materials for aircraft turbine engines at high temperatures of 700 F (*1, 2*) as well as in turbopump applications for rocket propulsion at liquid hydrogen temperatures, —423 F (*3*). It is feasible, therefore, that a carbon with or without adjuncts can be selected to perform satisfactorily in liquid oxygen and provide the necessary low friction and low wear required.

The low wear of mechanical carbons, as experienced in the more conventional applications, where air, moisture, or other vapors are present, is attributed to the self-lubricating characteristics of the carbon. It has been reported (*4*), that effective lubrication is accomplished only when an oriented surface layer of graphitic carbon is established on the mating surface, which in effect results in a sliding combination of carbon on carbon rather than carbon on metal.

Reference (*1*) hypothesized that graphite lubrication depends primarily upon adherence of the graphite to the metal mating surface. This adherence can be achieved by the presence of intermediate films of adsorbed moisture, gases, or by the presence of an oxide film on one or both of the surfaces to be lubricated. The more common theory for the mechanism of graphite lubrication, which suggests the shearing of interlamellar adsorption films between the graphite platelets, does not consider affinity or adhesion of graphite to the lubricated surfaces. Earlier liquid oxygen studies (*5*) have indicated that oxide films are beneficial in minimizing wear and friction in metal–metal combinations. Therefore, since beneficial oxide films form readily on metal surfaces in liquid oxygen and graphite effectively lubricates oxidized metals (*1*), it is likely that films of graphite on the mating surface will develop readily and lubrication will be enhanced. Such film formation is essential for the lubrication to provide low wear and friction as required in dynamic seals and bearings.

The objectives of this investigation were (a) to determine the influence of graphite content on wear and friction of carbon bodies, (b) to determine the influence of adjuncts to carbon bodies on wear and friction, (c) to investigate what effect, if any, the free energy of formation of metal oxides of the mating surfaces has on wear and friction of graphite, and (d) to suggest improved seal materials for liquid oxygen turbopump applications. Carbon with varied amounts of graphite content as well as carbons modified by means of adjuncts were run in sliding contact against metals having different oxidation characteristics in liquid oxygen at —298 F. Data were obtained with a $\frac{3}{16}$-inch-radius rider speci-

Contributed by the ASLE Technical Committee on Seals and Packings and presented at the Annual Meeting of the American Society of Lubrication Engineers held in New York, April, 1963.

[1] Research Engineer, NASA, Lewis Research Lab, 2100 Brookpark Road, Cleveland 35, Ohio.

[2] Head, Lubrication Section, NASA, Lewis Research Lab.

men sliding on a flat surface of a rotating 2½-inch-diameter disk. Runs were made with specimens submerged in liquid oxygen at surface speeds ranging from 1000 to 6500 feet per minute and a normal load of 1000 gm.

Apparatus and procedure

The apparatus used in this investigation is shown schematically in Fig. 1. The basic elements are a rotating disk specimen (2½-inch-diameter) and a stationary

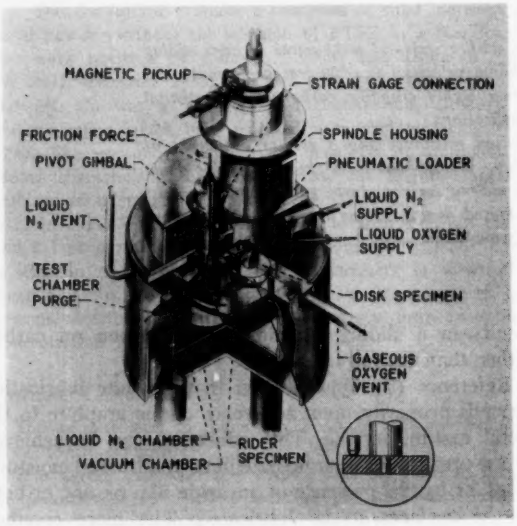

FIG. 1. Liquid oxygen friction apparatus

hemispherically tipped rider specimen (3/16-inch-radius) in sliding contact with the disk (see inset). The disk is rotated by a variable speed electric motor through a gear box speed increaser coupled to the specimen shaft. Disk speed is monitored by a magnetic pickup whose output is fed into a digital readout instrument.

The rider specimen is loaded against the disk by a pneumatic operated piston on the end of a gimbal mounted arm. Through this arm, pressurizing gas (dry He) is supplied. The arm is linked to a strain gage assembly for measurement of frictional force.

The apparatus consists of two sections which may be separated for changing specimens. The lower section consists of four separate chambers: The inner chamber, or test chamber, is located within a "jacket" which may be filled with liquid nitrogen for cooling. This cooling jacket is surrounded by a vacuum chamber to reduce the boil-off rate of the cooling and test fluids. The outermost chamber, or spill chamber, surrounds the three chambers and provides safe operation in the event excess amounts of the test fluid should escape. The upper section is a vacuum jacket through which passes the disk specimen drive shaft housing and the rider specimen arm assembly. A series of carbon face seals are employed to seal around the drive shaft and flexible bellows are used to seal the rider arm assembly. Fluorinated hydrocarbon oils are used to lubricate the gear box and the support bearings in the shaft housing to prevent a reaction of the oil with the liquid oxygen in case the shaft seals fail.

The test fluid, liquid oxygen in this investigation, passes through a coil within the cooling jacket before entering the test chamber near the bottom. In tests where the test fluid initially is in the gaseous state, the coil would condence the gas into the liquid state. Excess liquid and vapor are vented by a line leaving from a point near the top of the chamber. The liquid level within the test chamber is monitored by a capacitance probe and recorded on a circular chart capacitance recorder.

The cooling jacket is filled with liquid nitrogen and vented by two diametrically opposite lines. The coolant level is monitored with a carbon resistance probe, a full jacket being indicated by a sharp drop in output when the coolant absorbs the heater output.

Specimen Preparation and Test Procedure

The nonimpregnated carbon rider specimens were cleaned by soaking them in ACS certified acetone for 5 hours and placed in a vacuum (10^{-3} mm Hg) for 10 hours.

In cleaning the impregnated carbons it was discovered that in some cases the above procedure caused the impregnants to be leached out when they were placed in the vacuum. Therefore, the impregnated carbons were cleaned by wiping them with a soft cloth saturated with ACS certified acetone before being placed in the vacuum. All the carbon specimens were then stored in a desiccator until used.

The nonplated disk specimens used in this experiment were circumferentially finished to a surface roughness of 4–8 microinches RMS. The plated specimens, 440-C hardened to 52-54 R_c, were ground and lapped to 4–8 microinches RMS before plating (Table 1). The various platings were electro-deposited from electrolytes held in absorbent materials attached to portable electrodes (*6*).

All the disk specimens were then given the following cleaning treatment: (a) immersion in an ultrasonic cleaning tank filled with water, for ½ hour; (b) thorough rinsing with ACS certified acetone; (c) polishing with moist levigated alumina on a soft cloth; and (d) thorough rinsing with distilled water. The remaining water was removed using filter paper. Each disk specimen was prepared just prior to being placed in the test chamber.

After the desired liquid oxygen level was attained, the disk specimen was brought up to speed and the normal load was applied. Duration of runs was 60 minutes or less depending on the stability of operation. The frictional force was measured continuously by resistance strain gages mounted on a dynamometer ring whose output was fed into a recording potentiometer.

TABLE 1
Physical and Chemical Properties of Metal Disk Materials Used in This Study

Disk		Plate thick. (in.)	Standard hardness (BHN)[a]	Surface finish (μin. RMS)	$-\Delta F_{-298F}$[b]
Solid	Plate				
	Au	0.0030	110	4.2	0.30
Ag			36	6.2	7
	Ag	.0038	85	4.2	7
	Rh	.0020	925	4.0	20
Cu			82	6.2	35
	Cu	.0034	175	4.0	35
Co			101	8.4	55
	Co	.0015	—	8.4	55
Ni			68	5.5	56
	Ni	.0046	379	4.5	56
Fe			66	4.8	63
	Sn	.0042	<5	3.6	67
	Zn	.0035	50	12.0	82
Cr			120	8.4	87
	Cr	.0042	733	4.2	87
Ti			175	7.2	110
440-C			20-54 R_c	4.0-8.0	

[a] At 75 F.
[b] Reference (*10*) (Kcal per gram atom of O_2).

Rider wear was obtained by measuring the wear scar diameter and calculating the wear volume.

Results and discussion

Influence of Graphite Content on Wear and Friction

The importance of graphite content on the wear of carbon riders is demonstrated in Fig. 2. The carbon riders were run in sliding contact with 440-C stainless steel and chromium plate in liquid oxygen at 2300 feet per minute and a 1000-gm load. Rider wear decreased with increasing graphite content; the fully graphitized carbons gave the lowest wear against either 440-C stainless steel or chromium plate. In both series the wear of the amorphous carbons was about 20 times that of the fully graphitized carbon. Mechanical carbons that have operated successfully in liquid nitrogen and liquid hydrogen (*3*) have wear rates on the order of 10^{-11} inch^3 per foot of sliding, which is comparable to the wear rate of the 20% graphite sliding on chromium plate (Fig. 2) in this investigation.

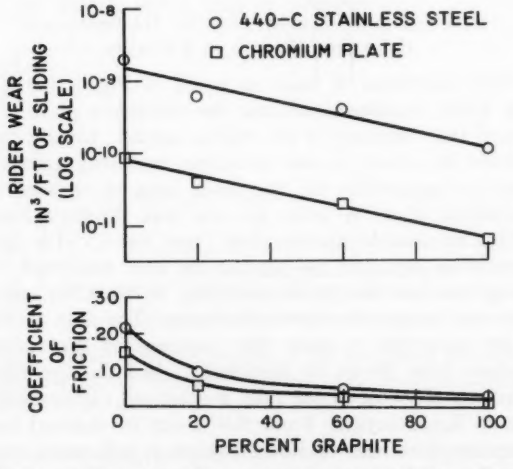

FIG. 2. Effect of graphite content on the lubricating properties of carbons in liquid oxygen (2300 fpm; 1000-gm load; duration, 1 hour).

The low wear exhibited by the fully graphitized carbon specimens is attributed in part to their greater resistance to oxidation than those carbons of lower graphite content.

It has been reported that amorphous carbon begins to oxidize in air at 622 F and that graphitic carbon begins to oxidize in air at 842 F (*7*). It would therefore appear that, in the highly oxidative environment of this investigation, even though the temperature is at —298 F, the sliding interface temperatures were sufficient to promote a more rapid and extensive oxidation of the carbons containing little graphite and resulted in excessive corrosive wear.

It appears also that, in this investigation, the greater capability of the fully graphitized materials to form a transfer film of graphite on the metal mating surface is important in reducing rider wear. Visual inspection of the disk specimens showed that an adherent graphite film was noted best with the fully graphitized rider run on chromium plate. It was also observed that the carbons of lower graphite content did not transfer sufficient graphite to the mating surface so that the carbon was continually sliding on bare metal surfaces. As a result, the lower graphitic carbons were more susceptible to wear by abrasive processes as well as oxidation. Figure 3 is a set of photomicrographs showing rider wear scars and the transfer film of graphite on the mating chromium plate surfaces.

The distinct separation of the two curves is very significant as it points out the importance of oxides being present on the metal surfaces when graphite is to be used as a lubricant in the absence of moisture or water vapor. The selection, therefore, of mating surfaces takes on increased importance when designing dynamic seals for liquid oxygen applications. Previous friction and wear studies with graphite at elevated temperatures (*1*) suggested that the presence of beneficial oxide films promoted an affinity of the graphite for the metal mating surface and was a requirement of graphite lubrication in unconventional systems. The 20-fold reduction in wear between the two curves was the basis for a more exhaustive study as to the role played by oxide films in graphite lubrication for liquid oxygen applications. These results will be presented and discussed subsequently.

Coefficient of friction data (bottom of Fig. 2) show a downward trend as the amount of graphite is increased

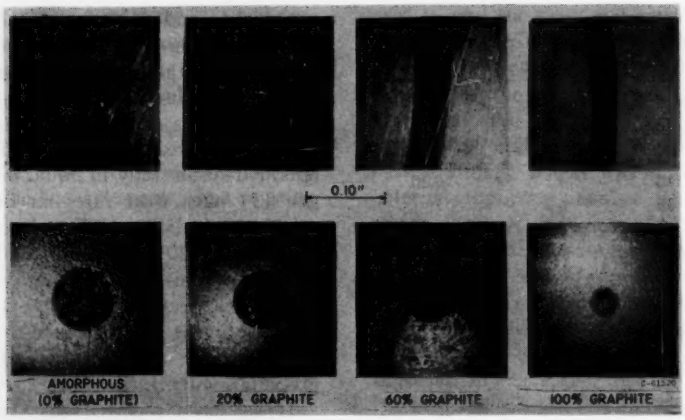

FIG. 3. Disk (top) and rider (bottom) wear areas of nonimpregnated carbons with various graphite content sliding on chromium plate in liquid oxygen (load, 1000 gm; sliding velocity, 2300 fpm; duration, 1 hour).

from 0 to 100%. The values reported are the values of friction after stabilization has occurred. The importance of graphite content in reducing friction is easily shown since the drop in friction, comparing the amorphous carbon to the 20% graphite carbon, is very pronounced: 0.22–0.10, when sliding on 440-C stainless steel and 0.10–0.06 when sliding on chromium plate. With further increases in graphite content, further reductions in the coefficient of friction are experienced with values reaching about 0.03 for the fully graphitized carbons sliding on 440-C and chromium plate.

Frictional force is the product of the effective shear area in sliding and the shear strength of the interface film (*8*). The harder amorphous carbons, having higher shear strength than the graphitic carbons, usually give minimum shear areas. The addition of minor amounts (20–30%) of graphite to the amorphous carbon usually gives an optimum combination of low shear strength (from the graphite) and low shear area (from the amorphous carbon matrix) that results in minimum friction. In liquid oxygen, however, the lowest friction values were obtained with the fully graphitic carbons. It is probable that the relative influence of the cryogenic temperature on the shear area (as determined by hardness) and the chemical behavior of the oxygen on the formation of adsorbates for easy surface shear, may have altered the optimum composition.

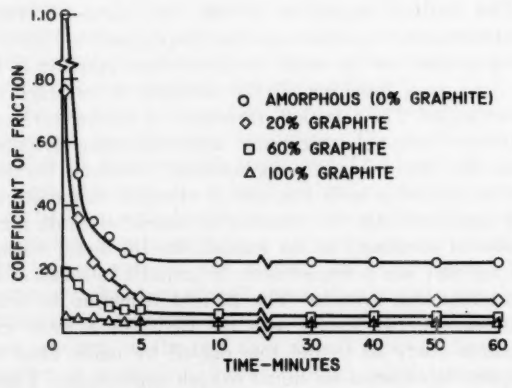

FIG. 4. Effect of graphite content on the friction of carbon on 440-C stainless steel in liquid oxygen (2300 fpm; 1000-gm load; duration, 1 hour).

The data of Fig. 4 are presented to show that high starting torques can be experienced with carbons of low graphite content and that for systems where high starting torques cannot be tolerated, fully graphitized carbons can provide low starting friction without extensive run-in periods. The values of friction attained after run-in are those shown in Fig. 2.

INFLUENCE OF METAL MATING HARDNESS ON GRAPHITE WEAR AND FRICTION

The differences in wear as noted in Fig. 2 between the 440-C stainless steel and the chromium plate suggested that hardness of the mating surface, usually considered important to wear of carbon type seal materials, may be responsible for the lower wear of carbons on chromium plate. A series of runs was therefore made with a hardenable stainless steel (type 440-C) of various hardnesses obtained by altering the heat treatment. In using one base metal, the variables of oxidation resistance and composition were eliminated. The data of Fig. 5 are presented to show that hardness of the mating surface from 20 to 54 Rockwell-C had no significant effect on the wear of the fully graphitized carbons when run in liquid oxygen. From this it can be deduced that graphite rider wear in liquid oxygen is influenced more by the oxidation resistance and composition of the mating surface than hardness.

Figure 5 data also show that the coefficient of friction

of a fully graphitized carbon sliding of 440-C of various hardnesses remained constant within the scope of this investigation.

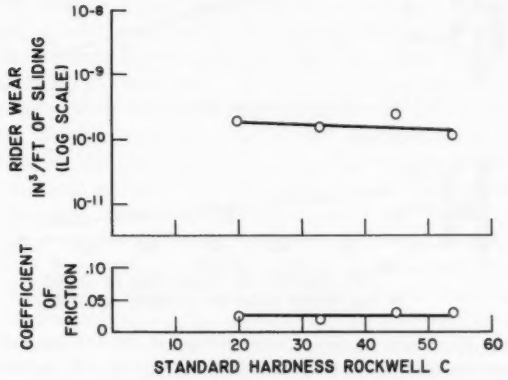

FIG. 5. Effect of surface hardness of 440-C stainless steel on the lubricating properties of graphite in liquid oxygen (2300 fpm; 1000-gm load; duration, 1 hour).

INFLUENCE OF SLIDING VELOCITY ON GRAPHITE WEAR AND FRICTION

The dissipation of frictional heat generated during sliding contact by dynamic seals in liquid oxygen could become of prime concern where substantial surface speeds are encountered. The additional heat experienced at the higher sliding velocities could increase the oxidation of the fully graphitized carbons which would lead to increased corrosive wear. A series of tests was conducted to show the effect of sliding velocity on the wear of a fully graphitized carbon rider sliding on 440-C stainless steel in liquid oxygen. Data of Fig. 6 present wear per unit distance of sliding at velocities from 1000 to 6500 feet per minute and a load of 1000 gm.

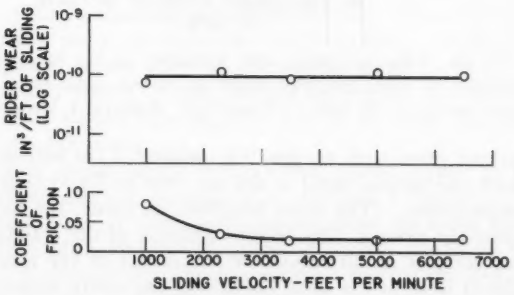

FIG. 6. Effect of sliding velocity on the lubricating properties of graphite sliding on 440-C stainless steel in liquid oxygen (1000-gm load; duration, 1 hour).

In this investigation, sliding velocity had no significant effect on graphite rider wear. Further increases in surface speeds, however, could bring about increased wear as the interface temperatures could become sufficiently high and cause extensive oxidation of the graphite. With the addition of adjuncts to the base graphite (to increase the oxidation resistance and improve physical properties) higher surface speeds may be tolerable. The selection of adjuncts is limited, however, to those that will remain stable in the highly oxidizing environment.

The coefficient of friction (bottom of Fig. 6) shows a decreasing trend to 3000 feet per minute, after which it remains constant within the limits of this investigation. The reduction in friction between 1000 and 3000 feet per minute (0.08–0.03) is not significant as both values are well below 0.10.

THE INFLUENCE OF IMPREGNANTS ON WEAR AND FRICTION

Two series of impregnated carbons, a 20% graphite base grade, and a 100% graphite base grade were run against 440-C stainless steel in liquid oxygen to study the effects of various impregnants on wear and friction of these carbons. The unimpregnated base grades were run against themselves for a comparison [note (A), Figs. 7 and 8].

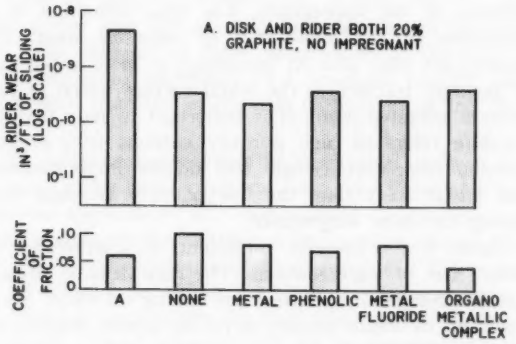

FIG. 7. Effect of impregnants on the lubricating properties of a 20% graphite sliding on 440-C stainless steel in liquid oxygen (2300 fpm; 1000-gm load; duration, 1 hour).

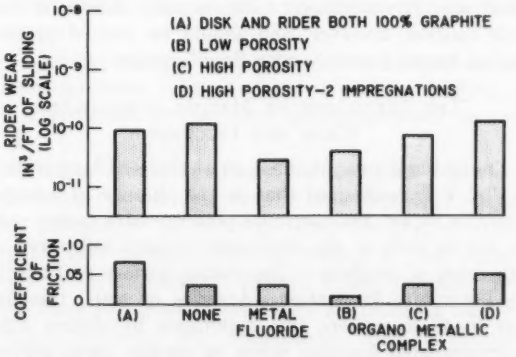

FIG. 8. Effect of impregnants on the lubricating properties of a 100% graphite sliding on 440-C stainless steel in liquid oxygen (2300 fpm; 1000-gm load; duration, 1 hour).

The wear data for the 20% graphite series, presented in Fig. 7, show that the impregnant had little effect on the wear of the carbon rider. The carbon with metal impregnation had the lowest wear: 2.2×10^{-10} inch^3 per foot of sliding for this series of runs.

The coefficients of friction of the variously impregnated 20% graphite riders are presented at the bottom of Fig. 7. The addition of the impregnants had no significant effect on the frictional properties of the carbons used in this investigation. The organo-metallic complex impregnated carbon had the lowest coefficient of friction (0.04) for this series.

The data in Fig. 8 show the effect of impregnants on the wear and friction of a 100% graphite rider sliding on 440-C in liquid oxygen. In general, additive impregnants did not significantly influence wear; however, the metal fluoride impregnant and the organo-metallic complex impregnant in a low porosity carbon did reduce wear by a factor of approximately 3. The metal fluoride impregnant had the lowest wear of the two: 3×10^{-11} inch^3 per foot of sliding.

This reduction in carbon rider wear indicates the oxidation resistance of the carbon was increased with the addition of the impregnant. The wear reduction is an indication of the importance of corrosive wear. The impregnant also acts to encourage a more rapid rate of graphite transfer to the metal surface which in turn reduces adhesive wear. It is important to note that the graphite riders of high porosity carbons with organo-metallic complexes (single and double impregnations) had higher wear than the low porosity graphite rider having the same impregnant.

Figure 8 also presents coefficients of friction for the same series of impregnations. The high density, organo-metallic complex, graphite rider sliding on 440-C stainless steel in liquid oxygen gave the lowest friction coefficient, 0.01.

From the results of Figs. 7 and 8, high density (low porosity) 100% graphite mechanical carbons can be considered for bearings and seals in liquid oxygen applications. The selection of impregnants should be made with caution, however, and should be limited to those having known stability with liquid oxygen.

The Influence of Mating Surface on Wear and Friction

Friction and wear studies (*9*) at elevated temperatures to 700 F hypothesized that in the absence of adsorbed water or vapor, the continual presence of a proper oxide on one or both of the lubricated surfaces influenced the adherence of graphite to the mating surface and affected good graphite lubrication. A series of tests, therefore, was made to explore this hypothesis by sliding 100% unimpregnated graphite riders on various metal surfaces in liquid oxygen. These data are shown on Figs. 9 (solids) and 10 (platings).

The abscissa, free energy of formation of the oxide, in

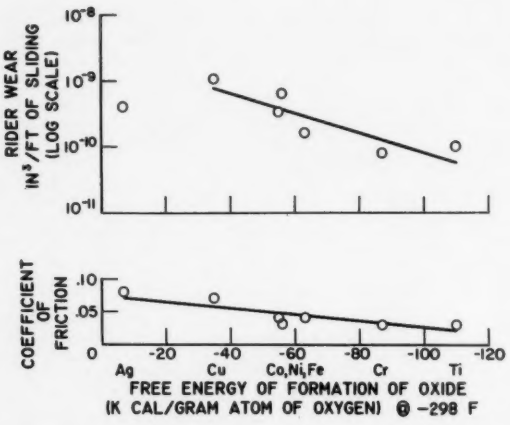

FIG. 9. Effect of metal oxide formation on the lubricating properties of a 100% graphite sliding on various solid metals in liquid oxygen (2300 fpm; 1000-gm load; duration, 1 hour).

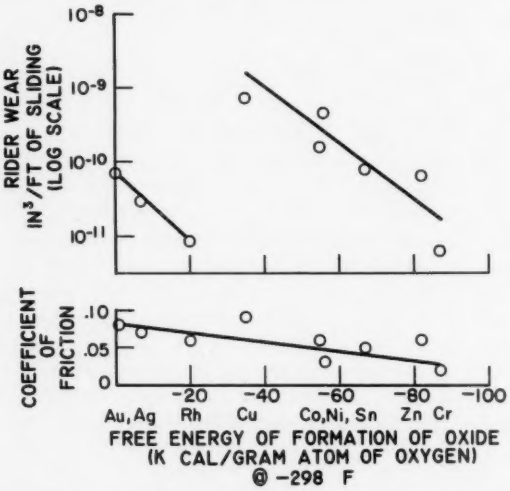

FIG. 10. Effect of metal oxide formation on the lubricating properties of 100% graphite sliding on various metal plates in liquid oxygen (2300 fpm; 1000-gm load; duration, 1 hour).

kcal per gram atom oxygen, is a measure of the ease with which the various metal oxides can form at liquid oxygen temperatures. (The more negative the value, the more stable the oxide.) The relative position of the standard free energies of formation for the oxides of the metals studied were in the same order over the entire temperature range that could be expected to result from local frictional heating on the surfaces. Reference (*8*) indicates that under conditions of boundary lubrication more favorable than in the present experiments, surface temperatures 900 F above the ambient might be obtained. On that basis, in these experiments, interface temperatures of about 600 F could be postulated. The surface temperatures, therefore, can be expected to range from the ambi-

ent of —298 to 600 F. The values used in plotting the relative position of the oxides formed were extrapolated from graphs down to —298 F, liquid oxygen temperature (*10*).

The data of Figs. 9 and 10 show a downward trend in graphite rider wear as the free energy formation of the oxide becomes more negative. This downward trend in wear is more pronounced with the plated specimens (Fig. 10) than with the solid disk specimens (Fig. 9). The break in the curve for the plated specimens, i.e., in separating the precious metals from the remaining specimens, could be caused by the presence of a contaminant, co-deposited from the electrolyte with the metal, remaining on the surface of the disk. Any contamination present in studies of this nature can have marked effect on the wear and frictional properties of the materials under investigation. The coefficient of friction also shows a downward trend with both the plated and solid disk specimens as the oxides that are formed become increasingly stable.

Those metals forming the more stable oxides developed transfer films from the graphitic carbon bodies (mechanical carbons); such films provided the most effective lubrication. The stability of the film is associated with the formation of a chemical bond between the graphite and the metal oxide. During sliding contact, penetration of the fluid (O_2) adsorbed on the surface would be achieved. Thus, with the mechanical carbon and the oxide-coated metal in intimate contact, a chemical reaction to form a carbon-oxygen-metal complex can occur. Conditions favorable for such reaction are that the contacting solids are under pressure (the yield strength of the softer slider material) and that sufficient frictional energy is available for reaction. The kinetics of such reactions are impossible to define because of transient conditions that are characteristic of sliding contact. The present reference to free energy relationships indicate the relative stabilities of potential chemical bonds in the postulated carbon-oxygen-metal complex. The chemical bonding energy is associated with stability of adhering graphitic carbon films on the mating metal surfaces as described herein. Thus, the sliding process was one of graphite sliding on a graphite film rather than graphite on nascent metal.

With those metals forming less stable oxides, it is thought that the graphite rider, through a chemical reaction, removes the bonded oxygen from the metal surface resulting in the formation of carbon monoxide or carbon dioxide. In these experiments, those metal oxides having a less negative ΔF than either carbon monoxide or carbon dioxide showed little or no graphite transferred to the mating surface. It is thought that in the liberation of these gases the nascent metal surfaces reoxidized from time to time leading to a corrosive type wear mechanism for the graphite rider. It appears that as the metal oxides become less stable, the degree of corrosive and adhesive wear increases.

Summary of results

An experimental wear and friction investigation of mechanical carbons for seals and bearings was conducted in an environment of liquid oxygen. The following results were obtained:

(1) Highly graphitic mechanical carbons had better wear and friction properties in liquid oxygen than more commonly used materials which have low graphite content. Of the graphitic materials tested, performance was best with those having high density (low porosity). Low wear values for graphitic carbon are attributed in part to its greater oxidation resistance in comparison with amorphous carbon. Also important to both wear and friction is the greater capability of the graphitic materials to form a transfer film of carbon on the metal mating surface; optimum performance appears to occur when a continuous transfer film is present on the mating metal so that the solid carbon can slide on a carbon film.

(2) Chromium plate was a better mating surface than any of the other metal platings, pure metals, or 440-C. Observations in these and other carbon wear studies suggest that the metal oxide films are of primary importance in effecting graphite lubrication. Metals forming the most stable and dense oxide films appear to perform best. The presence of these metal oxides on the mating surface promotes adherence of a beneficial transfer film of graphite from the mechanical carbons in sliding contact.

(3) Additive impregnants to mechanical carbons did not have a significant effect on wear and friction. Erratic data was experienced with impregnated carbons as compared to data for the nontreated base grade carbons; this was attributed to treatment inconsistencies. Where the use of treated carbons is preferred they should be impregnated in very nearly the final form so that the most effectively treated material will not be removed by machine finishing.

(4) Hardness of the mating 440-C material was varied from 20 to 54 Rockwell-C without significant influences on wear and friction of fully graphitized carbon rider specimens.

(5) Sliding velocity from 1000 to 6500 feet per minute had no significant effect on rate of wear or friction of fully graphitized carbon rider specimens when run on 440-C.

(6) Carbon wear problems are less severe in these liquid oxygen experiments than in liquid hydrogen studies made previously. A potential reaction hazard exists, however, with carbons in sliding contact at high surface speeds in liquid oxygen. Dense, highly graphitic materials have the greatest resistance to initiating such an oxidation reaction; any impregnants used to improve the performance of mechanical carbons in liquid oxygen applications must, therefore, have known stability in oxygen.

REFERENCES

1. BISSON, E. J., JOHNSON, R. L., and ANDERSON, W. J., "Friction and Lubrication with Solid Lubricants at Temperatures to 1000 F with Particular Reference of Graphite," Inst. Mech. Eng. Conf. on Lubrication and Wear. Paper no. 23, Oct. 1957.
2. PETERSON, M. B., and JOHNSON, R. L., "Friction Studies of Graphite and Mixtures with Several Metallic Oxides and Salts at Temperatures to 1000 F," *NACA (Natl. Aeron. Space Admin.) Tech. Note* 3657, 1956.
3. WISANDER, D. W., and JOHNSON, R. L., "Wear and Friction of Impregnated Carbon Seal Materials in Liquid Nitrogen and Hydrogen," *In* "Advances in Cryogenic Engineering," (K. D. Timmerhouse, ed.), Vol. 6, Plenum Press, Inc., New York, 1961.
4. SAVAGE, R. H., "Physically and Chemically Adsorbed Films in the Lubrication of Graphite Sliding Contacts," *Ann. N. Y. Acad. Sci.* **53**, 362-869 (1951).
5. HADY, W. F., ALLEN, G. P., and JOHNSON, R. L., "Boundary Lubrication Characteristics of a Typical Bearing Steel in Liquid Oxygen." *NASA (Natl. Aeron. Space Admin.) Tech Note* **1580**, 1962.
6. HUGHES, H. D., "Practical Brush-Plating," *Inst. Met. Finishing, Trans.* **33**, 424-442 (1955-56).
7. MANTELL, CHARLES L., "Industrial Carbon," 2nd ed., Van Nostrand, Princeton, N. J., 1946.
8. BOWDEN, F. P., and TABOR, D., "The Friction and Lubrication of Solids," Oxford Univ. Press (Claredon), London and New York, 1950.
9. SWIKERT, M. A., and JOHNSON, R. L., "Wear of Carbon-Type Seal Materials with Varied Graphite Content," *ASLE Trans.* **1**, 115-120 (1958).
10. GLASSNER, A., "The Thermochemical Properties of the Oxides, Fluorides, and Chlorides to 2500 K," Argonne National Laboratory Publication, ANL-5750.

ASLE TRANSACTIONS 6, 209-217 (1963)

The Effect of Adsorbed Films on the Attractive and Frictional Forces Developed in an Electrostatic Clutch

By W. C. CLINTON[1] and R. L. LYON[2]

An investigation has been made of the effect of adsorbed organic films at the solid/air interface of a rotor in an electrostatic clutch. The solid was a cured composition of butadiene-acrylonitrile novalak phenolic resin. The film substances included mono- and multilayers of a homologous series of fatty acids. These films were prepared by both the Langmuir-Blodgett technique and the static vapor-condensation method. A dynamic vapor-condensation oven for continuously adsorbing condensed films of polar compounds on rotor surfaces under specified clutch operating conditions is described. It is shown that the tension developed in the band can be calculated theoretically to within ±15% of that measured experimentally. It is shown that an adsorbed film, the thickness of which is less than the order of roughness of the rotor surface (20×10^{-6} inches), has no effect upon the measured values of the tension developed in the band. The ratio of the dielectric coefficient and the equivalent interface gap thickness is shown to be constant for all calculated values. Finally, it is concluded that the life expectancy of an electrostatic clutch can be infinite when the solid material is prevented from transferring to the band by maintaining one or more monolayers of polar-nonpolar compounds at the solid/air interface.

Nomenclature

$V_G =$ Generator voltage, volts
$R_G =$ Internal impedance of generator, ohms
$R_R =$ Bulk resistance of the rotor material plus its contact resistance to the metallic shaft, ohms
$V_R =$ Voltage across the rotor,[3] volts
$I_0 =$ Initial current flowing in the circuit, amps
$R_{g1} =$ Resistance at the rotor-band interface, ohms
$V_{g1} =$ Voltage at the rotor-band interface gap, volts
$I_{s1} =$ Steady state current, amps
$R_{g2} =$ Bulk resistance of the transferred material plus its contact resistance with the band, ohms
$V_{g2} =$ Voltage across the transferred material, volts
$I_{s2} =$ Steady state current flowing in the circuit after material transfer, amps
$K_e =$ Dielectric coefficient
$\varepsilon_0 =$ Permitivity of free space [farad^2/ (in^2 — lb)]
$W =$ Band width, inches
$r =$ Radius of rotor, inches
$\theta =$ Wrap angle of band, radians
$f_k =$ Dynamic coefficient of friction between rotor surface and the band
$V_{g1} =$ Voltage across the interface gap, volts
$t_g =$ Equivalent interface gap thickness, inches
$T_0 =$ Constant tension exerted by two springs, lb

Contributed to the American Society of Lubrication Engineers by the authors. Manuscript received February 25, 1963.

[1] Advisory Chemist, IBM, General Products Division, Development Laboratory, Endicott, New York.

[2] Staff Engineer, IBM, Endicott, New York.

[3] Voltage build-up is limited by the capacitance C_g (see Fig. 2).

I. Introduction

An electrostatic clutch is essentially an electromechanical transducer that is used in the present instance to operate print hammers. The basic principles involved in its design have been fully reported elsewhere (*1, 2*) and only a simple description of the operation of the clutch used in this investigation will be reviewed here. A schematic representation of the clutch assembly is shown in Fig. 1.

A narrow metallic band or tape is held with a small normal force by springs A and B against a rotor made

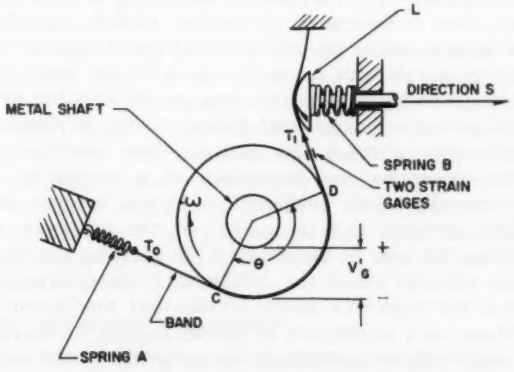

FIG. 1. Electrostatic clutch assembly

of semi-insulating electrical material cemented to a metallic shaft which rotates at a constant velocity (—ω). A potential (V_G') applied across the band and rotor will develop an attractive force at the rotor-band interface and cause an increase in the frictional force due to an increased normal force. Because of the increased friction, the band will be pulled by the rotor in the direction of rotation (clockwise in the present case) and, in doing so, will actuate the mechanism L (held under compression by spring B) in the direction S. Spring B will return L to the position shown in Fig. 1 when V_G' is removed.

In practice it has been found that, due to the normal welding and adhesion of two clean sliding surfaces, transfer of the semi-insulating material to the surface of the metallic band occurs as the assembly is rotated. Accompanying this transfer is a constant decrease of the force of electrostatic attraction, which approaches zero with time.

It follows that the usefulness of the transducer is limited unless means are employed to reduce the material transfer and to maintain a constant force of electrostatic attraction. Early experiments showed that fluid thicknesses of macrodimensions (>0.005 inches) reduced the force of electrostatic attraction to zero. Other experiments showed that useful forces could be produced when the fluids on the rotor surface were rubbed to film thicknesses of molecular dimensions. In the latter case the magnitude of the force was highly dependent upon the amount of rubbing.

This paper then is concerned with the investigation of four specific problems: (1) to determine what chemical specie can be adsorbed as a thin film at the sliding interface and also prevent material transfer, (2) to determine the frictional characteristics of the adsorbed film, (3) to determine the optimum molecular dimensions of the specie necessary to develop a useful tension in the band, and (4) to devise a practical dynamic method for adsorbing and maintaining the optimum molecular dimensions of the specie at the sliding interface of the band and rotor.

II. The adsorbed film

Since Hardy (*3*) first showed the ability of a homologous series of saturated, unbranched alcohols, paraffins, and acids to reduce the coefficient of friction between two rubbing metals with increasing chain length, numerous investigators have proceeded along similar lines but with more precise techniques and greater variety of chemical specie and substrate. In general, these investigators agree concerning the importance of a monolayer in reducing the kinetic coefficient of friction between two sliding surfaces, and the ability of the multilayer to decrease the wear of the substrate. In studying the effect of the adsorbed mono- and multilayers in the electrostatic clutch, our experience follows closely their conclusions.

Mono- and multilayers of species capable of floating on water can be easily built up on solids by the well-known Langmuir-Blodgett technique (*4*). Here, a monolayer of an insoluble substance, spread on the surface of water and kept under two-dimensional pressure, is transferred to the surface of a solid by raising or lowering the solid through the floating film. Repetition of this process will fold the monolayer back and forth on itself so that successive layers can be built up.

Another very simple way to adsorb a condensed monolayer onto a solid is to expose the surface of the solid to the vapors of the chemical compound in a closed system maintained at a temperature high enough to provide an adequate vapor pressure but low enough to adsorb a close-packed condensed film. Recently, investigators (*5*) have shown quite clearly that a single condensed monolayer of exceptional durability can be prepared by this method with polar-nonpolar compounds. This is accomplished by removing the excess material, which accumulates during evaporation, by vigorous rubbing with clean grease-free tissue paper or absorbent cotton after the solid has been allowed to cool to room temperature.

A procedure of more recent origin is known as the "retraction" or "withdrawal" method (*6*). In this case the carefully cleaned solid is dipped into a solution of the chemical specie and a nonpolar solvent. The solid is withdrawn after equilibrium is established. The excess liquid on the solid retracts, leaving a film of monomolecular dimensions on the surface of the solid.

In nearly all cases reported using these techniques, the substrates were very smooth solid metals, evaporated metals on glass, or glass alone. Such materials offer infinite loci for adsorbing. In this investigation we are concerned with a solid (butadiene-acrylonitrile novalak phenolic resin; see Table 1 for composition), the surface

TABLE 1
Composition of Solid Material Cemented on Metallic Rotor Shaft

Parts by weight	Name
0.1	Dimethyldithiocarbamate
0.5	Mercaptobenzothiazole
1	Antioxidant
1	Stearic acid
1.5	Sulphur
3	Zinc oxide
40	Butadiene-acrylonitrile copolymer
42.5	Conductive carbon
60	Phenolformaldehyde resin
100	Asbestos fiber

of which is of an indeterminate nature. This surface possesses loci that, in all probability, are random and far apart, and the energy of adsorption of which for a given chemical specie is nonuniform over the surface of the solid. Nevertheless, successful mono- and multilayers of polar-nonpolar compounds were adsorbed on the surface of this material by each of the methods reviewed. However, difficulty was experienced with the "retraction" procedure owing to the attack of the solid by the solvents usually employed. Some liquids which do not attack the solid are monohydric and polyhydric alcohols, organic acids and

amines, mineral oil, and silicones. Since each of these groups spreads readily on the solid surface, examples of these chemical species were chosen for studying the effect of the adsorbed boundary film on the mechanical efficiency of the electrostatic clutch.

The compounds used in this study were derived from the sources listed in Table 2. This was not primarily a

TABLE 2
Chemical Specie Adsorbed on Rotor Surface

Compound	Chemical name	Melting point (°F)
n-$C_{17}H_{35}COOH$	Stearic acid	156.2
n-$C_{13}H_{27}COOH$	Myristic acid	127.4
n-$C_{11}H_{23}COOH$	Lauric acid	108.5
n-$C_{9}H_{19}COOH$	Capric acid	87.1
n-$C_{7}H_{15}COOH$	Caprylic acid	59.9

study in basic adsorption but rather the application of surface chemistry techniques to a practical problem where a solution which depended on materials of high purity would be useless for practical purposes. Therefore, all materials were used as received and no attempt was made to remove more strongly adsorbable impurities.

III. The electrical model

A better understanding of the part played by an adsorbed film in the operation of an electrostatic clutch can be gained by first considering the electrical model of the system. Its equivalent circuit is shown in Fig. 2.

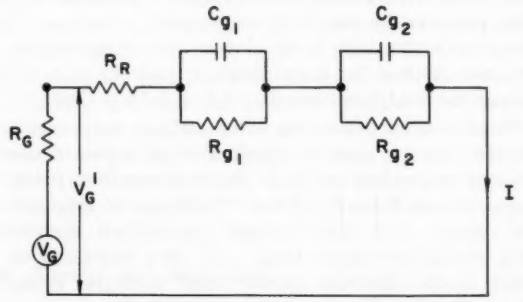

FIG. 2. Equivalent circuit of electrostatic clutch

Measurement of the initial surge current flowing in the circuit when the rotor is idle and before any material transfer has occurred allows determination of both the bulk resistance of the rotor material and the voltage across the rotor, since

$$R_R = \frac{V_G}{I_0} - R_G \qquad [1]$$

and

$$V_R = I_0 R_R \qquad [2]$$

If the rotor is now pulsed and rotated and the steady state current is measured before transfer has occurred, the voltage and resistance across the rotor-band interface can be calculated as follows:

$$R_{g1} = \frac{V_G}{I_{s1}} - (R_G + R_R) \qquad [3]$$

$$V_{g1} = I_{s1} R_{g1} \qquad [4]$$

After transfer occurs, and assuming that R_{g1} in Eq. [3] remains constant, the resistance of the transferred material and the voltage across it can be calculated as follows:

$$R_{g2} = \frac{V_G}{I_{s2}} - (R_G + R_R + R_{g1}) \qquad [5]$$

and

$$V_{g2} = I_{s2} R_{g2} \qquad [6]$$

It follows that after transfer occurs, Eq. [4] no longer holds and the voltage at rotor-band interface gap becomes

$$V_{g1} = I_{s2} R_{g1} = \frac{V_G}{1 + (R_G + R_R + R_{g2})/R_{g1}} \qquad [7]$$

In this paper the values of V_{g1} measured under the experimental conditions of Eq. [4] are designated initial values (V_{g1i}), and those measured under the experimental conditions of Eq. [7] are designated final values (V_{g1f}). These two values of V_{g1} are determined experimentally and are used to calculate the theoretical values of the initial and the final tension developed in the band. The theoretical tension values are then compared with the initial and final tensions measured experimentally.

The calculations of the theoretical tension in the band are based on a model in which the band and rotor are regarded as forming a parallel plate capacitor. It can be shown that the tension (T_1) developed in the band at point D in Fig. 1 may be expressed as follows:

$$T_1 = 7.27 \times 10^{11} \frac{K_c f_0 V_{g1}^2 W_r \left[\exp(f_k\theta) - 1\right]}{2t_g^2} + T_0 \exp(f_k\theta) \qquad [8]$$

Since the term $T_0 \exp(f_k\theta)$ is small compared with the other terms in Eq. [8], it is neglected in all subsequent calculations.

The initial and final experimental tension values were measured with the use of the two active strain gages which are bonded facing each other on opposite sides of a metal band at approximately the location shown in Fig. 1. Two other inactive strain gages, bonded to large static metal masses, were used to complete a conventional Wheatstone bridge circuit. Both an oscilloscope and tape recorder were used to continuously monitor and record the tension developed in the band as the electrical system was pulsed by voltage V_G.

IV. Experimental procedure

Extreme care was used in degreasing each sliding surface prior to each experiment because it is well known

that the friction and adhesion between two rubbing surfaces is highly dependent upon the presence or absence of an adsorbed film. The rotors were scrubbed with a grease-free sable hair brush and an aqueous solution of detergent because it has been shown, by frictional measurements on dry abraded plastics, that such surfaces can be freed of adsorbable contaminants by this technique (*7*, *8*). After this degreasing, each rotor surface was abraded under running tap water with 600 A Grit silicon carbide paper, rinsed thoroughly in distilled water, and dried over anhydrous $CaCl_2$.

The slider and a suitable holder were rinsed five times in boiling CP benzene and then scrubbed with detergent. After rinsing thoroughly with flowing distilled water, they were immediately dried with CP acetone and transferred to a benzene vapor degreaser for 30 minutes.

The metal bands used in the pilot model of the electrostatic clutch were given a high polish with the use of a levigated polishing compound. They were then scrubbed with an aqueous solution of detergent, rinsed in distilled water, and finally dried over anhydrous $CaCl_2$.

A. Langmuir-Blodgett Films

Known amounts of two different fatty acids adsorbed as oriented films on the rotor surfaces were studied to determine, first, the molecular dimensions necessary to prevent material transfer to the band. These films were adsorbed by the Langmuir-Blodgett technique; a Hydrophil balance was modified to contain a deep section so that the rotors could be completely immersed in water (pH 6.2). A surface pressure of 28.3 dynes per centimeter was applied to the floating acid films by the use of a piston oil of purified oleic acid.

Monolayers of stearic acid successively added to the number of six were adsorbed by raising and lowering a rotor through the compressed acid film. This process was repeated with myristic acid. The first layer was always deposited with the carboxylic group adjacent to the rotor surface. The successive even-numbered layers were always deposited with the hydrocarbon end nearer the rotor surface, and the odd-numbered layers were always deposited with the carboxylic group nearer the rotor surface. It is believed that the orientation of the first layer was that the plane of the methylene groups was nearly parallel to the rotor surface and the chain itself nearly perpendicular to the surface.

After the adsorption of the required number of monolayers, the initial coefficient of kinetic friction (f_{ki}) between the coated surface and a ½-inch diameter, hemispherically ended metal slider was measured with our modified Bowden-Leben (*9*) "stick-slip" machine at a sliding velocity of 0.005 cm per second and a normal load of 500 gm.

Later it will be shown that the values of f_{ki} measured at the sliding velocity of 0.005 cm per second, as contrasted to the higher sliding velocity of the rotor and band, gave good correlation between the calculated and the observed values of the tension developed in the band. Hence, for all practical purposes it can be assumed that f_{ki} remains constant.

Immediately after measuring f_{ki}, the durability of each coated surface was evaluated on a pilot robot with a degreased metal band (rotor speed, 1200 rpm; rotor radius, 1.25 inches; band width, 0.063 inches; wrap angle, 136°; generator voltage, 300 volts). The durability of the films was evaluated by monitoring the steady-state current, I_{s1}. A measurable decrease in this current indicated that the films had changed, and visual observation showed that rotor material had transferred to the band. The criterion for discontinuing a given test run was the value of V_{g1} calculated from the monitored steady-state current. When a useful voltage could no longer be obtained, the test was discontinued.

Following the film-durability evaluations, a final kinetic coefficient of friction (f_{kf}) was measured for each coated surface with a degreased, hemispherically ended slider traversing only the area of the wear track worn on the rotor by the rubbing band. The measured values of f_{kf} were assumed to be practically independent of the sliding velocity. The values obtained were used to calculate the final tension (T_{tf}) values developed in the band.

B. Evaporated Films

Because the results obtained with the Langmuir-Blodgett films showed that one or more monolayers could prevent material transfer for a finite time, the adsorption experiments were extended to the study of films prepared by the static evaporation technique. This was done with a view to developing this technique into a dynamic method for maintaining a constant film thickness at the solid/band interface for an infinite time.

Several clean, grease-free rotor surfaces were each suspended over crystals of stearic acid in separate closed systems maintained at 20 F above the melting point of the acid (see Table 1). After 10 minutes of exposure to the vapors, each rotor surface was rubbed vigorously with grease-free paper tissue and then evaluated in a robot in the identical manner used with the Blodgett films. The experiment was repeated with the use of myristic acid maintained at 30 F above its melting point (see Table 2).

Thus, a dynamic evaporation technique was devised to continuously adsorb organic films onto rotor surfaces. Figure 3 shows a sketch of an oven evaporator designed to maintain an adequate vapor pressure of any low melting point hydrocarbon over a rotor surface under the dynamic conditions of normal clutch operation. After a few milligrams, or milliliters, of the compound under investigation have been placed in cavity A, a clean, grease-free abraded rotor is rotated under the oven which is gradually elevated to the desired temperature by a cartridge heater. A grease-free, polished band, which has, in addition to the two bonded strain gages referred

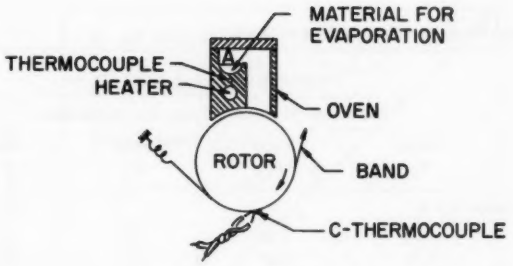

FIG. 3. Oven evaporator

to earlier, a thermocouple welded to the outside of the tape approximately at the position C, is then attached to the system. The welded thermocouple is used to monitor the approximate temperature of the rubbing surfaces.

The evaluation procedure with the oven evaporator differed from that described earlier with the Blodgett films. Here the parameters f_{ki}, I_0, I_{s2} and T_{1i} were not measured. Instead, after the oven had reached a state of equilibrium at a preselected temperature (a temperature at which an adsorbed film was clearly visible on the rotor surface), only the stabilized steady-state current I_{s1} and the tension T_{1f} developed in the band were measured. The rotor was then removed and the coefficient of kinetic friction (f_{kf}) was measured with a hemispherically ended slider traversing only that area of the rotor on which the band had rubbed. The rotor was returned to the robot and, without attaching the band, rotated about its axis while the oven temperature was elevated 2–5 F. After the oven reached equilibrium, the band was reattached and new values of I_{s1} and T_{1f} were measured. This routine was continued until, at some elevated oven temperature, either the value of T_{1f} became excessive, or material transfer occurred. The latter occurred whenever the rotor surface temperature reached a certain critical value at which the desorption rate exceeded the adsorption rate for a given compound, i.e., the films become nonunimolecular or are nonexistent.

V. Results and discussion

A. Langmuir-Blodgett Films

The results obtained for all parameters, both measured and calculated for stearic acid films adsorbed on three different rotors, are listed in Table 3.

The values of f_{ki} vary from 0.10 to 0.18 for a single monolayer and from 0.06 to 0.09 for two or more layers. This is as expected since it has been clearly shown (*10–12*) that only a small decrease in friction occurs when the number of layers is greater than one.

Early in this study, experiments showed that the film thickness employed could have no appreciable effect upon the tension developed in the band because even the thickness of nine monolayers of stearic acid is small compared to the surface roughness of the rotor. This was shown when five different thicknesses of stearic acid were adsorbed on five different rotors and measurements were made of K_e/t_g^2 at five different areas on each rotor. It was found that the average value of this ratio was 2.185×10^9 in.$^{-2}$. This same experiment was repeated with a carboxylic acid of only 14 carbon atoms (myristic acid) and an identical average value was obtained. For a clean surface, K_e is nearly 1, and t_g is approximately 21×10^{-6} inches, which is the order of magnitude of the surface roughness. The thickness of one monolayer of stearic acid and the thickness of one monolayer of myristic acid are, respectively, 8.94×10^{-8} and 6.97×10^{-8} inches. The thickness of a single monolayer of the other carboxylic acids referred to later in this report (caprylic, capric, and lauric acids) in even less.

It can be concluded that the adsorbed films are very thin compared to the gap thickness and that they do not have any significant effect upon the value of either K_e or t_g. It is assumed that the average value of K_e/t_g^2 practically remains constant for all adsorbed films, and hence the numerical value of 2.185×10^9 in.$^{-2}$ is used in all calculations of the values of T_{1i} and T_{1f} shown.

Note in the tabulation (Table 3) that different values of V_{g1f} are listed for films of identical thickness adsorbed on the same rotor. This is due to the fact that V_{g1f} was measured at any time that a decrease in V_{g1i} was judged to be significant. The magnitude of the decrease was arbitrarily selected for each evaluation.

Comparison of the values of f_{kf} with V_{g1f} shows in general that an inverse linear relationship exists, i.e., the final coefficient of friction increases as the value of V_{g1f} decreases. This relationship is a reflection of the amount of transfer that has occurred rather than the thickness of the remaining adsorbed film, because the average kinetic coefficient of friction of a clean, grease-free, abraded rotor is only 0.22–0.28, although many of the tabulated values of f_{kf} are much greater. Apparently, there is a corresponding increase in friction as the surface roughness increases with material transfer.

The most revealing data shown in Table 3 are the good correlations between the measured and calculated values of T_{1i} and T_{1f}. This is clearly shown in Fig. 4, where the measured values in Group A[4] are plotted versus their calculated values. For comparison purposes, it is convenient to show a one-to-one correspondence between calculated and measured values with the use of a straight line.

The correlation of the tension values tabulated in Groups B and C of Table 3 is shown in Fig. 5. Included are values measured with adsorbed films of myristic acid, the molecule of which has a chain length of only 14 carbon atoms. This plot reflects the effect which two different fatty acids have on the correlation. It includes the deviations introduced by four different rotors, as well as the deviations introduced when the tension measure-

[4] The band is rubbing on the hydrocarbon end of the molecule each time that T_{1f} is measured, since only the odd-numbered layers were evaluated.

TABLE 3
Friction, Voltage, and Tension Data for Langmuir-Blodgett Films of Stearic Acids

Number of monolayers n-$C_{17}H_{35}COOH$	Average kinetic coefficient of friction		Voltage at Rotor-band interface		Tension developed in band (lbs)			
					Measured		Calculated	
	Initial f_{ki}	Final f_{kf}	Initial V_{g1_i}	Final V_{g1_f}	Initial T_{1_i}	Final T_{1_f}	Initial T_{i_i}	Final T_{i_f}
Group A—Adsorbed on rotor No. 6								
1	0.08	0.23	246	123	1.95	1.95	2.38	2.11
3	0.10	0.24	191	121	1.79	1.46	1.85	2.17
3	0.06	0.20	222	139	1.46	1.94	1.42	2.25
3	0.08	0.26	264	154	2.27	2.58	2.81	3.31
5	0.08	0.40	248	83	2.92	1.95	2.42	2.15
5	0.08	0.23	269	160	2.75	2.94	2.85	3.58
7	0.08	0.23	275	156	2.58	2.58	2.98	3.40
9	0.06	0.19	246	109	1.65	1.10	1.74	1.29
Group B—Adsorbed on rotor No. 2								
1	0.10	0.22	108	70	0.66	0.66	0.59	0.57
1	0.10	0.27	124	66	0.77	0.66	0.77	0.66
2	0.18	0.30	120	50	1.10	0.51	1.30	0.43
2	0.18	0.30	136	50	1.10	0.55	1.61	0.43
3	0.07	0.18	136	80	0.51	0.48	0.57	0.58
3	0.07	0.18	130	86	0.77	0.55	0.51	0.66
4	0.07	0.26	130	60	0.49	0.44	0.52	0.52
4	0.07	0.33	150	50	0.66	0.44	0.69	0.50
5	0.07	0.10	136	110	0.49	0.44	0.57	0.54
5	0.07	0.10	132	110	0.49	0.44	0.54	0.54
6	0.07	0.17	180	100	0.88	0.77	0.99	0.84
6	0.07	0.07	156	90	0.90	0.70	0.74	0.68
Group C—Adsorbed on rotor No. 4								
1	0.08	0.29	180	50	0.99	0.40	1.14	0.42
1	0.08	0.29	195	60	1.65	0.44	1.34	0.60
2	0.09	0.50	150	40	1.32	0.81	0.90	0.61
2	0.09	0.50	140	30	1.32	0.73	0.79	0.35
3	0.09	0.32	200	50	1.58	0.44	1.61	0.48
3	0.09	0.60	150	20	0.77	0.44	0.91	0.21
4	0.09	0.60	150	26	0.99	0.48	0.91	0.36
4	0.09	0.60	120	33	0.88	0.55	0.58	0.58
5	0.07	0.12	170	140	0.77	0.88	0.89	1.09
5	0.07	0.16	160	120	0.66	0.79	0.78	1.12
6	0.08	0.70	210	32	1.54	0.55	1.56	0.74
6	0.08	0.70	170	36	1.35	1.01	1.05	0.93

ments are made on the even-numbered layers where the band rubs on the carboxylic end of the molecule. Thus, it is clear that the tension developed in the bands can be calculated by using Eq. [8], and that film thicknesses equivalent to from one to nine monolayers of stearic acid do not change the values of K_e and t_g corresponding to clean, grease-free, abraded surfaces.

B. Evaporated Films

The results obtained with each acid were identical to those reported previously for a single monolayer of each adsorbed by the Blodgett method. However, in each case the high temperature required to maintain adequate vapor pressure was considered excessive for practical purposes because a reasonable oven-evaporation temperature should not elevate the rotor surface temperature above 140 F. Since the melting points of caprylic, capric, and lauric acid (see Table 2) are considerably less than stearic and myristic acid, a single monolayer of each was adsorbed on three different rotors at temperatures 10 F above the respective melting points of these acids. The results obtained under normal clutch-operating conditions were identical to those measured with the longer chain acids.

The compounds studied with the oven evaporator were the four monocarboxylic acids, caprylic, capric, lauric, and myristic. For brevity, a tabulation of all recorded data is excluded. Only the temperature curves and the correlation diagram of all measured and calculated values of T_{1f} with the four monocarboxylic acids are shown.

Curves of the tension-oven temperature and the tension-rotor temperature with evaporated caprylic acid

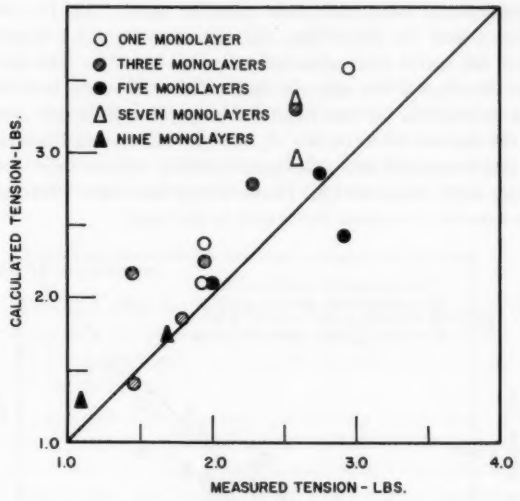

FIG. 4. Correlation of calculated and measured values of initial and final tensions developed in band for films adsorbed on rotor 6.

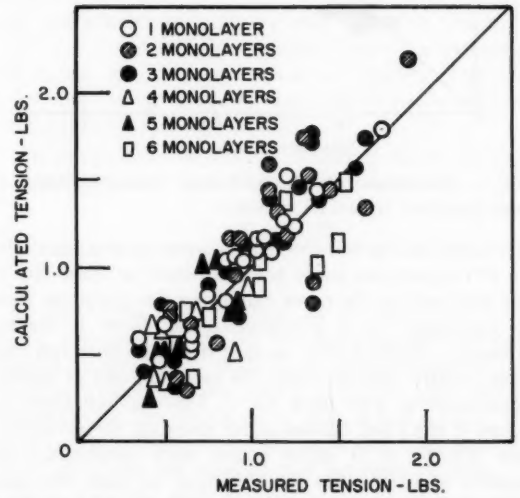

FIG. 5. Correlation of calculated and measured values of initial and final tensions developed in band for films adsorbed on rotors 2 and 4.

adsorbed on rotor No. 5 are shown in Fig. 6. Note that a sharp increase develops in band tension when the oven temperature is 87 F and the rotor temperature is 112 F, and that another sharp increase occurs when both the oven and rotor temperature are 120 F. These transition temperatures differentiate the molecular dimensions of the adsorbed film. For example, it can be shown by ellipsometric measurement that when the oven temperature is between 87 and 120 F and the rotor temperature is between 112 and 120 F, a single monolayer of caprylic acid is adsorbed at the solid/band interface. Above an

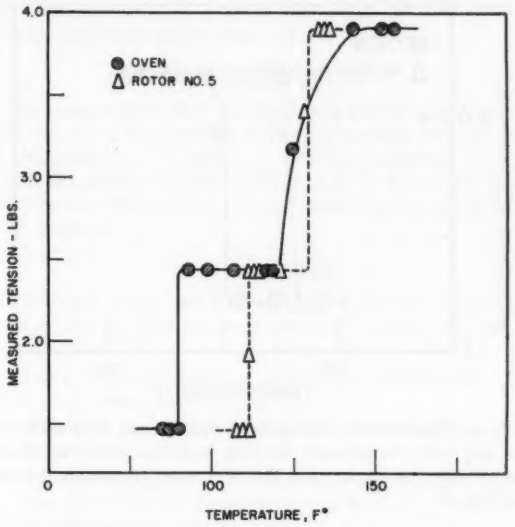

FIG. 6. Variation of tension developed in band with respect to oven and rotor temperatures.

oven and rotor temperature of 130 F, the film is either nonexistent or nonunimolecular. At oven temperatures less than 87 F or rotor temperatures less than 112 F, two or more monolayers of caprylic acid can be measured. These transition temperatures reflect the energy level necessary to desorb the first and second monolayers. Transition temperatures were not detected for films thicker than two monolayers; apparently, the differences in the energy levels necessary to desorb each successive monolayer above two are much smaller than those required to desorb the first and second monolayers.

Examination of Fig. 6 also shows that above 130 F the rotor temperature is always less than the oven temperature, but between 87 and 130 F it is generally higher. This is explained by the fact that the tension developed in the band was measured with a decreasing oven temperature and before complete equilibrium had been established between oven and rotor temperature. In all other tension measurements the oven temperature was always higher than the rotor temperature because measurements were made with an increasing oven temperature. In any case, however, the rotor temperature is the important parameter.

The transition temperatures were found to be dependent on the rotor surface temperature and on the chemical specie and its molecular structure. The amount of tension developed at the transition was dependent upon the value of $R_{\phi 1}$, which varies with each rotor and the particular area on the rotor surface rubbed by the band.

Figure 7 shows another tension-temperature curve of caprylic acid adsorbed on rotor No. 5. Only that part of the curve exhibiting the transition from two monolayers to one monolayer is shown. This graph not only illustrates

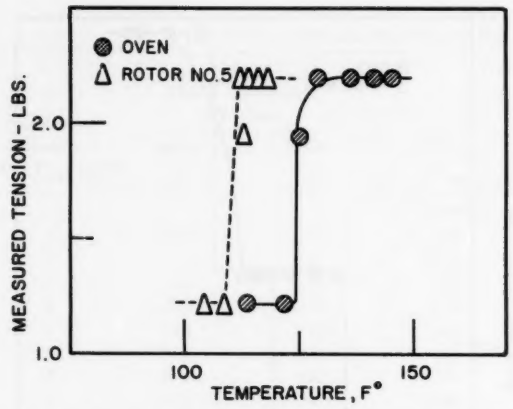

FIG. 7. Variation of tension developed in band with respect to oven and rotor temperature, showing transition from two monolayers to one monolayer when the band slides on an area different from Fig. 6.

that a change in the amount of tension can occur when a different area of the rotor surface is rubbed by the band, but also shows that, for a given chemical specie and molecular structure, the transition from two monolayers to one monolayer always occurs at some critical rotor temperature irrespective of oven temperature.

A demonstration of the effect of molecular structure on the transition temperature for evaporated lauric acid adsorbed on rotor No. 5 is shown in Fig. 8. Again, only that part of the curve exhibiting transition from two monolayers to one monolayer is shown. Here, the critical transition temperature of the rotor surface is 130 F and is easily reproducible; this contrasts with the

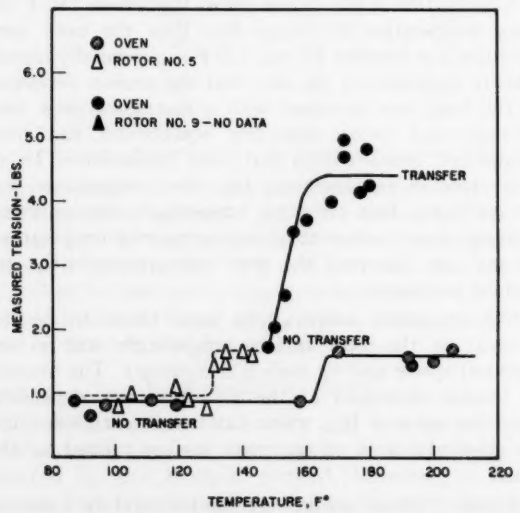

FIG. 8. Variation of tension developed in band with respect to oven and rotor temperature, showing effect of increased chain length.

temperature measured with caprylic acid, 112 F (see Figs. 6 and 7). Note that the amount of tension developed for lauric acid adsorbed on rotor No. 5 is less than that developed for caprylic acid. This difference may be due completely to the band rubbing on a different area of the surface of rotor No. 5, but the correlation diagram of the measured and calculated tension values (see Fig. 9) strongly suggests that chain length has some effect on the amount of tension developed in the band.

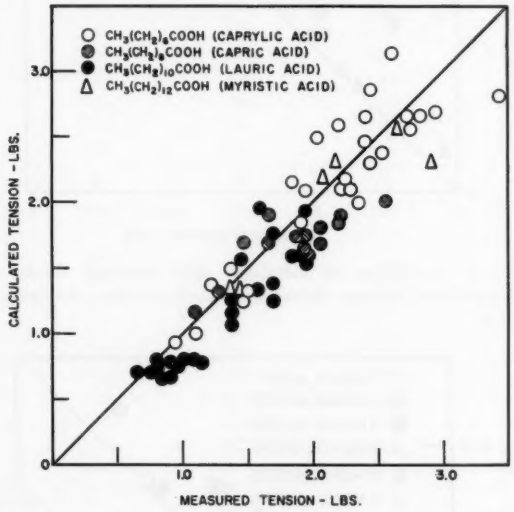

FIG. 9. Correlation of calculated and measured values of tension developed in band for all liquids.

Included in Fig. 8 is the tension-oven temperature relation of evaporation lauric acid adsorbed on rotor No. 9. Only that part of the curve exhibiting the transition from one monolayer to a nonunimolecular layer is shown. Although a different rotor is used it will be observed that before transfer has occurred, the same amount of tension is developed as with rotor No. 5. This was not found to be true if the band rubbed other areas on the surface of rotor No. 9, or if other rotors were employed; the diameter of each rotor was different so that the oven temperature necessary to reach a critical rotor-transition temperature varied with each rotor.

This curve serves to illustrate that, for a given compound, the transition temperatures are not always identical for all rotors. For example, note that the transition from one monolayer to a nonunimolecular layer occurs with rotor No. 9 when the oven temperature is between 150 and 160 F; however, with rotor No. 5 two or more monolayers are still adsorbed at this temperature interval.

The correlation of all measured and theoretically calculated values of the tension developed in the band with four different evaporated monocarboxylic acids is shown in Fig. 9. The results strengthen the reliability of Eq. [8] and indicate that the average value assumed

for K_e/t_g^2 (2.185×10^9 in.$^{-2}$) is also applicable to dynamically evaporated films, even though the diagram indicates that, except for the myristic data, the band tension decreases with increasing chain length. Evidently, the observed inverse relationship arises from the fact that with condensed films of monocarboxylic acids f_k decreased with increasing chain length, reaching an asymtotic minimum with a 12-carbon compound (*3*, *9*, *10*).

VI. Conclusions

This investigation has shown that condensed mono- and multilayers of monocarboxylic acids adsorbed at the rotor-band interface can prevent transfer of rotor material to the band.

It was discovered that dynamically evaporated films show a transition temperature, different for each compound and for each rotor, above which one monolayer is maintained and below which two or more monolayers are maintained as adsorbed films on the rotor surface. A similar temperature exists for the transition of one monolayer to a nonunimolecular layer. A single monolayer can be maintained as an adsorbed film on the rotor surface at any temperature between the two transition points; the force developed will be constant and of a predictable magnitude. At least one or more monolayers of adsorbed films must be continuously maintained on the rotor surface to prevent material transfer.

An analysis of the tension developed in the band has shown that it can be calculated from the equation.

$$T_1 = 7.27 \times 10^{11} \frac{K_e \varepsilon_0 V_{g1}^2 W_r}{2 t_g^2} \exp(f_k \theta - 1)$$

It was found that the value of K_e/t_g^2 (2.185×10^9 in.$^{-2}$) remained practically constant for all compounds studied. Experiments with clean surfaces showed that K_e is approximately one and t_g is of the same order of magnitude as the roughness of the surface (21×10^{-6} inches). Since the adsorbed films are very thin, the values of K_e and t_g are the same as that for clean surfaces.

Measurements with rotor and band surfaces whose roughness was of the order of 21×10^{-6} inches showed that the amount of tension developed in the band is greater for a monolayer than for multilayers.

ACKNOWLEDGMENT

The excellent work of W. C. Chocholaty and R. A. Schumacher, who obtained a large portion of the experimental data and aided in the preparation of tables and figures, is gratefully acknowledged. The authors are also indebted to T. C. Ku for his help in planning this study and for valuable suggestions during the course of its progress.

REFERENCES

1. Johnsen, F. A., and Rahbek, K., "A Physical Phenomenon and Its Application to Technology," *I.E.E. Journal* **61**, 713-725 (1923).
2. Fitch, C. J., "Development of the Electrostatic Clutch," *IBM J. Res. Develop.* **1**, 49-56 (1957).
3. Hardy, W. B., "Collected Scientific Papers." Cambridge Univ. Press, 1936.
4. Blodgett, Katharine B., "Films Built by Depositing Successive Monomolecular Layers on a Solid Surface," *J. Am. Chem. Soc.* **57**, 1007-1022 (1935).
5. Levine, O., and Zisman, W. A., "Physical Properties of Monolayers Adsorbed at the Solid-Air Interface. II. Mechanical Durability of Aliphatic Polar Compounds and Effect of Halogenation," *J. Phys. Chem.* **61**, 1188-1196 (1957).
6. Levine, O., and Zisman, W. A., "Physical Properties of Monolayers Adsorbed at the Solid-Air Interface. I. Friction and Wettability of Aliphatic Polar Compounds and Effect of Halogenation," *J. Phys. Chem.* **61**, 1068-1077 (1957).
7. Bowers, R. C., Clinton, W. C., and Zisman, W. A., "Frictional Behavior of Polyethylene, Polytetrafluoroethylene and Halogenated Derivatives," *Lubrication Eng.* **9**, 204-208 (1953).
8. Bowers, R. C., Clinton, W. C., and Zisman, W. A., "Friction and Lubrication of Nylon," *Ind. Eng. Chem.* **46**, 2416-2419 (1954).
9. Bowden, F. P., and Tabor, D., "The Friction and Lubrication of Solids." Oxford Univ. Press, London and New York, 1950.
10. Langmuir, I., "Mechanical Properties of Monomolecular Films," *J. Franklin Institute* **218**, 143-171 (1934).
11. Bowden, F. P., and Leben, L., "The Friction of Lubricated Metals," *Phil. Trans. Roy. Soc.* **239A**, 1-27 (1946).
12. Hughes, F. P., and Whittingham, G., "The Influence of Surface Films on the Dry and Lubricated Sliding of Metals," *Trans. Faraday Soc.* **38**, 9-27 (1942).

ASLE TRANSACTIONS 6, 218-226 (1963)

The Behavior of a Silicone-Lubricated Electrostatic Clutch

By P. J. MAGILL,[1] R. E. McCURRY,[1] and
R. R. SCHAFFER[2]

The performance of a silicone-lubricated electrostatic clutch, as originally reported by Fitch [IBM J. Res. Develop. **61**, No. 1 (1957)], *differs considerably from that of one using dry surfaces or boundary lubricants. The study reported here, of constriction resistance and the dependence of the coefficient of friction on the bearing modulus* (μ v/p), *provides a qualitative and quantitative explanation of this behavior. The existence of an air film was experimentally observed for the first time. This film, occurring under proper speed and loading conditions, explains the low residual torque. Effects due to voltage, rotor surface speed, fluid viscosity, band width, and surface roughness are shown to exist and are discussed. The lubricating film thickness, determined by a radioactive tracer technique, is shown to depend on rotor surface speed and voltage.*

I. Introduction

THE electrostatic clutch, as originally conceived, is based on the Johnson-Rahbek effect (*1*). This effect depends upon the existence of a large constriction resistance between two mating surfaces. Due to this resistance and the fact that the major part of the surfaces is separated by a narrow gap (insert of Fig. 1), an applied voltage produces an electrostatic force. It is this force that has been utilized in the development of the clutch. In its early versions (*2*) the clutch was operated using dry surfaces, although the original studies (*1*) showed a need for the presence of minute quantities of moisture. Subsequent studies (*3, 4*) yielded inconsistent results, a conclusion being that the clutch was unreliable and, therefore, not usable. Actually what these studies point out is that the clutch characteristics depend on the surface properties and that the preservation of these properties is essential to continued satisfactory operation.

Fitch (*2*) conceived the idea that a silicone lubricant would preserve these surface properties and simultaneously reduce the operating temperatures. The clutch utilized by Fitch, and reported here (Fig. 1), consisted of a metallic band wrapped around a portion of a rotating cylinder (rotor) composed of a highly polished, high-resistivity material. The band and rotor comprise concentric plates between which the electrostatic force exists when a voltage is applied. With the cylinder rotating a tension is developed in the band that depends on the normal force and the coefficient of friction. This relationship is given by (*5*):

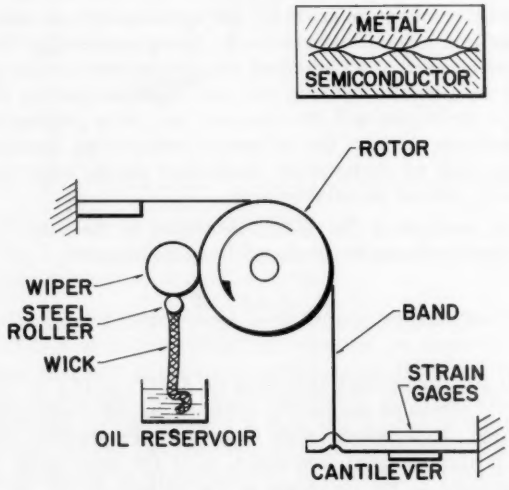

FIG. 1. Schematic diagram of clutch used for measurement of dynamic behavior.

$$F = 4.52\,Klr\frac{V^2}{h^2}\,(e^{f\theta} - 1) \times 10^{-10} + F_0\,e^{f\theta} \quad [1]$$

where F is the resultant tension (gm), K is the dielectric constant of the gap material, l is the band width (cm), r is the cylinder radius (cm), V is the interface voltage (volts), h is the gap separation (cm), f is the coefficient of friction, θ is the wrap angle (radians) and F_0 is the initial tension (gm).

Earlier investigators (*3, 4*) (utilizing basically dry surfaces) were unable to find a definite dependence of tension (or normal force) on the square of the applied voltage. The silicone lubricant introduced an unexplained dependence of tension on the speed of the rotor.

Contributed to the American Society of Lubrication Engineers by the authors. Manuscript received April 22, 1963.

[1] Staff Physicist, IBM, General Products Division, Development Laboratory, Endicott, New York.

[2] Advisory Engineer, IBM, General Products Division, Development Laboratory, Endicott, New York.

In order to explain these observations the present authors postulated the following:

(1) The constriction resistance and its variation with load may account for the lack of dependence of tension on the square of the applied voltage.

(2) The clutch mechanism was, in essence, a type of a fluid film bearing. Consequently, the coefficient of friction should depend on the so-called "bearing-modulus," $\mu\ v/p$. Here μ is the viscosity (centistokes), v is the speed (cm/sec), and p is the pressure (gm/cm^2).

As a result of these postulates it appeared that the constriction resistance, voltage, coefficient of friction, and fluid film thickness should be interdependent. The experimental work described in this report and the subsequent analysis support the above hypothesis.

II. Experimental methods and results

A. Constriction Resistance

Both static and dynamic measurements of constriction resistance were performed. The former was carried out by the crossed bar technique (*6*) using a small steel bar and a bar of the moulded clutch material with surface preparation similar to that used by Fitch (*2*). A load range of 0–500 gm was employed and currents were minimized to prevent excessive heating. The relationship $R \propto L^{-1/2}$ (L is the normal load) was observed and is indicative of plastic deformation (*6*). To study the effects of higher voltages, without introducing large electrostatic forces, it was necessary to replace the steel bar with a steel pin (tip radius approximately 0.01 cm). *V-I* characteristics (0–400 volts) were obtained for various loads. The effects at higher voltages were determined relative to those existing at 10 volts. At 10 volts the constriction resistance (R_c) was attributed solely to that of the mechanical load. The departure from this value of R_c at higher voltages was assumed as being due to the creation of conduction paths in parallel with the constriction resistance. This effective resistance was then calculated from the total resistance (measured) and the constriction resistance (measured at $V = 10$ volts). Its contribution to the *V-I* characteristic was evaluated and plotted in Fig. 2 as emission current vs. voltage. No hysteresis between R and V was observed at the higher voltages.

All dynamic measurements were taken utilizing silicone oil (a dimethyl polysiloxane) with a viscosity of 1000 centistokes at 25 C. For studying the constriction resistance of the clutch under dynamic conditions, a simulated clutch test robot was assembled (Fig. 1). It consisted of six ganged rotors with a common oiler system. Steel bands (.005 × .95 cm) were attached to give a wrap angle of 90°. One end was attached to an adjustable arm which could be positioned to control the initial tension. The other end was attached to a force transducer consisting of two strain gauges mounted on a cantilever beam.

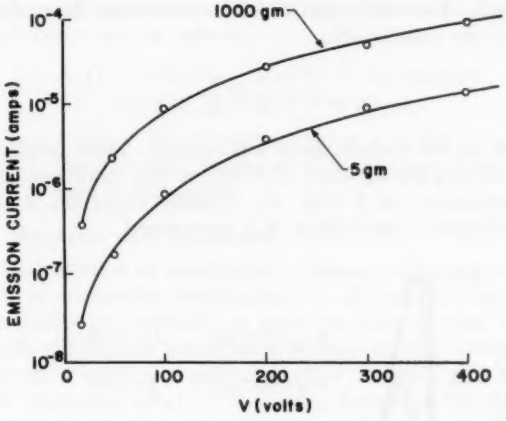

Fig. 2. Field emission current as a function of voltage

The resistance measurements were made by monitoring the current when a voltage pulse was applied to the clutch. Assuming a parallel circuit of a resistance and a capacitance, in series with the bulk resistance of the rotor, calculations are readily made from the measured current-voltage values. Representative values of R are plotted against the applied voltage in Fig. 3. The influence of rotor speed is evident from the family of curves for various speeds.

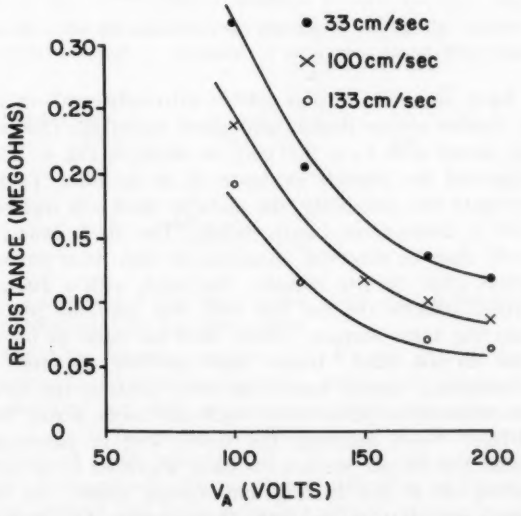

Fig. 3. Resistance as a function of applied voltage with rotor surface speed as a parameter.

B. Coefficient of Friction and Influence of Lubricant

To determine the dependence of f on the loading and speed, a single stage robot was constructed. It permitted measurement of initial tension and tension at various

speeds. The coefficient of friction was then determined from the relationship,

$$f = \frac{1}{\theta} \ln \frac{F}{F_0} \qquad [2]$$

since no electrostatic force was applied. These measurements indicate the effect of F_0 on the film conditions, and consequently on f (Fig. 4). Equally important is the simultaneous dependence of f upon speed.

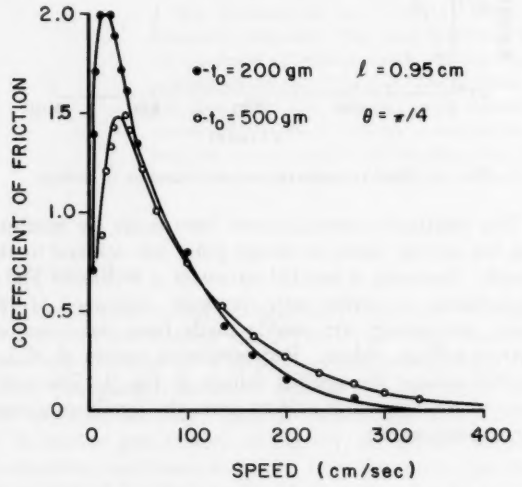

FIG. 4. Coefficient of friction as a function of rotor surface speed with initial tension as a parameter.

Most important to note are the extremely small values of f under proper loading and speed conditions (300 cm per second with $F_0 = 200$ gm), as shown in Fig. 4. This suggested the possible existence of an air film. To investigate this possibility, the metallic band was replaced with a transparent plastic band. The fluid behavior could then be observed visually. At high rotor surface speeds (400 cm per second), the band, with a 200-gm weight attached to the free end, was carefully placed onto the rotor surface. There were no signs of oil or wear on the band. Under light touching, to promote translational motion across the rotor surface, the band was observed to glide freely, back and forth, across this surface. Upon reducing the speed, and in particular below 300 cm per second, the band appeared to be contacting oil at the leading and trailing edges. As the speed was further reduced, these regions of contact spread out. Finally, in the vicinity of 33 cm per second, the entire band was dragging through the oil. Under this condition, the plastic band exhibited signs of wear. Thus, it was shown for the first time that an air film can, and does, exist under proper conditions. Furthermore, the dragging effect at low speeds contributes to the high effective coefficient of friction, as seen in Fig. 4. The uncertainties in data at the lower speeds (10–15%) are far from sufficient to account for the large observed values of f.

All of these measurements illustrated the residual tension of the clutch, i.e., the tensile force when $V = 0$. To determine tension under actuated conditions ($V > 0$), the test robot previously described was used. The tension was recorded via the strain gauge output by use of an oscilloscope strain gauge plug-in unit. Its maximum sensitivity was approximately 110 gm per centimeter deflection on the oscilloscope. The experimental results, shown in Figs. 5a and 5b, are similar to those

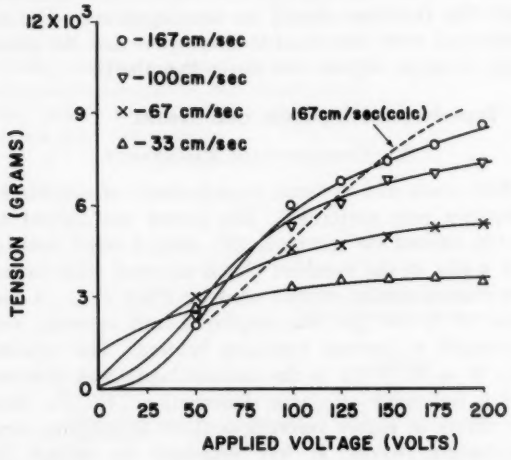

FIG. 5a. Tension as a function of applied voltage with rotor surface speed as a parameter.

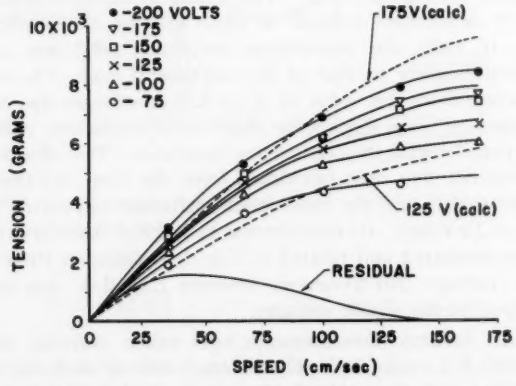

FIG. 5b. Tension as a function of rotor surface speed with applied voltage as a parameter.

originally observed by Fitch (*2*) for tension vs. voltage and tension vs. speed, even though the techniques used were not similar. Since both graphs are families of curves for various speeds and voltages respectively, it is obvious that one could be inferred from the other. Consequently, the residual torque curve ($V = 0$) must account for the crossover of the tension vs. voltage curves. It should

also be noted that the tension approaches limiting values for both voltage and speed. The "calculated" curves are the result of the work discussed in Section III, B.

C. Additional Studies

No study was made of other viscosities except for the evaluation of some recent unpublished work by Fitch (Section III, B). Other factors that would influence the operation of the clutch are band width, surface roughness, and rate of oil application. All of the preceding data were taken using 0.95-cm width bands. To determine the influence of band width, several bands varying in width from 0.200 to 3.17 cm were installed (on the robot) in place of the original bands. The results showed that the tension/width was not independent of band width, for either constant applied voltage or constant gap voltage. What was observed was a maximum (in both cases) occurring in the region of 0.9-cm band width.

For surface roughness influence, several rotors were prepared, with surface roughnesses varying from 1×10^{-5} to 4×10^{-5} cm. The roughness measurements were made with a profilometer-type instrument, so these measurements are only approximate. Nevertheless, the spread in roughness noted was still indicative of the variance in surface properties. The tension measurements showed decreasing values with increasing roughness. Due to the dependence of tension on $1/h^2$ (Eq. [1]) this result should be expected. On the other hand, the constriction resistance increased and then showed a slight decrease at maximum roughness.

The study of influence of oiler rate was restricted to a band width of 0.95 cm. The oil rates studied were 1, 2, and 3.5 rpm of a 1.5-cm radius oil cylinder supporting the pile fabric wiper (Fig. 1). The results observed for a rotor surface speed of 133 cm per second, at voltages (V_A) of 150 and 200 volts were: (1) approximately a 10% increase in tension over the range of increased oiler speed; and (2) an increase in gap resistance (R_g) and gap voltage (V_g) over the same range.

At a rotor surface speed of 67 cm per second the tension decreased by approximately 10%, with increasing oiler speed, but with a similar increase in gap resistance and gap voltage.

Finally, as an added and very important study, the thickness of the fluid film was determined by a radioactive tracer method. A radioactive silicone oil, having the same viscosity as the silicone oil used as the lubricant, was applied to the rotor. A geiger counter, mounted close to the rotor, measured the radiation emitted from a constant area of the oil film on the rotor. The count rate obtained was converted to the thickness of oil film by suitable conversion factors.

The results of these measurements as a function of speed and voltage were analyzed and equations approximating each set of data were developed. These calculated relationships are as follows:

$$h \approx h_0\,(1 - 0.003V_g);\ 50 < V_g < 125 \text{ volts } DC$$
$$\approx 0.4\,h_0;\ V_g > 125 \text{ volts } DC \qquad [3]$$

where $h_0^2 \approx 5 \times 10^{-12}\,(520 - v)$; $0 < v < 300$ cm per second. The restricted ranges of V_g and v are those of main concern in this report.

III. Analysis and Discussion

The variation of constriction resistance with load permits a qualitative explanation of the tension-voltage characteristics. Initially, it must be realized that the clutch mechanism serves as a voltage divider network with the constriction resistance (R_C) in series with the bulk resistance (R_B) of the rotor. Secondly, the constriction resistance is a variable, depending upon the load ($R_C \propto L^{-1/2}$). The load, in this case, is the electrostatic force

$$L \text{ gm} = 4.5K\frac{AV_g^2}{h^2} \times 10^{-10} \qquad [4]$$

where V_g is the voltage across the gap separating the band and rotor, and A is the area (cm^2). Consequently, the constriction resistance is inversely proportional to the gap voltage ($R_C \propto 1/V_g$), all other factors assumed constant.

Using the voltage divider network where $V_g = R_C/(R_C + R_B) \times V_A$, the variation of R_C with the load, and Eq. [4], the gap voltage may be expressed by the following relationship:

$$Vg = -\frac{\alpha h}{2R_B\sqrt{l}} + \frac{\alpha h}{2R_B\sqrt{l}}\left(1 + \frac{4R_B\sqrt{l}}{\alpha h}V_A\right)^{1/2} \qquad [5]$$

where

$$\frac{4R_B\sqrt{l}}{\alpha h} \sim 10^{-3},$$

α is a constant, l the band width (cm), and h the film thickness (cm) or gap separation.

Assuming constant values of l, h, and R_B, V_g approaches V_A for small values of V_A only. As V_A increases, V_g deviates and then approaches a fixed percentage of V_A. If R_B is increased, the deviation of V_g is greater, starting at lower values of V_A than in the preceding case. Consequently, for maximum utilization of the applied voltage the bulk resistance should remain small compared to the constriction resistance.

As the voltage range is extended to higher values another limiting factor is introduced. This factor is the creation of conduction paths (by virtue of field emission) in parallel with the constriction resistance. Work by Stuckes (*4*) and Sillars (*7*) substantiate this. Stuckes used high bulk resistance material and neglected any variation of constriction resistance with load. Figure 2 was

plotted on the assumption of this parellel conduction path. The resultant current voltage relationship is of the form $I = A\,V^n\,e^{-B/V}$ (A, n, B are suitable constants). Calculations show that $n \approx 2$, as predicted by Sillars. Thus, at sufficient voltages the constriction resistance is effectively altered and the actual resistance can no longer be attributed to one parameter (R_C). This effect certainly places a limitation on achievable gap voltages.

In considering the tension-voltage relationship, therefore, the influence of constriction resistance and field emission explain the departure from the anticipated. In brief, at low voltages the tension will be proportional to the square of the applied voltage, deviating from this at higher voltages due to variation of constriction resistance and finally approaching a limiting value due to the onset of field emission.

B. Coefficient of Friction and Influence of Lubricant

In lubrication studies, the coefficient of friction (f) is usually expressed as a function of the parameter ($\mu\, v/p$). When f is shown graphically as a function of this parameter, two general regions of lubrication are indicated: boundary and hydrodynamic (*8*). These two regions are joined by a transition region of mixed lubrication. The slope of f vs. $\mu\, v/p$ is negative in the mixed lubrication region and increasingly positive in the hydrodynamic region. Kriesle (*9*) has noted that the minimum thickness for complete hydrodynamic lubrication occurs at a spacing equal to the sum of the surface roughness values. Below this thickness the lubrication is quasi-hydrodynamic and eventually enters into the boundary region. For the silicone-lubricated electrostatic clutch tested, the sum of the surface roughnesses was about 2×10^{-5} cm, and the measured (rms) values of the fluid thickness determined by the tracer technique were $2\text{–}4 \times 10^{-5}$ cm. This indicates that the lubrication could be quasi-hydrodynamic or hydrodynamic.

The preceding conclusion is interesting in view of the previous experimental work by Fitch on both residual and applied voltage tension, which indicated that the coefficient of friction increased positively with speed. This lends support to the hydrodynamic form of lubrication. To more clearly illustrate this, we use the coefficient of friction measurements similar to those shown in Fig. 4. The values measured (calculated from Eq. [2]) are plotted against $\mu\, v/p$, as shown in Fig. 6. As a guide, separate regions showing dependence on $(\mu\, v/p)^n$ are illustrated. At low values of $\mu\, v/p$, a type of Couette flow exists ($n = 1$). As the bearing modulus increases, the dependence changes to a converging wedge of Blok "foil" type of bearing ($n = 1/2$). Unusual care is important in interpreting the data beyond this point. As was so strongly indicated in Section III, B, air is introduced (under residual torque conditions) beyond certain rotor speeds. The point at which admittance begins is governed largely by the distribution of oil on the surface.

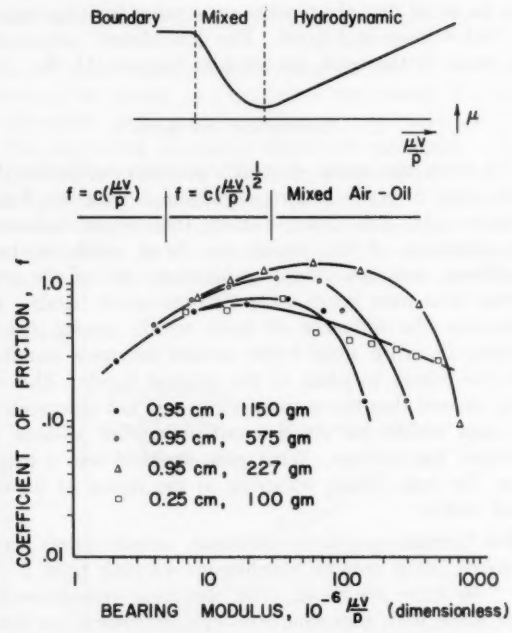

FIG. 6. Coefficient of friction as a function of bearing modulus

Thus, the oiler speed, initial tension, and rotor surface speed are all supporting parameters. After the introduction of air has commenced, a transition region of air and oil exists. This extends over a broad range of speeds, until the point is reached at which a complete air bearing is developed between the band and the surface supporting the oil.

As a result of this action, the plot of f vs. $\mu\, v/p$ (Fig. 6) is somewhat misleading. In this plot the viscosity (μ) was assumed constant. It should be quite apparent that due to the varying admixture of air and oil, the true value of (μ) is unknown. The important point to remember is that, in spite of plotting against increasing values of $\mu\, v/p$, the actual value of $\mu\, v/p$ is probably decreasing. The negative slope region, therefore, should be reflected onto the positive slope or reduced $\mu\, v/p$ values. Thus, over the entire region f is a function of $(\mu\, v/p)^n$, where n is positive.

Two major conclusions arise from the over-all evaluation of the coefficient of friction studies. First, there exist, in some regions, large values of the coefficient of friction. Such values (> 1) are seldom observed in hydrodynamic lubrication, presumably because high viscosity fluids are inconsistent with the need for hydrodynamic lubrication. In the present case the large coefficient of viscosity is desirable; obviously, a viscous drag on the band results. This drag, in simplified form, is equal to the coefficient of viscosity multiplied by the velocity gradient. In view of its contribution to the coefficient of friction, one might prefer to call the latter an effective coefficient. In any event, the resultant values

(Fig. 4) incorporate this influence. In the present case, to compare Fig. 6 with the over-all picture of f vs. $\mu\, v/p$, the latter is inserted in Fig. 6. The experimental data projects only onto the positive-slope region of the inserted graph.

Second, there exists under some operating conditions a complete air film. This film—which has been observed visually—cannot be overemphasized. It allows the extremely low residual torque and simultaneously aids in maintaining cool the rotor surface. The latter is important in maintaining thermal stability of the fluid. As a consequence of this film, the electrostatic force, when applied, forces the band through the air film and onto the oil surface covering the rotor. At that time, a tension develops in the band that is due to the Johnson-Rahbek effect and also due to a viscous drag by the oil. That the latter is true is indicated by previous work that yielded smaller tensions for unlubricated (nonsilicone) surfaces. Further evidence is obtained in the subsequent analysis on the dynamic behavior of the clutch.

The dynamic behavior of the clutch has been illustrated in Figs. 5a and 5b. Using this data in conjunction with Eq. [1] ($V = V_g$) and Eq. [3], the coefficient of friction was calculated. The values of f so determined were plotted against $1/V_g$ (Fig. 7). Using the linear relationship of f to $1/V_g$, Eq. [1] becomes:

$$F = \frac{270\, V_g^2\, (e^{33/V_g} - 1)}{(520 - v)\,(1 - 0.003\, V_g)^2} \qquad [6]$$

This holds for a .95-cm band width, a wrap angle of 90°, and a rotor radius of 3.17 cm.

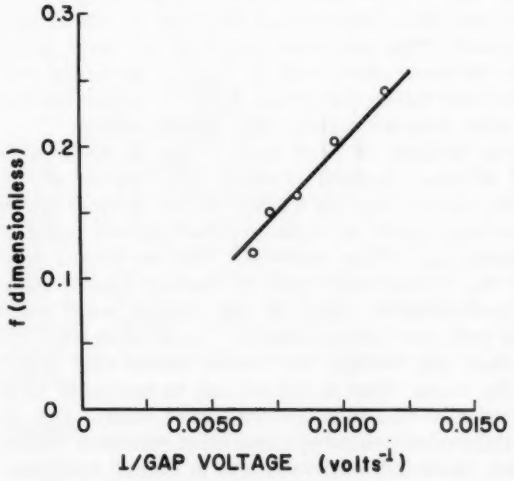

Fig. 7. Coefficient of friction (calculated, see text) as a function of reciprocal gap voltage.

Since the exponential term, $f\theta$, is dependent upon $1/V_g$ ($V_g \sim p^{-1/2}$) the previous conclusion of $f = (\mu\, v/p)^n$ is now utilized. Here p^{-n} is assumed to be correlated directly with $1/V_g$ and Eq. [6] may be expressed in the form

$$F = \frac{C_1 V_g^2 \left(eC_2 \dfrac{(\mu v)^n}{V_g} - 1\right)}{(C_3 - v)\,(1 - 0.003\, V_g)^2} \qquad [7]$$

where C_1, C_2, and C_3 are constants. Over most of the speed and voltage ranges of interest the exponential term may be expanded and the logarithm taken.

$$\ln F = \ln C_4 + n \ln \mu + n \ln v + \ln V_g - \ln (C_2 - v) - 2 \ln (1 - 0.003\, V_g) \qquad [8]$$

where $\ln C_4$ results from grouping constant terms. For a given viscosity and gap voltage a plot of $\ln F$ vs. $\ln v$ should yield a straight line. Data plotted in this way are shown in Fig. 8 and the slope indicates a value of $n \approx 1/2$.

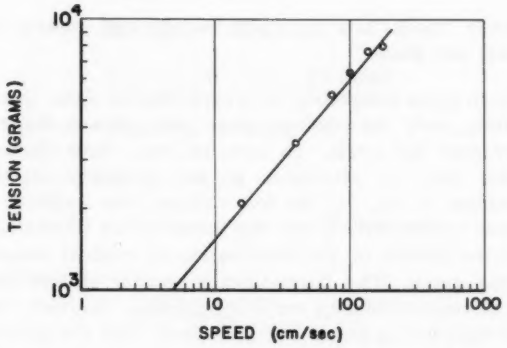

Fig. 8. Tension as a function of speed with constant viscosity and gap voltage.

Similarly, for a given speed and gap voltage, $\ln F$ vs. $\ln \mu$ should be a straight line with $n = 1/2$. In this case use was made of data taken by Fitch. The data shown in Fig. 9 are for different viscosity oils of similar VTC (viscosity temperature coefficient). The slope of the line is $n \approx 0.45$. Thus, reasonable support has been obtained for the assumption that $f \sim (\mu\, v/p)^{1/2}$. For the case studied here ($\mu = 1000$ cs) calculations of C_2 yielded a value of 2.5. Equation [7] becomes

$$T = \frac{270\, V_g^2 \left(e \dfrac{2.5 v^{1/2}}{V_g} - 1\right)}{(520 - v)\,(1 - 0.003\, V_g)^2} \qquad [9]$$

for the geometry stated for Eq. (6).

A quantitative comparison of Eq. [9] is shown with the experimental curves in Figs. 5a and b. Beyond 60 volts of applied voltage the approximate relationship of $V_g \approx 0.65\, V_A + 20$ was used to interchange V_g and V_A. This latter relationship was determined experimentally, coincident with R_g measurements. A plot of Eq. [9] superimposed on Figs. 5a and b shows that the theory

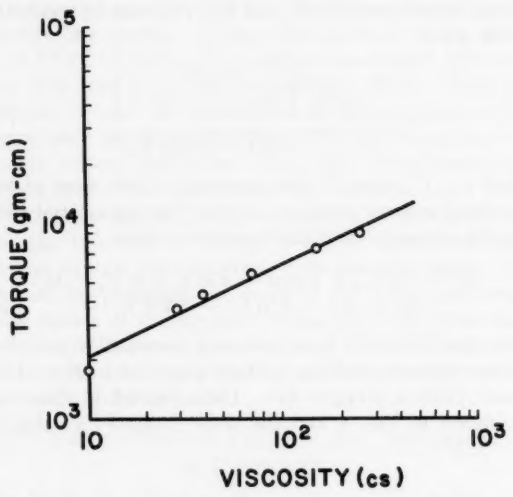

FIG. 9. Torque as a function of viscosity with constant gap voltage and speed.

fails to agree completely with experimental data. Qualitatively, only the tension-voltage plots show a discrepancy near the origin. In part, at least, these discrepancies may be attributed to the invalidity of the expansion of Eq. [8] for low voltages, the inability to account quantitatively for any air-oil mixed lubrication, and the neglect of the contribution of residual torques at low speeds. This latter effect is peculiar, in that now the electrostatic forces are being applied. However, the film thickness is greatest at low speeds, and the electrostatic forces are inversely dependent on the square of this thickness. Figure 5a shows but little difference in tension at low speeds ($<$ 33 cm per second) whether or not the voltage is applied. The viscous drag is very definitely significant in this range.

In spite of the lack of direct correspondence between experiment and theory, sufficient correlation exists to support the statement of the dependence of f on speed and loading. This, coupled with the coefficient of friction analysis from direct experimental data, is fairly conclusive. The inclusion of a study of the influence of the viscosity of fluids was neglected, other than Fitch's data, since it had been rather well established that the 1000 cs oil was one of the most stable for clutch usage. Consequently, all experimentation was restricted to this fluid. The dependence on viscosity was not included in the tension equation (Eq. [9]) due to the lack of knowledge of the dependence of viscosity on shear rate. Published data on the silicone oil shows the 1000 cs oil to be Newtonian up to shear rates of 10^4 sec^{-1}; no data is available for greater shear rates. The electrostatic clutch operates at least two orders of magnitude greater in shear rate. However, Fitch had tested some of the non-Newtonian silicone oils (i.e., $\mu >$ 1000 cs) and observed almost identical results as with 1000 cs oil. The dependence of torque on viscosity for various oils is illustrated in Fig. 9 for a range of viscosities (10–1000 cs). Not all oils obeyed this relationship strictly. However, as stated, it was fulfilled by those with similar VTC values. From this, it was concluded that the effect of shear rate may not be as pronounced as one might believe.

C. Surface Conditions and Band Width

The measurements taken with varying surface roughness indicate that close control on this parameter is needed for reproducible results. It should be apparent that the reduction in tension with increasing roughness follows directly from Eq. [1]. The important point to bear in mind is that any given rotor may vary (even slightly) from one region to another on the surface. As a consequence, the tension cannot be attributed to the rotor as a unit but rather to a given portion of the surface. Of the six rotors initially prepared for this study, one was completely out of tolerance with the rest. After reworking the surface, it gave results consistent with the others.

The variation of fluid thickness with speed and applied voltage has been shown previously (Eq. [3]). Another parameter influencing the film thickness is the oiler rate. Results (Section III, B) had indicated that in spite of similar increase in constriction resistance and gap voltage (as oiler rate increased), the tension increased for the higher rotor speed and decreased for the lower speed. Radioactive tracer measurements showed that increased oiler rates increase fluid film thickness. Thus, at the higher rotor speed and higher oiler rate, the increase in tension must be attributed to additional viscous drag. At the lower rotor speed, the increased oiler rate reduces the electrostatic force due to the increased thickness. That this latter effect did not occur in both cases of rotor speeds tends to support the earlier statement that the torque at low speeds is almost the same as that observed without any applied voltage.

The influence of band width is not as direct as Eq. [1] indicates. Analysis of tension as a function of band width showed that the tension did not increase directly with band width for either constant applied voltage or constant gap voltage conditions. That the tension should not vary directly with width for constant applied voltage is understandable, since the gap voltage might readily vary from one width to another. On the other hand, with constant gap voltage, the tension should vary directly as the width. That it did not can be attributed to the variation of film thickness with band width. This was partially substantiated by constriction resistance measurements which indicated variations in loading conditions.

D. Lubricant Properties

The silicone fluid studied in this report has a dielectric constant of 2.8 and a volume resistivity of the order of 10^{15} ohm-cm. From the dependence of tension on viscosity (Fig. 9) for fluids of different dielectric constants in

the range of 2–10, there is no apparent dependence on the dielectric constant. Furthermore, the admixture of air and oil would seemingly reduce the effective dielectric constant toward that of air. Therefore, the effect of the dielectric constants is likely to be insignificant for values in the range of 2–10. Such was assumed in this report and the dielectric constant of air was used throughout.

On the other hand, the volume resistivity is an important factor, intimately associated with the Johnson-Rahbek effect. What is essential is the stability of the fluid resistivity and its being large compared to the resistivity of the rotor material. If the resistivity approaches that of the rotor then additional conduction paths occur. Taken to the limit, a good conducting fluid would place both surfaces (rotor and band) at the same potential thereby reducing the electrostatic force of attraction to zero.

Finally, the lubricant should retain its viscous properties. As Fig. 9 illustrates the tension is definitely dependent on viscosity. Lubricants with higher viscosity than the 1000 cs silicone oil were tried by Fitch. However, they had poor shear properties and behaved like the 1000 cs silicone oil (i.e., their effective viscosity was reduced to that of the 1000 cs silicone oil).

IV. Conclusions

The operational characteristics of the silicone-lubricated electrostatic clutch have been shown to depend on the nature of the surface and upon the fluid lubrication. The former, by virtue of constriction resistance and its dependence on load, aid in explaining the tension-voltage characteristics. The latter, by virtue of the dependence of the coefficient of friction on speed, load, and viscosity, presents a model that is consistent with experimental results. This model also provides a basis for further investigative work. The lack of complete correlation of the proposed model (expressed in Eq. [9]) with experiment implies the need of such an investigation. For example, the complete behavior of the fluid during the engage time of the clutch should be analyzed. It is conceivable that the properties of the fluid may change during this time. Furthermore, it is plausible that both surface and lubricant properties may be altered under severe, and localized, conditions of temperature and mechanical stresses. These properties must be maintained stable if a reliable and reproducible device is to be realized.

Appendix

Tension-Voltage Relationship for the Electrostatic Clutch

Figure 10 illustrates the forces acting on the clutch mechanism. From this figure the following equilibrium conditions are obtained assuming that the band is stationary.

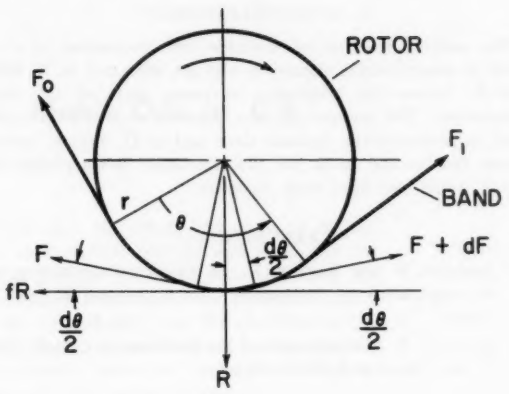

dE — Electrostatic Force

F — Tensile Force

f — Coefficient of Friction

R — Reaction Force

θ — Wrap Angle

Fig. 10. Forces acting on clutch mechanism

Normal Forces

$$R - dE - 2F \sin\frac{d\theta}{2} - dF \sin\frac{d\theta}{2} = 0 \qquad [10]$$

Tangential Forces

$$-fR + dF \cos\frac{d\theta}{2} = 0 \qquad [11]$$

Combining Eqs. [10] and [11] and making the approximation, $\sin d\theta/2 \approx (d\theta)/2$, and neglecting second order terms,

$$\frac{dF}{f} - dE - Fd\theta = 0 \qquad [12]$$

where $dE = (\varepsilon_0 KV^2/2h^2) \times dA$, and $dA = lr\, d\theta$. Letting $\beta \equiv (\varepsilon_0 K\, lrV^2)/2h^2$, then $dF/f - [\beta + F]\, d\theta = 0, dF/\beta + F) = f\, d\theta$.

Integrating from $\theta = 0$ to $\theta = \theta$, and

for $F = F_0$ at $\theta = 0$

and $F = F_1$ at $\theta = \theta'$,

$$\ln\left[\frac{F_1 + \beta}{F_0 + \beta}\right] = f\theta',$$

$$F_1 + \beta = [F_0 + \beta]\, e^{f\theta'},$$

$$F_1 = \beta\,[e^{f\theta'} - 1] + F_0\, e^{f\theta'},$$

or $$F_1 = \frac{\varepsilon_0 K\, lrV^2}{2h^2}\,[e^{f\theta'} - 1] + F_0\, e^{f\theta'}. \qquad [13]$$

V. ACKNOWLEDGMENT

The authors wish to acknowledge the cooperation of C. J. Fitch in many fruitful discussions and the assistance of R. Miller and A. Cooper for fabrication of many parts of the clutch mechanisms. The authors are also indebted to E. Clark, for his work in procuring the dynamic data, and to D. Krouse, without whose radioisotope work on film thickness measurements this report would not have been complete.

REFERENCES

1. JOHNSON, F. and RAHBEK, K., "A Physical Phenomenon and Its Application to Technology," *I.E.E. Journal* **61**, 713-725 (1923).
2. FITCH, C. J., "Development of the Electrostatic Clutch," *IBM J. Res. Develop.* **1**, No. 1 (1957).
3. BALAKUSHNAN, C., *Brit. J. Appl. Phys.* **1**, 211 (1950).
4. STUCKES, A. D., *Proc. Inst. Elec. Engr.* **103B**, 125 (1956).
5. SCOTT, M., "Mechanics," 1st ed. p. 95. McGraw-Hill, New York, 1949. (Normal force due to electric field added to derivation given here.)
6. HOLM, R., *In* "Electrical Contacts," 1st ed., p. 79. Gebers-Stockholm, 1946.
7. SILLARS, R. W., "The Effect of Field Emission on the Behavior of Semi-Conductor Contacts," *Proc. Phys. Soc.* (*London*) 68, 881 (1955).
8. FULLER, D. D., "Theory and Practice of Lubrication for Engineers," p. 236. Wiley, New York, 1956.
9. KRIESLE, L. F., "Surface Roughness—A Criterion for Minimum Hydrodynamic Oil-Film Thickness of Short Journal Bearing," *Trans. ASME* **78**, 955 (1956).

ASLE TRANSACTIONS 6, 227-232 (1963)

Classification of Multigrade Motor Oils at 0°F

By D. E. NEUNHERZ[1]

Viscosities of polymer-oil blends do not plot as straight lines throughout the range of ASTM Viscosity-Temperature Chart D 341. One consequence is that SAE 10W/30 motor oils can be formulated from borderline 20W base stocks and high-potency V-I improvers. Compared to 10W/30 oils based on true 10W stocks, these anomalous representatives are relatively hard-starting at low temperatures. The heavy-base group can be excluded from the classification by specifying that the maximum extrapolated viscosity shall apply to sonic-irradiated rather than to new oils. This approach appears more attractive than published procedures based on the Brookfield and Ferranti-Shirley viscometers, or on identification of base stocks by dialysis.

Introduction

THE SAE classification for winter-grade motor oils is based on viscosities at 0 F extrapolated, by means of ASTM Viscosity-Temperature Chart D 341, from viscosities measured at higher temperatures. The extrapolated viscosity of a 10W oil, for example, must fall between 6000 and 12,000 Saybolt Universal Seconds at 0 F (approximately 1300–2600 centistokes). Extrapolated viscosities are specified because wax interferes with kinematic or Saybolt viscosity measurements of many petroleum oils at 0 F. By contrast, engines are relatively insensitive to wax so that cold-cranking performances, of single-grade oils at least, have always correlated well with their extrapolated viscosities. Unfortunately, no such simple relation exists with modern multigrade motor oils. The problem is to find a relation that does and apply it to the job of establishing a technically sound classification.

A major difficulty is that oils blended with Viscosity-Index improvers are non-Newtonian, that is, their viscosities depend upon the rate of shear (*4*). The ASTM chart is valid only for Newtonian oils; viscosities of waxy oils or of polymer-oil blends do not plot as straight lines but curve upward at low temperatures. One peculiar consequence is that a 10W/30 oil can be formulated from a 20W base stock and a viscous V-I improver, which obviously must do some thickening. In an engine, a 10W/30 oil made in this way will not perform as a 10W oil at low temperatures (*7, 11*).

Evidently, a reliable laboratory method is needed for measuring viscosities of multigrade motor oils at shear stresses and rates encountered by the oils in engines during cold-starting. Despite considerable effort (*3, 8, 12*) there is no agreement to date on the magnitude of this shear rate. Neither is there agreement on a suitable viscometer to use for purposes of correlation. The one common denominator in the investigations has been the use of new oils for comparative measurements. Even this approach is of unproven merit inasmuch as the motorist is concerned with how his *used* oil performs.

The present objective is to extend knowledge of viscosities of multigrade oils at 0 F to used as well as new oils. From this broader background, generalization leading to a tighter SAE specification hopefully might be drawn. The approach has been first to simulate, by sonic irradiation, the breakdown in polymeric V-I improvers that causes permanent viscosity losses in used oils from engines. Next, the probable shear rate of interest for these oils has been bracketed by measurements with the Brookfield and Ferranti-Shirley viscometers. Finally, to assess proximity to complete breakdown, kinematic viscosities of these oils have been compared with those of the base stocks extracted therefrom by dialysis. Application of the proposed revision to the 10W/30 classification is illustrated by means of six new reference oils on which cranking data are available.

Experimental

Selected combinations of three different V-I improvers and three base stocks were used in formulating the commercial (fully formulated) 10W/30 motor oils. Direct comparisons between polymethacrylate (A) and polyisobutylene (B) V-I improvers in the same base stock were included. API gravities and cloud and pour points of all the test oils are listed in Table 1, and original viscosity data of blends and base stocks are given in the tables of results.

Polymer breakdown was accomplished by vibrating the oil samples at a frequency of 10 kilocycles per second in a sonic oscillator. The principal features of this device have been described in conjunction with an ASTM proposed test method (*2*). For the present work, the treatment unit was modified by incorporation of a motor-

Contributed to the American Society of Lubrication Engineers by the author. Manuscript received February 4, 1963.

[1] Research and Development Department, American Oil Company, Whiting, Indiana. Present address: 8636 Greenwood Avenue, Munster, Indiana.

TABLE 1
Test Oil Inspections

Blend No.	Base oil No.	V–I imp. No.[a]	V–I imp. %[b]	Grav. (API)	Cloud pt. (°F)	Pour pt. (°F)
ASTM 5	—	A–1	5.15	27.5	16	—30
ASTM 6	—	B–1	12.9	28.7	24	—35
Coml. 1a	1a	B–1	10.0	29.7	—	—20
Base	1a	—	0.0	29.7	—	—20
Coml. 1b	1b	B–1	10.0	29.8	8	—10
Coml. 2	1b	A–2	6.1	29.7	8	—50
Coml. 3	1b	A–2	6.6	29.7	8	—45
Coml. 4	1b	A–2	7.1	29.7	8	—55
Base	1b	—	0.0	29.7	8	—10
Coml. 5	2	A–2	4.3	28.7	8	—40
Coml. 6	2	A–2	4.8	28.7	8	—40
Base	2	—	0.0	28.7	8	— 5
Coml. 7	3	A–3	5.0	28.5	—	—45
Base	3[c]	—	—	—	—	—

[a] A, polymethacrylate; B, polyisobutylene. Numbers indicate variations.
[b] Concentrations in reference and commercial blends are in weight and volume per cents, respectively. Base oils contain detergent and zinc dialkyl dithiophosphate inhibitor.
[c] No data are available.

driven glass stirrer in the sample cup. The preferred method of operation comprised irradiation at 0.9 amp of 50 ml of oil for the time indicated. Sample temperature was controlled at 115 F ± 0.5 F by varying the rate of stirring, a practice that appears to reduce the tedium of frequent recalibration for degradation severity.

The two viscometers used are commercially available. The Brookfield viscometer, Model LVF, is a low-shear (<2 sec^{-1}) instrument of the rotating spindle type. Application of this instrument has been described in detail (*9, 11*). The Ferranti-Shirley, or cone-plate viscometer (*10*), is capable of much higher shear rates (8600 sec^{-1} at 0 F), but such utilization is not without problems (*1, 3*). Between the two viscometers, the probable shear rates of interest should be pretty well bracketed, and the magnitude of temporary viscosity losses should be evident.

Separation of base oils from their blends by dialysis closely followed a published procedure (*5*). The technique involves overnight leaching of the sample through a thin-walled rubber sac and the use of a solvent such as hexane or heptane. Solvent was removed from the dialysate by means of rotary vacuum evaporator and boiling-water bath.

Discussion

Losses in viscosity of V-I improved oils are of two types that depend upon the severity of treatment. When the lengthy polymer molecule is ruptured, as by engine operation or sonic irradiation, the loss in viscosity is permanent. When polymer molecule is merely distorted and aligned under shear, as in some bearings and viscometers, the viscosity losses sustained are only temporary.

PERMANENT VISCOSITY LOSSES

Meaningful viscosity data on used oils from engines are difficult to obtain because of conflicting effects of contamination, oxidation, and fuel dilution. However,

TABLE 2
Effect of Turnpike Test on Viscosities of Dissimilar 10W/30 Motor Oils

Oil No.[a]	V–I imp.	Miles	Viscosity (cs) 100 F	210 F	V–I
Coml. 1b	B-1	0	68.55	10.97	138
		410	58.65	9.53	137
Coml. 3	A-2	0	56.5	10.82	150.5
		410	42.8	7.88	144.5

[a] These oils are reblends of compositions elsewhere described. The same base oil is used in each blend.

Table 2 affords comparisons of two dissimilar 10W/30 oils before these road factors become appreciable. After only 410 miles, the blend containing polymethacrylate shows signs of a greater breakdown than the same base oil containing polyisobutylene V-I improver. These data were obtained in an 8-cylinder 1960 automobile operated on a turnpike at high speed. More pronounced differences may be expected at higher mileages or with heavier duty. In taxicab fleet tests, for example, permanent losses of nearly one-third the original viscosity at 100 F have been observed in some 10W/30 oils after 1000 miles of operation.

Simulation of this substantial degree of breakdown is readily accomplished in the sonic oscillator. As shown in Table 3, irradiations of 90 minutes duration suffice. In contrast to used oils from engines, these samples are perfectly clean. The extensive data on commercial oil

TABLE 3
Effect of Sonic Irradiation on Viscosities of 10W/30 Motor Oils

Oil No.	V-I imp.	Irrad. (min)	Viscosity (cs) 100 F	210 F	V-I
ASTM 5	A–1	0	71.4	11.46	138.5
		90	50.5	7.19	110.5
Base	—	0	47.1	6.40	91.5
ASTM 6	B–1	0	72.0	11.38	137.5
		90	55.3	8.99	135.5
Base	—	0	24.5	4.44	100.5
Coml. 1a	B–1	0	63.6	10.33	138.0
		15	56.9	9.27	136.5
		30	53.2	8.74	136.0
		45	51.7	8.48	135.0
		90	47.4	7.86	134.0
Base	—	0	27.7	4.95	115.5
		45	27.3	4.88	113.0
Coml 1b	B–1	0	66.7	10.87	137.0
		90	47.5	7.76	131.5
Base	—	0	28.7	5.15	120.5
Coml. 2	A–2	0	54.7	10.41	150.0
		90	33.4	5.94	131.0
Coml. 3	A–2	0	57.3	10.97	150.0
Coml. 4	A–2	0	60.0	11.48	150.5
		90	33.8	6.15	136.0
Base	—	0	28.7	5.15	120.5
Coml. 5	A–2	0	66.4	10.61	137.5
Coml. 6	A–2	0	69.0	11.17	138.5
		90	46.6	7.07	118.5
Base	—	0	44.1	6.44	105.0
Coml. 7	A–3	0	72.2	11.29	136.5
		30	56.2	8.14	120.0
		90	54.3	7.71	114.5
Base[a]	—	—	—	—	—

[a] Compare with dialysis data, Table 5.

1a indicate that any given breakdown on the road can be approximated in the laboratory by varying the time of sonic irradiation. In general, the viscosities of sheared blends containing polymethacrylates approach the viscosities of the respective base stocks as a limit. The viscosities of the blends containing polyisobutylene show no such breakdown under similar conditions of sonic irradiation. These observations are valid whether the base stocks are the same, as in the indicated commercial oil examples, or different, as with the ASTM reference oils. Figure 1 brings out the relationships quite clearly. The plots are reductions of the standard ASTM Chart and illustrate the extrapolation procedure described in the SAE classification. ASTM 5 is an example of a 10W/30 oil made from a 20W base stock. In engines, ASTM 5 and 6 exhibit viscosities at 0 F of about 4000 and 2450 cs, respectively (*7*).

TEMPORARY VISCOSITY LOSSES

At first glance the number of variables exhibited in Table 4—oil type and extent of degradation, viscometer type and rate of shear—would appear to make comparisons of viscosity measurements very complex. Fortunately, some simplifications are possible.

In the first place the cone-plate viscosities seem relatively insensitive to reductions in the shear rate (from 8600 to 4300 sec^{-1}), and to sonic irradiation (compare ASTM reference oils and commercial oils 1a and 7). These observations are reassuring because the instrument appears easier to calibrate reliably at the lower shear rate and because correlations with cold-starting need not be vitiated as the motor oils become used.

In the second place, in contrast to oils containing polyisobutylene, oils containing polymethacrylate tend, at 4300 sec^{-1}, to approach the base oil in viscosity. As a consequence, Brookfield viscosities on sonic-irradiated wax-free oils, such as commercial 2 and 4, approximate cone-plate viscosities at 4300 sec^{-1}; this is just what would be expected with the equivalent of a Newtonian base oil.

Finally, extrapolated viscosities of only those oils made

TABLE 4
Comparison of Viscosity Measurements at 0 F

Oil No.	V-I Imp.	Irrad. (min.)	Viscosity (cs)[a] Extrapolated[b]	Brookfield	Ferranti-Shirley 4300 sec^{-1}	Ferranti-Shirley 8600 sec^{-1}
ASTM	A-1	0	2300	5200	3730	3840
		90	3065	4290	3730	3840
Base	—	0	3655	—	—	—
ASTM 6	B-1	0	2420	4580	2430	2320
		90	1945	3535	2870	2320
Base	—	0	960	—	—	—
Coml. 1a	B-1	0	2085	3055	1890	1725
		15	1955	2640	—	1890
		30	1840	2510	1920	1810
		45	1825	2355	—	1880
		90	1695	2230	1770	1780
Base	—	0	1045	1110	1010	1110
		45	1040	—	—	—
Coml. 1b	B-1	0	2110	3350	2050	—
		90	1785	2360	1900	—
Base	—	0	1045	1300	1170	—
Coml. 2	A-2	0	1160	2040	1380	—
		90	1135	1470	1290	—
Coml. 3	A-2	0	1170	2000	1430	—
Coml. 4	A-2	0	1205	2130	1430	—
		90	1050	1430	1380	—
Base	—	0	1045	1300	1170	—
Coml. 5	A-2	0	2230	3540	2550	—
Coml. 6	A-2	0	2220	3250	2490	—
		90	2345	2420	2520	—
Base	—	0	2675	Waxy	2390	—
Coml. 7	A-3	0	2520	4755	3750	3530
		30	2965	4080	3585	4080
		90	3165	—	—	—
Dialysate		0	2930	—	—	—

[a] Viscosities measured by the Ferranti-Shirley and Brookfield viscometers are in centipoises (= centistokes × density at 0 F). Densities at 0 F (approx. 0.9) were estimated by means of Standard API Gravity Temperature Correction Tables.

[b] Extrapolated values of all blends were calculated from viscosities at 100 and 210 F by means of the Walther equation:
$\text{Log log } (\eta + 0.6) = m \log T + a.$

with polymethacrylates in the heavier (more conventional) base stocks tend to increase with sonic irradiation. How these observations are turned to good account will be shown after a discussion of the dialysis results.

VISCOSITIES OF DIALYSATES

The direct approach to the elimination of anomalous 10W/30 oils is to require that 10W (or lighter) base oils be used in their formulations. Adherence of the refiner to this specification could be monitored by means of the dialysis technique (*6*). Table 5 shows some kinematic viscosity comparisons of interest on such dialysates. Dialysates from new or used motor oils do not differ materially from each other or from their respective base stocks (cf. Table 3). However, dialysis separates not only V-I improver but detergent from base oil, as shown by published and current results. From the rheological standpoint this selectivity may be unfortunate, inasmuch as some detergents contribute little to non-Newtonian behavior in the dosages normally used (cf. Commercial 1a base oil, Table 4).

REVISED EXTRAPOLATION PROCEDURE

Both the Ferranti-Shirley and the Brookfield viscometers have been investigated for use in cold-starting correlations. The former viscometer in its present construction is costly and ill-adapted to routine measurements at 0 F; requirements in time and skill seem exorbitant. The latter viscometer, although comparatively inexpensive and simple to operate, tends to read high on waxy oils. Substitution of observed Brookfield for extrapolated viscosities at the present maximum of 2600 centistokes

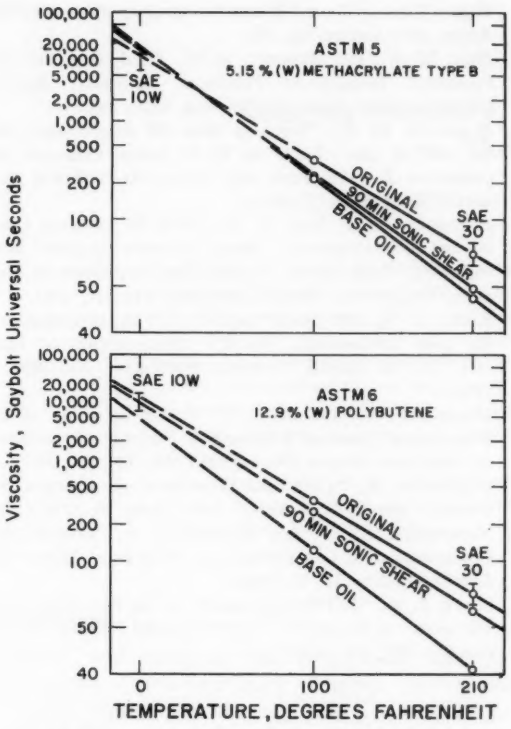

FIG. 1. ASTM low temperature reference oils

would eliminate most of the 10W/30 oils in this study. In short, neither viscometer is well suited to the task at hand. Nor is the time-consuming dialysis technique wholly satisfactory.

TABLE 5
Viscosities of Motor Oil Dialysates

Oil No.	Irrad. (min)	Dial. (%)	Res. (%)	Viscosity (cs) 100 F	210 F
ASTM 5	0	96.43	3.36	44.48	6.42
	90	96.36	3.45	43.92	6.19
ASTM 6	0	94.45	4.99	24.62	4.41
	90	94.45	5.13	24.01	4.29
Coml. 1a	0	95.23	4.74	24.1	4.57
	15	94.74	5.04	23.7	4.16
	30	94.92	4.97	24.3	4.29
	45	94.95	5.03	23.8	4.21
	90	94.79	5.07	23.8	4.31
Base	0	97.11	2.92[a]	22.9	4.16
Coml. 1b	—	94.83[b]	4.96	24.9	4.38
	—	94.35[c]	5.22	25.3	4.45
Coml. 3	—	95.68[b]	4.21	25.7	4.54
	—	94.69[c]	4.54	24.9	4.58
Coml. 7	0	96.47	3.45	44.5	6.36

[a] The "base" oil contained a barium phosphonate detergent and a zinc dialkyl dithiophosphate inhibitor.

[b] 0 road miles.

[c] 410 road miles.

A better proposal stems from the observation that the extrapolated viscosities at 0 F of many blends decrease slightly with sonic irradiation. As indicated above, only the 10W/30 oils made up with the polymethacrylates in the heavier (sometimes 20W) base stocks exhibit significant increases with sonic irradiation. It is precisely just such oils that should be eliminated from the SAE 10W/30 classification—not because they are poor lubricants, but because they don't belong in the category. This exclusion could be accomplished by substituting used (sonic-irradiated) oils for new in the existing (or slightly narrower) SAE specification. Table 6 shows how this works out on a new series of reference oils.

TABLE 6
Extrapolated Viscosities at 0 F of Cranking Oils

No.[a]	V-I imp.	Blend	Base	Dialysate	90-min. sonic	Engine[b]
I	B–1	2210	735	865	1745	1760
II	A–4	1900	1910	1790	2055	2300
III	A–3	2105	3450	3135	2720	3000
IV	B–1	2190	805	885	1915	1760
V	A–4	2200	2170	2025	2200	2010
VI	A–3	2240	2895	2800	2720	3430

[a] All blends contain zinc dialkyl dithiophosphate inhibitor but no added detergent (A–3 possesses some detergency). The base oils used in Nos. I–III were low in wax. Base oils used in Nos. IV–VI were high in wax.

[b] Average of duplicate determinations on a 6-cylinder 1961 automobile, based on starter current. These preliminary values are subject to adjustment as the cranking technique undergoes revision.

Sonic irradiation lines up the oils in much the same order as the engines. Extrapolated sonic values for oils I and IV (containing polyisobutylene) are realistic and markedly different from base-oil values. Oils III and VI, containing polymethacylate, exceed 2600 cs and should be excluded from the 10W/30 category. Wax, this time in conjunction with V-I improvers, once again exhibits little effect on engine cranking.

Conclusion

Revision of the viscosity-extrapolation method for winter-grade motor oils is a solution to the SAE classification problem not anticipated at the outset of this program. Nevertheless, as a compromise measure involving no radical changes, the sonic-irradiation proposal should be acceptable to refiner and consumer alike. The fact that the irradiation procedure is undergoing standardization in the ASTM is an added attraction.

Although the method is primarily designed to screen out the anomalous 20W base-oil representatives, it appears capable of discriminations within the normal 10W/30 class as well. More work with fully formulated (detergent-bearing) motor oils will be required to establish this broader indication, however. Because extrapolated viscosities of a polymethacrylate in a lighter base

stock remain virtually unchanged by irradiation, extension of the method to the 5W/20 classification is unlikely.

Contrary to expectation, viscosities at moderate shear rates of new and used oils, as measured by the cone-plate viscosities, are about the same. By implication, cold-cranking characteristics of motor oils should not be altered greatly as mileage accumulates. Further correlation efforts along these lines might well be supplemented, if not supplanted, by the sonic-extrapolation method.

ACKNOWLEDGMENTS

Most of the commercial oil blends were prepared by J. E. Clevenger. L. J. Allman performed the turnpike tests in Table 2, and R. H. Bunting the cranking tests in Table 6.

REFERENCES

1. "American Oil Company Procedure for Ferranti-Shirley Viscometer at Low Temperatures." *ASTM Special Technical Publication No.* **299**, 153 (1962).
2. ASTM Committee D-2, "Proposed Method of Test for Shear Stability of Polymer-Thickened Oils." Preprint 35S, Philadelphia, Pennsylvania, 1961.
3. FORSTER, E. D., and HOROWITZ, H. H., "Application of the Cone-Plate Viscometer to Non-Newtonian Systems," *ASTM Special Technical Publication No.* **299**, 85 (1962).
4. GEORGI, C. W., "Viscosity Characteristics of Motor Oils at Higher Rates of Shear," *World Petrol. Cong. Proc. 4th Congr. Rome, 1955* Section VI, 211.
5. HILL, M. W., and MUNSELL, M. W., "Dialysis of Petroleum Products." Division of Petroleum Chemistry. American Chemical Society, New York Meeting, Sept., 1960.
6. HOROWITZ, H. H., "Proposed Base Oil Specification Limit for 10W/30 Oils." Letter to W. S. James, Chairman Subcommittee B, SAE Fuels and Lubricants Technical Committee, dated May 2, 1961.
7. HOROWITZ, H. H., VICK, G. K., "Low Temperature Cranking and Flow Properties of Waxy, Polymer-Thickened Motor Oil," SAE International Congress and Exposition of Automatic Engineering, Detroit, Michigan, January, 1961.
8. KOHL, G. A., and SKOGLUND, R. D., "An Investigation of the Low Temperature Viscosity Characteristics of Motor Oils," *ASTM Special Technical Publication No.* **299**, 123 (1962).
9. MALONE, G. K., and SELBY, T. W., "Relationship of Low Temperature Cranking Resistance to Viscosity Characteristics of Multigrade Engine Oils," *SAE Trans.* **64**, 602 (1956).
10. MCKENNEL, R., "Cone-Plate Viscometer—Comparison with Coaxial Cylinder Viscometer," *Anal. Chem.* **28**, 1710 (1956).
11. NEWINGHAM, T. D., and ZIEGLER, J. B., "Cold-Cranking Characteristics of Conventional and Multigrade Motor Oils," *Lubrication Eng.* **18**, 71 (1962).
12. SELBY, T. W., "ASTM Investigation of the Low-Temperature Viscometry of Engine Oils," *ASTM Special Technical Publication* No. **299**, 136 (1962).

ASLE TRANSACTIONS 6, 233-238 (1963)

Relating Humidity Cabinet Life of Lubricants to Their Service Life

By R. F. McKIBBEN (ASLE)[1] and D. M. FORINASH (ASLE)[2]

In the past the results obtained from humidity cabinet corrosion tests have been useful for comparing one protective material with another, but of little value for predicting the protective life of any given material under atmospheric exposure conditions.

A corrosivity factor, arbitrarily developed, has been found invalid. A method has been developed from experimental data by which the humidity cabinet life of a lubricant may be used to predict its protective life on steel when exposed to the atmosphere. This method is expressed mathematically as a function of temperature, humidity, and protective life (time). It is applicable for world-wide use by using local temperature and humidity data for the location under consideration.

The same general equation appears to be applicable for any lubricant. Each lubricant has its own constants, which must be determined from experimental data. The constants for two lubricants have been determined.

Introduction

RUSTING and corrosion are ever-present hazards to mechanisms or structures made of metal. The amount of corrosion required to seriously affect a mechanism or structure may vary widely. In some cases severe corrosion, removing several thousandths of an inch of metal, can be tolerated before a piece becomes scrap. On the other hand, where appearance is of prime importance, a minute stain is reason for scrapping or reoperation. In between these two extremes lie most corrosion problems.

In this paper consideration is limited to atmospheric effects on ferrous metals. Although industrial contaminants, salt air, and air circulation are among the factors contributing to atmospheric corrosion, consideration is further limited to the effects of temperature and humidity.

There are two concerns regarding corrosion in business machines. First is the matter of functional operation. With thousands of closely fitting parts, many of which are operated with light springs, very small amounts of corrosion in bearing areas can cause malfunctioning, or very small attacks of corrosion on the springs can cause fatigue failure. Second is appearance, since rusty parts may cause unfavorable reactions on the part of customers or servicemen, even though this visible rust is unlikely to cause malfunctioning.

Contributed by the ASLE Technical Committee on Properties of Lubricants and presented at the Annual Meeting of the American Society of Lubrication Engineers held in New York, April, 1963.

[1] Section Head, Lubrication Laboratory, The National Cash Register Company, Main and K Streets, Dayton 9, Ohio.

[2] Analytical Chemist, Lubrication Laboratory, The National Cash Register Company, Dayton 9, Ohio.

Many parts may be protected from corrosion by plating; however, there are also many parts where plating interferes with proper operation, and the lubricant is required to provide protection. Accordingly, these parts are not plated, as well as many other parts which could otherwise be plated. Instead, a corrosion protective lubricant is applied.

Atmospheric corrosion has been studied from many different points of view. Copson (*1*) reported an extensive study in atmospheric corrosion on low alloy steels, using one industrial and two marine locations as test sites. The U. S. Navy (*2*) investigated corrosion of metals in the Panama Canal Zone. The *Iron Age* (*3*) reported an evaluation of atmospheric corrosion in many areas of this country and published a corrosion map of the United States. All three of these investigations were made using unprotected steel directly exposed to the elements.

It is well known that corrosion preventives—or perhaps corrosion protective materials would be a preferable name—may be used to greatly reduce the amount of corrosion that develops under atmospheric exposure. Sawyer (*4*) found a correlation between corrosion due to exposure in the JAN-H-792 Humidity Cabinet and corrosion due to atmospheric exposure, using for the latter three widely separated areas of the United States. His findings indicated that rust preventives showing superior humidity cabinet life give superior protection for both indoor and outdoor service. Trigg (*6*) described a 1-year atmospheric exposure evaluation of several protective materials. On the basis of one series of tests, he concluded that thin-film protectives should be reapplied every 3 months and mineral-jelly protectives every 9 months. Other references to studies of corrosion

and corrosion protection could be cited; but nowhere in the literature is found anything to show that a lubricant having a humidity cabinet life of H hours will assure a protective life of Y years when applied to a mechanism which will be located in climatic condition C.

Business machines are used wherever men trade. Obviously, such equipment must operate satisfactorily in all climatic conditions. If a corrosion preventive will give a humidity cabinet life of 300 hours, how long will it protect equipment located at Dayton, Ohio; Miami, Florida; Tel Aviv, Israel; San Juan, Puerto Rico; or Rangoon, Burma? A final answer to this question has not been and may never be obtained, but some progress has been made and an indication has been obtained which can be used until a better method is developed.

As stated previously, there are many factors contributing to atmospheric corrosion. Likewise, there are many factors contributing to the degradation of corrosion protective materials. However, the ones which are universally present and which no doubt account for the most corrosion and the most degradation of protectives are temperature and humidity. In general, chemical reaction rates double for each 18 F increase in temperature, and reaction rates are directly dependent on the concentration of active material which in this case is water vapor. The tendency of a climate to cause corrosion—identified as corrosivity (C)—is therefore a function of the humidity (H) and of the temperature (t). Recognizing that the rate of corrosion will approach but never equal zero as temperatures and humidities are reduced, corrosivity was arbitrarily made equal to 1 when the temperature was 40 F and the relative humidity was 35%. These limits were selected since corrosion proceeds at a negligible rate at lower temperatures and humidities. On these bases, the equation

$$C = \left(\frac{H}{23.4} - 1.28\right) \times 2^{\frac{t}{18}} \qquad [1]$$

was derived.

Using this equation, with average temperatures and humidities, Dayton, Ohio, has a corrosivity of 15 and Rangoon, Burma, has a corrosivity of 55. This would indicate that a machine at Rangoon would corrode in about one-fourth of the time required for equivalent corrosion to develop at Dayton. To determine the validity of this relation, a program was established to determine humidity cabinet life under various corrosivity factors; the severity of the exposure was reduced until the test time became unreasonably long.

Out of the large number of environmental test devices which have been developed, the JAN-H-792 Humidity Cabinet is perhaps the best known. Tests conducted in this cabinet are more repeatable than many other humidity tests. It is designed to operate continuously under a condition of 100% relative humidity. The usual operating temperature is 120 F, although lower temperatures may be used where the severity of exposure must be reduced; but this cabinet does not have the wide range of possible test conditions desired for this investigation.

On the other hand, the test chamber shown in Fig. 1 is readily adjustable to various temperatures and humidities. It will duplicate the standard conditions of the

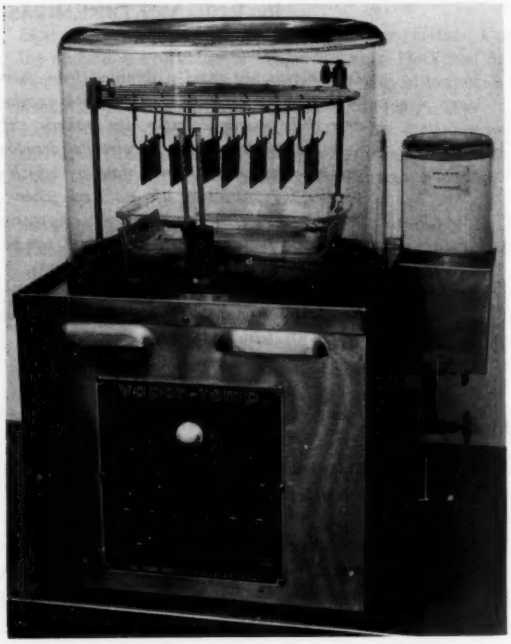

FIG. 1. Test chamber—humidity and temperature variable

JAN-H-792 Humidity Cabinet. Lower temperatures may be obtained, limited only by the ambient temperature surrounding the chamber; and lower humidities may be obtained, limited only by the temperature of the water put through its cooling system. For these reasons, this device (Fig. 1) was selected as being suitable for conducting a step-wise investigation, planned to start with the severe exposure of the JAN-H-792 Humidity Cabinet and progressively going toward milder conditions.

The test pieces used for each determination consisted of five 2 × 4 inches by .035 inch sand blasted steel test panels, prepared by the standard procedure of NCR Process Specification No. 2021.16, dipped in the desired lubricant, and drained overnight in the laboratory atmosphere. Following this, they were exposed continuously in the test chamber at the desired conditions. Observations were made at least once each working day during the exposure period. The test was terminated when six of the ten faces had failed. A face was considered failed when 0.2% of its significant area was corroded. The hours of failure of the fifth and sixth faces were noted. Their numerical average, representing a median value for the ten faces, was recorded as the

life of the protective material under the given set of exposure conditions. The median value is approximately equal to the average value, and its use as a criterion of failure results in a substantial reduction in test time (*5*).

Parallel investigations of two protective materials were conducted. These materials were selected because they represent a wide range in protective ability. Lubricant No. 1 consisted of a turbine quality oil having a viscosity of 150 Saybolt Seconds at 100 F. Panels dipped in this oil at 100 F retain a film approximately 0.0002 inch thick after a 24-hour drain. Lubricant No. 555 consisted of a 20% dispersion of a grease in Stoddard Solvent with a sodium sulfonate corrosion inhibitor added. The grease was composed of a turbine quality oil having a viscosity of 150 Saybolt Seconds at 100 F, thickened with aluminum soap and mineral wax. Panels dipped in this grease dispersion retain a film of lubricant approximately 0.0001 inch thick after evaporation of the solvent. Initially, a material having greater protective ability than Lubricant No. 555 was considered, but it was canceled when it became evident that the exposure time required would be longer than practical.

Procedures

Life determinations were made of both lubricants in both cabinets at 100% relative humidity and 120 F. In both cabinets, Lubricant No. 1 had a life of about 3 hours. In the JAN-H-792 Humidity Cabinet, Lubricant No. 555 had a life of about 300 hours, and in the test chamber (Fig. 1), 312 hours. This was an excellent check between the two cabinets. Milder conditions were then imposed in the test chamber (Fig. 1) by reducing the relative humidity while maintaining the temperature at 120 F. At 93% relative humidity, Lubricant No. 1 had a life of 1023 hours and Lubricant No. 555 had a life of 5400 hours. Determinations were also made at 76% relative humidity, giving 7000 and 22,500 hours, respectively. Due to the excessive time involved, no further reduction in humidity was attempted.

In the next phase of the investigation, the milder conditions were obtained by reducing the temperature while maintaining the relative humidity at 100%. Determinations were made with Lubricant No. 1 at eight steps, the lowest being 84 F; and with Lubricant No. 555 at four steps, the lowest being 109 F.

Analysis and discussion

According to Eq. [1], a lubricant exposed to a given corrosivity should have a constant life no matter what combination of temperature and humidity was used to obtain it. Early in the investigation, it became apparent that this relation was not valid. For instance, a corrosivity of 275 obtained with 118 F and 100% relative humidity and again with 120 F and 93% relative humidity gave a life for Lubricant No. 555 of 324 hours under the first conditions and 5400 hours under the second. Obviously, the effect of humidity was much greater, and that of temperature much smaller, than indicated by Eq. [1], and a new relation had to be developed.

In analyzing the results, it was evident that absolute humidity rather than percent relative humidity should be considered in plotting this data. Humidity was therefore expressed as grains of moisture per pound of dry air. Similarly, absolute temperature in degrees Rankine was used rather than temperature in degrees Fahrenheit.

The life of each lubricant was plotted against the variable characteristics. First, curves were prepared plotting the life of Lubricant No. 1 and Lubricant No. 555 in hours as the abscissa, against the temperature as the ordinate (Figs. 2 and 3, respectively); then curves were

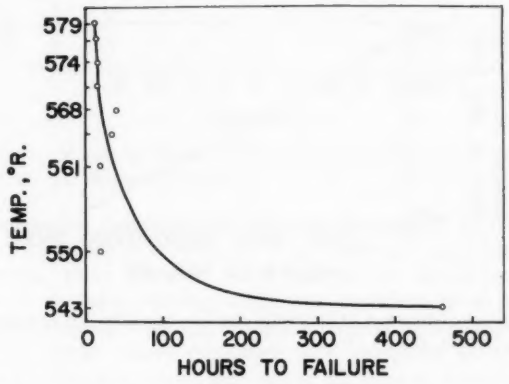

FIG. 2. Variation of life with temperature for Lubricant No. 1 at 100% relative humidity.

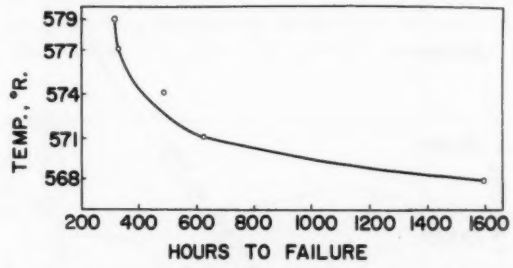

FIG. 3. Variation of life with temperature for Lubricant No. 555 at 100% relative humidity.

prepared plotting the life as the abscissa against the humidity as the ordinate (Figs. 4 and 5, respectively). The data plotted in this manner on rectangular coordinate paper did not produce straight lines from which equations could be derived. By plotting the data in several different relations, it was found that approximately straight lines were obtained when the life in hours was plotted on rectangular coordinate paper as the ordinate, against the reciprocal of the humidity as the abscissa, with the temperature held at 120 F (Fig. 6). Approximately straight lines were also obtained by

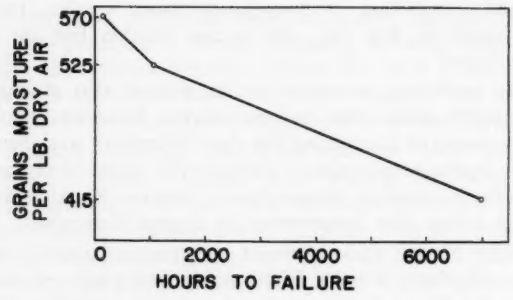

Fig. 4. Variation of life with absolute humidity for Lubricant No. 1 at 120 F.

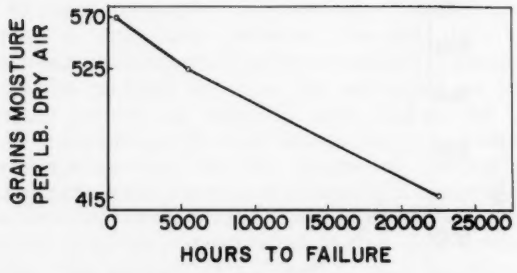

Fig. 5. Variation of life with absolute humidity for Lubricant No. 555 at 120 F.

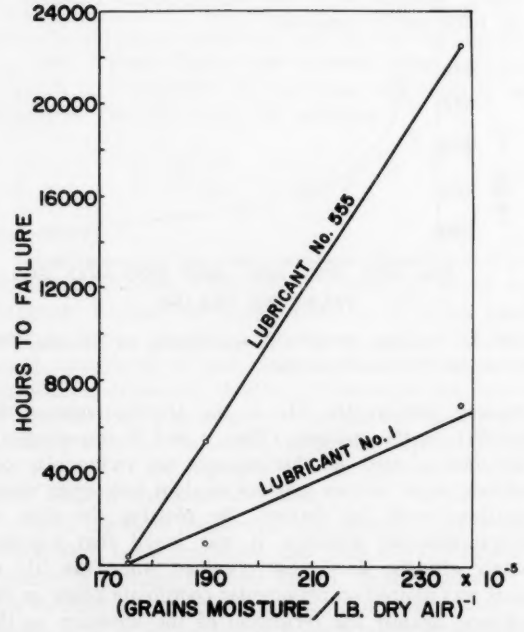

Fig. 6. Variation of life with inverse of absolute humidity at 120 F.

plotting the life in hours on semilogarithmic paper as the ordinate, against the reciprocal of the temperature as the abscissa, with the relative humidity maintained at 100% (Fig. 7). From these curves, equations relating life and humidity and life with temperature were ob-

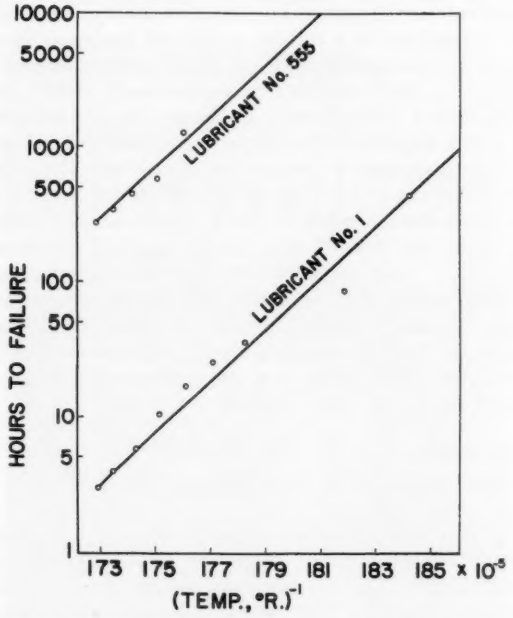

Fig. 7. Variation of life with inverse of absolute temperature at 100% relative humidity.

tained. For Lubricant No. 555, these equations were combined into one as follows:

$$L = 10^{(1.8935\times10^4)/(t-30.225)} + \frac{3.5556\times10^7}{H} - 6.2368\times10^4 \qquad [2]$$

This equation fitted the curve when the temperature was held constant and the humidity was varied. However, it did not fit the curve when the temperature was varied and the relative humidity was held at 100%. It was concluded that this was due to the variation in absolute humidity with variation in temperature. It was therefore apparent that variation in humidity with temperature has a different relation to life than does direct variation of humidity. By adding appropriate factors involving the temperature differential from the maximum (579 R) the following equation was derived:

$$L = 10^{(1.8935\times10^4)/(t-30.225)} + \frac{3.5556\times10^7}{H} - 6.2368\times10^4 - 2111(579-t) - 2.9(579-t)^{2.8} \qquad [3]$$

This represents both plots of data reasonably well.

Although the two lubricants differ widely in protective

characteristics, the equation for Lubricant No. 1 has the same form as Eq. [3], but has different constants.

In applying Eq. [3] for calculating life at various locations, average temperatures and humidities were used, but it is recognized that there are daily and seasonal variations in both. To determine if these variations are significant, tests were made in the test chamber by cycling the temperature and humidity to simulate climatic variations. In these tests the lubricants appeared to have a substantially longer life than they had under constant conditions. There is no apparent explanation why this should be. However, it appears that by using average conditions, the life calculated by using Eq. [3] is on the conservative side.

All of the data reported so far was obtained under laboratory control, using clean test panels. Mechanisms which have been assembled by workmen who handle each part, and which are dipped in the appropriate lubricant as the final operation, would not be expected to give the same results. To check this point, some assemblies which had been dipped in Lubricant No. 555 were subjected to exposure at 120 F and 100% relative humidity. It was found that corrosion developed approximately twenty times as fast as it did on the laboratory prepared panels. Thus, in a practical application, only 5% of the life predicted by Eq. [3] might be expected.

Applying this 5% factor, the protection to mechanisms which may be expected may now be calculated for various localities. At Dayton (Fig. 8), where the average temperature is 52.2 F and the average relative humidity is 71%, a machine using Lubricant No. 555 can be expected to give more than 40 years service before corrosion develops. Using the same lubricant in Rangoon (Fig. 9), where the average temperature is 81.1 F and the average relative humidity is 87%, corrosion may be expected to develop after 7 months of service. As an example, several years ago when Lubricant No. 1 was used as a protective material, three machines were returned to the factory due to excessive rusting, which was sufficient to cause malfunctioning, after approximately 1 year in San Juan, Puerto Rico. These machines were reworked at the factory. The rusty parts were either derusted or scrapped and replaced. The machines were rebuilt and relubricated with a lubricant having about 500 hours life in the JAN-H-792 Humidity Cabinet. Five years after being returned to San Juan, they showed no evidence of corrosion. In San Juan (Fig. 10), where the average temperature is 77.9 F and the average relative humidity is 78%, corrosion may be expected to develop after 0.1 month with Lubricant No. 1 and after 11 months with Lubricant No. 555. Since the 500-hour lubricant mentioned gave substantially greater humidity cabinet life than Lubricant

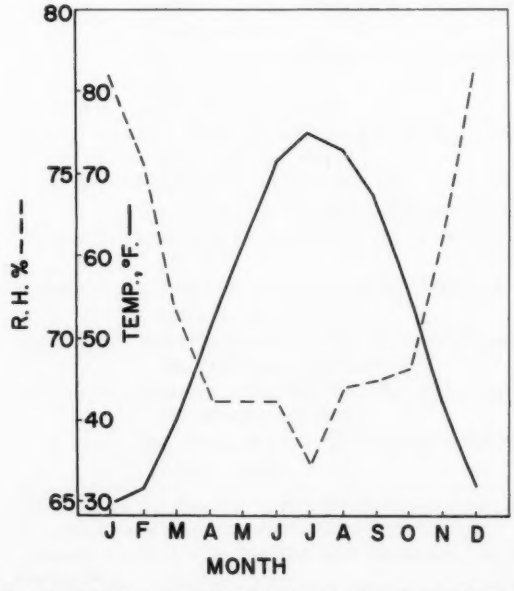

FIG. 8. Month to month variation of mean temperature and humidity for Dayton, Ohio.

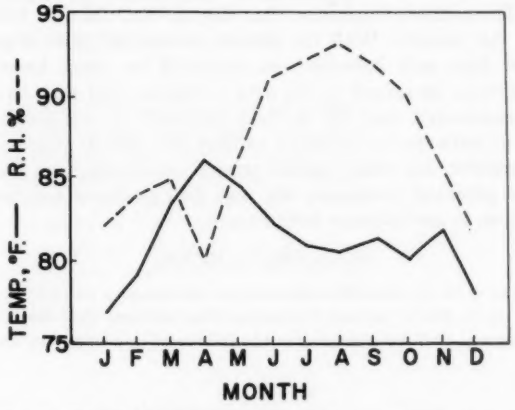

FIG. 9. Month to month variation of mean temperature and humidity for Rangoon, Burma.

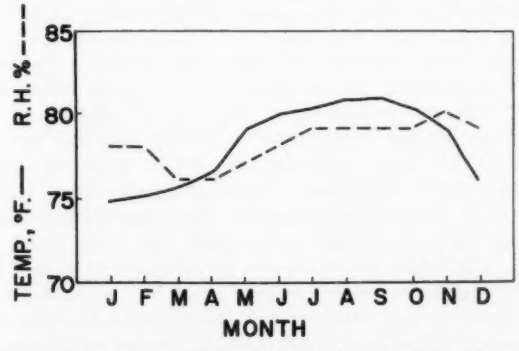

FIG. 10. Month to month variation of mean temperature and humidity for San Juan, Puerto Rico.

No. 555, the greater service life observed is understandable, although no equation has been developed for this material.

Conclusion

The authors emphasize that they do not claim to have all the answers. With the limited amount of work done, they have only indicated one approach by which knowledge may be gained in this field of interest, but they have demonstrated that for a given lubricant, a relationship exists between its humidity cabinet life and its potential protective life under known service conditions; and that this potential protective life may be calculated for conditions at any location in the world.

ACKNOWLEDGMENTS

The authors gratefully acknowledge the support of this work by the Technical Services Division of The National Cash Register Company, and the assistance in obtaining and presenting the data which was given by University of Cincinnati cooperative students working under the NCR Educational Training program.

REFERENCES

1. COPSON, H. R., "Long Time Atmospheric Corrosion Tests on Low Alloy Steels," presented at the Annual Meeting of the American Society for Testing and Materials, June, 1960.
2. FORGESON, B. W., SOUTHWELL, C. R., ALEXANDER, A. L., MUNDT, H. W., and THOMPSON, L. J., "Corrosion of Metals in Tropical Environments," *Corrosion* **14**, 73t–81t (1958).
3. "New Corrosion Index Shows Nation's Rust Pattern," *Iron Age* **182**, 54-56 (1958).
4. SAWYER, D. W., "Evaluation of Rust Preventives for Ferrous Alloys," *Lubrication Eng.* **17**, 334-341 (1961).
5. Technical Report PC-1059-5 (unpublished), "Statistical Analysis of Corrosion Preventive Materials." Technical Services Division, The National Cash Register Company.
6. TRIGG, C. F., "An Engineer's Approach to Corrosion," p. 118. Pitman, London, 1951.

ASLE TRANSACTIONS 6, 239-248 (1963)

Calculated Performance of Greases in Journal Bearings

By H. H. HOROWITZ[1] and F. E. STEIDLER[2]

A digital computer analysis has been made of the effects of non-Newtonianism on the performance of greases in finite width journal bearings. As anticipated, the extreme nonlinearity of the shear rate-shear stress relation exhibited by greases makes their deviations from "normal" behavior very marked. Among the effects noted are (1) apparent "anisotropic viscosities," i.e., viscosities in the side leakage direction as much as 30 times as high as those in the direction of motion, (2) reduced side leakage, (3) flatter pressure profiles, (4) reduced sensitivity of load and friction to speed changes relative to Newtonian lubricants, and (5) the occurrence of "cores" of plug flow. Theoretically interesting is the fact that the apparent axial viscosity approaches the true viscosity while the circumferential viscosity approaches the slope of the flow curve. Many of the conclusions obtained here, especially the advantages of greases at low speeds, are confirmed in practice.

Nomenclature

$x =$ length in circumferential direction, cm
$z =$ length in axial direction, cm
$y =$ length in radial direction (through film), cm
$\tau =$ shearing stress, dynes/cm^2
$\tau_0 =$ yield stress, below which velocity gradient $= 0$, dynes/cm^2
$\mu =$ viscosity, poises
$\mu_\infty =$ viscosity at infinite shear stress
$\Gamma =$ shear rate, reciprocal seconds
$n, K, b, N =$ empirical constants in flow equations
$\mu_x(\mu_z) =$ apparent local viscosity in $x(z)$ direction, poises
$\tau_x(\tau_z) =$ shear stress component in $x(z)$ direction, dynes/cm^2
$p =$ pressure, dynes/cm^2
$Q_x(Q_z) =$ flow rate per unit width in $x(z)$ direction, cm^3/sec/cm
$h =$ height of lubricant film, cm
$\mathbf{v} =$ linear velocity of moving surface cm/sec
$\mathbf{v}_x(\mathbf{v}_z) =$ local lubricant velocity in $x(z)$ direction, cm/sec
$f(\tau_x) =$ a function of the shearing stress as defined in the text
$\tau_{x0}(\tau_{z0}) =$ shearing stress in the $x(z)$ direction at the stationary surface
$\tau_{xh}(\tau_{zh}) =$ shearing stress in the $x(z)$ direction at the moving surface
$\alpha =$ the slope of the shear stress-shear rate curve, poises
$e =$ the eccentricity, cm
$C =$ the radial clearance, cm
$\varepsilon = e/c =$ eccentricity ratio, dimensionless
$L =$ bearing width, cm

Contributed to the American Society of Lubrication Engineers by the authors. Manuscript received February 22, 1963.

[1] Research Associate, Esso Research and Engineering Co., Box 51, Linden, N. J.

[2] Senior Engineer, Esso Research and Engineering Co., Box 51, Linden, N.J.

Introduction

An ever increasing portion of the commercial lubricants of all types are non-Newtonian, i.e., they follow a non-linear relation between shear rate and shear stress. This behavior occurs because the lubricants contain polymeric additives or suspended materials, like graphite or molybdenum disulfide, or soaps, as in greases. The authors have developed a procedure for calculating the effects of non-Newtonianism, as defined above, on the performance of lubricants in journal bearings operating in the hydrodynamic regime (without metallic contact) (*1, 2, 3*). This procedure has so far been applied only to polymer thickened motor oils. The results showed a number of effects that could be ascribed to non-Newtonianism, such as a flattening of the pressure profile, a decrease in the per cent of oil leaking out the sides of the bearing, apparent "anisotropic" viscosities, etc. However, these effects were relatively small, due to the fact that the change in viscosity with shear rate or shear stress is relatively small with polymer solutions. It takes a change of at least four or five decades of shear stress to reduce the viscosity of a typical SAE 10W-30 oil by a factor of two or three. Greases, on the other hand, are far more non-Newtonian. They often have a shearing stress below which their viscosity is virtually infinite. They suffer decreases in viscosity of a factor of two or three within one decade of shear stress. Therefore, the object of the current work was to calculate the performance of greases in journal bearings to determine how large the effects of this increased non-Newtonianism can become.

There has been continued interest in the use of greases

in journal bearings, as evidenced by a number of publications. Grease lubrication with considered briefly by Michell (*4*) in 1929 and by Hersey (*5*) in 1936. In 1949 Cohn and Oren (*6*) measured the pressure profiles in a grease-loaded, full journal bearing and showed that the integrated pressure projection equalled the applied load, just as in ordinary hydrodynamic lubrication. In 1953 Milne (*7*) analyzed an infinite width slider bearing operating on a Bingham plastic and showed how the existence of "cores" of unsheared grease could increase the friction and affect the load to a lesser extent. At the same time Umstatter (*8*) made an inexact analysis of what he called "structurally viscous" oils in journal bearings and came to the conclusion that they should give flatter pressure profiles than oils and should react less to changes in operating conditions. In 1957 Slibar and Pasley (*9*) analyzed the performance of a Bingham plastic in a thrust bearing and again found that the existence of the yield stress causes an increase in friction, but has less affect on the load carried. In 1961 Bradford *et al.* (*10*) carried out experimental studies on grease loaded journal bearings and noted effects due to non-Newtonianism and thixotropy. Thus, interest has continued up to the present.

Review of calculation

The calculation method used here has been adequately described (*1, 16*) but will be reviewed briefly to aid the reader's understanding of the current work. The geometry of the journal bearing is illustrated in Fig. 1. The eccentricity of the rotating journal drags the lubricant into a channel of ever decreasing cross section, causing pressures to arise in the lubricant. This is the "hydrodynamic wedge" effect. The resultant of the pressures balances the load, an applied force tending to push the journal and bearing together. Beyond the point of minimum clearance, in the divergent region of the film, the pressures tend to go negative. However, in actual practice the film cavitates and becomes discontinuous because of its inability to sustain any appreciable tensions. This is expressed mathematically by the use of the boundary condition that both the pressure and the pressure gradient go to zero simultaneously at the trailing edge of the film, no negative pressures being permitted.

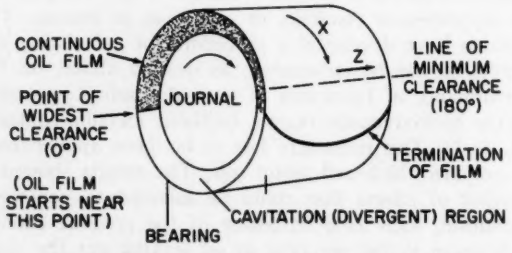

FIG. 1. Geometry of finite width journal bearing

The steps in the calculation procedure are as follows: The bearing surface is divided into a mesh containing as many as 480 points. A trial constant viscosity is chosen in the range of the apparent viscosity of the grease. The pressures are determined at all the mesh points by numerical solution of the Reynolds equation. This well-known expression combines force balances and flow balances into a relation between pressures at neighboring points. Next, from these trial pressures, the pressure gradients in the circumferential (x), and axial (z), directions are calculated at each surface point. Using these pressure gradients, it is possible to calculate the flow rate in each direction that the actual grease would have. This is done by means of numerical integrations in the y direction (the direction through the lubricant film) at each point in the xz surface. At each point in the y direction the viscosity is taken to be a function only of the resultant of the shear stresses in the x and z directions, that is, there is only one viscosity at each point in the grease film. The newly calculated flow rates are not consistent with those that would be calculated on the basis of the original trial viscosities. However, these new flow rates and the associated pressure gradients serve to define new averaged viscosities, which turn out to be different in the x and z directions. Despite the fact the pressure gradients are inexact, the apparent viscosities will be close to the true ones. These new viscosities are reinserted into a modified form of the Reynold's equation and an improved pressure distribution is obtained. The whole procedure is repeated until it converges on a single set of apparent average viscosities, pressures, and flow rates, which are all consistent with one another.

In the particular calculations described here a slow moving bearing with a large clearance was used, in order to emphasize the non-Newtonian properties of the greases. At higher speeds or lower clearances the greases tend to reach a limiting viscosity and act like Newtonian fluids. The operating ranges are listed in Table 1.

TABLE 1
Bearing Operating Ranges

Diameter	10 cm
Width	10 cm
Radial clearance	0.1–0.3 cm
Speed	3–300 rpm
Eccentricity ratios	0.60–0.95

Two important assumptions need to be pointed out. Time effects are not included in these calculations. First, it is assumed that the grease has been in the bearing long enough to have reached a steady state in which the shear rate-shear stress curve no longer is changing with further working of the grease. Secondly, it is assumed that the grease reacts instantaneously to changes in the shearing stress, that is, that the shear rate is determined solely by the shear stress and not by the time it has been at that shear stress, or its history prior to that time. For a slow moving bearing the latter assumption may be valid. The first assumption is often invalid in experimen-

tal studies as, for example, in reference (*10*), where fresh grease was fed into a relatively fast moving bearing. Here the characteristics of the grease may have been changing with time as it flowed through the bearing. These calculations cannot be applied to such studies.

Of course, there are many other simplifications included in this study, such as the omission of temperature and pressure effects. Only the effects of non-Newtonianism per se have been treated.

Characterization of the greases

Many empirical and semibasic equations have been developed for characterizing the flow properties of greases (*11, 12, 13*). The numerical procedure used here will handle any of these. However, it is most convenient to use an expression where the shear rate is given as a function of the shear stress. Some are written so that the shear rate is difficult to evaluate given the shear stress, the former being the independent variable in the expression (*11*).

The equation used for the bulk of these studies is that of Forster (*13*):

$$(\tau - \tau_0)^n (\mu - \mu_\infty) = K$$

where τ is the shear stress (dynes/cm^2), τ_0 is the yield stress, n is an empirical exponent, μ is the viscosity (poises), μ_∞ is the viscosity at $\tau = \infty$, and K is an empirical constant.

Also tested, for comparison, was the Bauer expression (*12*):

$$\tau - \tau_0 = b\Gamma^N$$

where Γ is the shear rate and b and N are empirical constants.

The best values for the constants for these equations had been determined by Zakin (*14*) for a 4% lithium stearate grease in a mineral oil of 750 Saybolt Universal Second viscosity. The original data used were those of Shuster (*15*), obtained at 77 F with a cone and plate viscometer, shearing the grease to equilibrium at each shear rate. These constants are given in Table 2; they

TABLE 2
Constants in Grease Equations

Forster constants		Bauer constants	
Symbol	Value	Symbol	Value
τ_0	1500	τ_0	1500
n	0.98	b	53
μ_∞	4.7	N	0.75
K	43,500		

fitted the actual data, which extended over a range of 5 to 180 poises, to 11 and 6%, respectively (average deviation).

It was first verified that the calculation procedure could handle either equation and that for one particular case it made little difference in the bearing performance which equation was used (Table 3). In view of this, the Forster equation was arbitrarily chosen for all further studies. In a number of cases the constants were varied to determine the effect of changes in the viscosity-shear curve on bearing performance, as will be discussed below.

TABLE 3
Comparison of Bauer and Forster Grease Equations
10-cm diameter "square" bearing, 0.1 cm radial clearance; 0.9 eccentricity ratio, 30 rpm.

	Forster equation	Bauer equation
Load (megadynes)[a]	68.55	71.35
Coeff. Frict.	0.0182	0.0178
Load angle (degrees)	32.8	32.2
In flow (cc/sec)	9.93	10.00
End flow (cc/sec)	0.965	0.962
Max. pressure (megadynes/cm^2)[b]	2.38	2.54
Angle of max. pressure (degrees)	166	166

[a] 1 megadyne = 2.248 lb weight.
[b] 1 megadyne/cm^2 $\cong$ 1 atmosphere.

Results of Calculations

Apparent Anisotropic Viscosities

An interesting result of the calculations was that the averaged viscosities in the side-leakage (axial) direction were always higher than those in the direction of motion. While this effect had been observed before in calculations on polymer thickened oils, it had amounted to differences of the order of 10%. With greases, however, the effect is much larger, going up to factors of 20–30 in extreme cases. Table 4 gives examples of the viscosity values in a fairly severe case.

The very high values of μ_z generally occur at points where plug flow occurs over part of the film thickness. At these points the resultant shear stress has taken on values below 1500 dynes/cm^2 at a series of locations in

TABLE 4
Apparent Anisotropic Viscosities in a Grease Lubricated Full Journal Bearing
Bearing diameter, 10 cm; width, 10 cm; clearance, 0.1 cm; speed, 3 rpm; eccentricity ratio, 0.8.

Circumferential location (degrees)[b]	Outer edge		Quarter point		Mid-point	
	μ_x[a]	μ_z[a]	μ_x	μ_z	μ_x	μ_z
0	26	199	31	630	45	1208
50	33	141	37	325	43	1010
100	34	74	36	111	33	450
125	28	53	24	96	21	159
150	20	40	17	51	16	52
163	17	37	15	44	15	45
174	15	37	15	45	15	47
190	[c]	[c]	15	43	15	44

[a] μ_x is viscosity in circumferential direction; μ_z in side leakage direction, in poises.
[b] O° is point of widest clearance, 180° narrowest clearance; pressure peak at 157°.
[c] Cavitation appears at this point and is complete at 200°.

the y direction. In this range dv/dy is zero, since the yield stress of the grease has not been exceeded, and a flat velocity profile is presented. The shear stress in the axial direction, τ_z, always passes through zero, and τ_x sometimes passes through zero, but only at certain locations does the resultant of the two approach zero. Plug flow does not occur over the majority of the bearing surface. Furthermore, at higher bearing speeds the extent of plug flow is much diminished.

SIDE EFFECT OF ANISOTROPIC VISCOSITY: DECREASED SIDE LEAKAGE

The increased viscosity in the axial direction relative to the circumferential direction naturally leads one to expect that relatively less lubricant will leak out the sides of the bearing in the case of a grease than in the case of a Newtonian fluid. This indeed turns out to be the case. In these calculations only the flow rates in the continuous portion of the film were determined. Some of the oil entering the hydrodynamic wedge leaks out the sides. The remainder passes through to the film end and reenters the continuous film on the next cycle. The deficit is presumably made up by fluid that is sucked or pumped into the bearing on its divergent (vacuum) side through an oil fill hole or groove or through the sides of the bearing. The mechanics of the feeding procedure were not treated. But the percentage of oil that did reach the end of the film was calculated. This percentage was in all cases increased by the apparent anisotropy of the grease. Those operating conditions which tend to emphasize the non-Newtonianism of the grease, low speeds and low eccentricity ratios (wide minimal clearances), tend to give maximum increases in the percent end flow, as shown in Table 5.

TABLE 5
Per Cent End Flow[a]—Grease vs. Mineral Oils

Eccentricity ratio	Grease Speed (rpm) 3	10	30	300	Newtonian fluids (all speeds)
0.95	6.9	5.3	4.5	4.3	4.0
0.90	13.3	11.2	9.7	8.5	7.9
0.80	25.8	21.4	19.2	17.0	15.6
0.60	—	—	—	34.3	31.9

[a] The per cent of oil taken from an axial groove located at the point of maximum clearance that does not leak out the sides but travels around the bearing.

MAIN EFFECT OF NON-NEWTONIANISM: FLATTER PRESSURE PROFILE

A good measure of the "pointedness" of the pressure distribution is the ratio of the peak pressure to the load per unit projected area. For a fluid of constant viscosity this ratio depends only on the eccentricity ratio. Increasing the viscosity of the lubricant or the speed increases both the load and the peak pressure so that the ratio remains constant. With a non-Newtonian fluid, however, the viscosity is higher near the beginning of the film, where the clearances are large, than near the point of minimum clearance. This tends to increase the pressures in the high clearance areas and reduce them near the peak. Therefore the ratio of peak pressure to load is decreased relative to a Newtonian oil. Furthermore, the percentage reduction in this ratio increases as the speed decreases and the effects of non-Newtonianism are emphasized, as shown in Table 6.

TABLE 6
Per Cent Reduction in Peak Pressure—Grease Compared to Oil at Same Load and Eccentricity[a]

Eccentricity ratio	Speed (rpm) 3	10	30	300
0.95	24	14	5	3
0.90	23	18	14	5
0.80	19	15	12	7
0.60	—	—	—	4

[a] Inaccuracies of as much as 5% in these figures are possible due to difficulty of interpolation between mesh points near sharp pressure peak.

Other indications of the flatter pressure profile are the shift of the peak pressure away from the point of minimum clearance and the increased angle between the direction of the minimum clearance and the load (see Appendix II). It should be emphasized that this flatter pressure profile is not primarily due to the apparent anisotropic viscosities mentioned earlier. It has to do with the non-Newtonianism itself and was observed even in bearing calculations that neglected side leakage (*2*).

The flatter pressure profile accounts for the bulk of the effects of non-Newtonianism discussed here, but not for the side leakage effect mentioned earlier. In that case the flatter pressure distribution worked in opposition to the side-leakage reduction. This is because most of the oil leakage occurs in the wide clearance region. Non-Newtonianism increases the pressures in this region and thereby tends to increase side leakage, partially counteracting the anisotropy effect.

EFFECT ON MAIN OPERATING VARIABLES: LOAD AND FRICTION

Non-Newtonianism produces large changes in the relations between the main bearing operating variables, load, speed, friction, and minimum clearance. For a given bearing operating on an oil of a fixed viscosity, the load/speed ratio determines the minimum clearance. This is not so for this grease; the curves for different speeds are far apart (Fig. 2) because the average grease viscosity goes up as the speed goes down. Therefore, operating at a fixed minimum clearance for safety, the sensitivity of the load capacity to speed changes is less for the grease than for a mineral oil (Fig. 3). This figure verifies the well-known fact that grease-lubricated bearings tolerate low speeds better than oil-lubricated bearings.

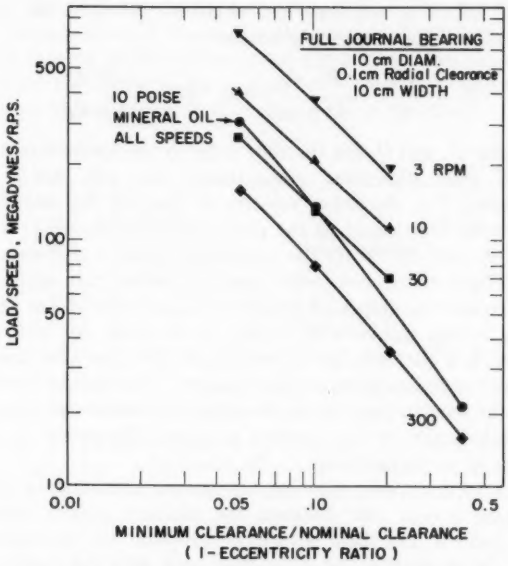

FIG. 2. Effect of speed on load-eccentricity relation

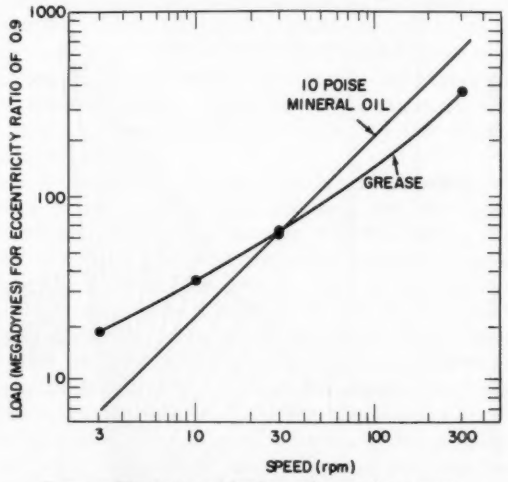

FIG. 3. Flattening of load-speed curve by a grease

The coefficient of friction curves show a similar dispersion. A mineral oil gives a single curve of coefficient of friction versus the ratio of load to speed, regardless of the actual load or speed. The grease gives a family of curves (Fig. 4).

At a given eccentricity and speed one can estimate from the load carried that the grease is acting over-all like a mineral oil of a particular viscosity. On the other hand, under the same conditions one can calculate another apparent viscosity based on the friction.[3] It turns

[3] Three different kinds of viscosity have now been introduced whose relation may need to be clarified. One is the true local viscosity at a point determined from the shearing stress. The second type consists of the set μ_x and μ_z, determined at each point in the x-z plane from the pressure gradients and flow rates at that point. The last, just mentioned, are over-all average viscosities based on the load or friction of the total bearing.

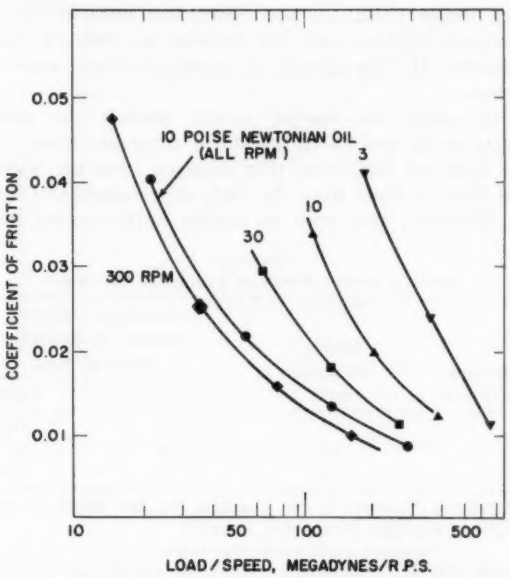

FIG. 4. Effect of speed on friction-load relation

out that, for greases, in common with other non-Newtonian fluids, the apparent viscosity based on the friction is always higher than that based on the load (Table 7).

TABLE 7
Over-All Apparent Viscosities (Poises)[a]

Eccentricity ratio	at 3 rpm		at 30 rpm	
	Based on load	Based on friction	Based on load	Based on friction
0.95	22.8	36.5	8.9	11.2
0.90	28.4	48.1	10.3	13.1
0.80	35.0	61.9	12.3	16.5

[a] The numbers give the viscosity of a Newtonian oil that would carry the same load, or give the same friction, as this grease at the speed and eccentricity shown.

In other words, at a given speed and eccentricity ratio the coefficient of friction, the ratio of the friction to the load, is higher for a grease than for a Newtonian oil. This is a consequence of the flattening of the pressure distribution, as explained in a previous publication (*2*). Another explanation is that the friction depends on the viscosity throughout the oil film, while the load depends chiefly on the viscosity under the pressure peak, where the viscosity is at its minimum.

MISCELLANEOUS EFFECTS OF VARIATION OF THE GREASE AND BEARING PARAMETERS

A number of variations were made in the bearing geometry and in the grease flow curve to determine how

they would affect the non-Newtonian behavior of the lubricant. (These runs are detailed as runs 21–30 in Appendix II.) In general the expected effects were observed.

Increasing the bearing width, holding the eccentricity ratio and other variables constant, brings the two types of viscosities, that obtained from the friction and that obtained from the load, closer together (Table 8). However, even with an infinite width bearing these

TABLE 8
Effect of Bearing Width on Equivalent Viscosities[a]

Bearing width (cm)	Width/diameter ratio	Equivalent viscosity (poises) of Newtonian fluid for equal	
		Load	Friction
5	0.5	9.66	13.61
10	1.0	10.34	13.12
20	2.0	11.34	12.80

[a] Bearing diameter, 10 cm; clearance, 0.1 cm; speed, 30 rpm; data from Appendix II runs 3, 4, 23-26.

would not be completely equal, as based on previous work. Thus, part of the higher coefficient of friction of a grease is due simply to its higher viscosities where the clearance is widest. But the complex flow patterns accompanying increased side leakage also contribute significantly.

Next, the grease flow curve parameters were varied so that the yield stress, the ultimate viscosity, and the viscosity at 10,000 dynes/cm^2 were unaffected, but the transition region was sharpened or broadened. This was accomplished by varying the parameters n and K in the Forster expression. Low values of n and K mean a sharp transition from infinite to low viscosities; high values of n and K mean a broad transition. The effects were surprisingly small, the high n and K values causing an increased coefficient of friction but little else (see Appendix II, runs 27 and 28).

Similarly, doubling the yield stress, with everything else constant, raises the over-all apparent viscosities somewhat and raises the coefficient of friction about 8% (Appendix II, runs 3 and 30).

Discussion

There are two points concerning the bearing performance of a grease that merit discussion. One is the reason for the apparent anisotropic viscosities that occur even though at each point in space the viscosity had only one value. Particularly mystifying, in this connection, is the fact that at locations where both dp/dx and dp/dz are nearly zero, meaning that the local viscosities are nearly constant, the apparent μ_x and μ_z still are widely different. The second point for discussion is the practical meaning of these results as to the utility of greases in bearings.

Meaning of Apparent Anisotropic Viscosities

In the derivation of the Reynolds equation for hydrodynamic lubrication with lubricants of constant viscosity, the following relations are obtained between the flow rates and the pressure gradients:

$$Q_x = \frac{Vh}{2} - \frac{h^3}{12\,\mu}\frac{dp}{dx} \quad \text{and} \quad Q_z = \frac{-h^3}{12\,\mu}\frac{dp}{dz}$$

where Q_x and Q_z are the flow rates in the circumferential and axial directions, respectively, per unit width or length; V is the linear velocity of the rotating member; h is the film height at the point; μ is the viscosity; and dp/dx and dp/dz are the respective pressure gradients.

These expressions were used to define the apparent viscosities μ_x and μ_z of non-Newtonian fluids. What they say is that the velocity profile in the axial, i.e., z direction, is a parabola for a Newtonian fluid, the area under which is proportional to the viscosity. The velocity profile in the longitudinal, i.e., x direction, is a linear one, bowed parabolically by the pressure gradient. The extent of the bowing is proportional to the viscosity.

A typical point showing anisotropic viscosity for this grease is near 100° between the mid and quarter points in Table 4. The shear stresses at this point are represented by the vectors in Fig. 5, as they vary with the height y.

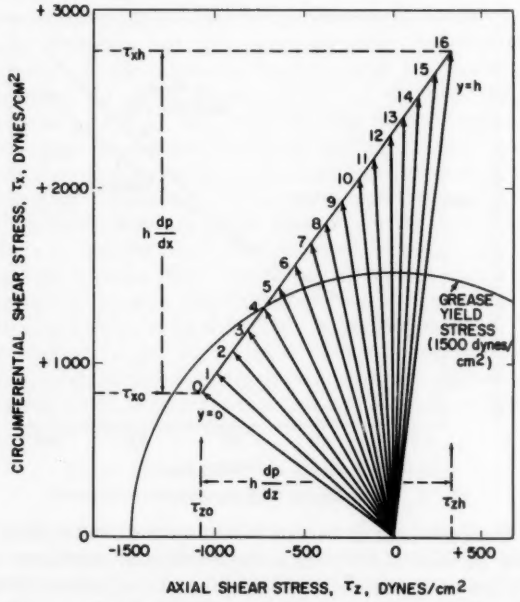

FIG. 5. Shear stress vectors as a function of distance through lubricant film (16 equal increments, point 0 at stationary surface, point 16 at moving surface).

The vector ends lie along a straight line in the τ_x-τ_z plane. The radius of the circle shown is equal to the yield stress of the grease. All vectors terminating within the circle represent shearing stresses less than the yield stress and correspond to infinite viscosities, zero velocity gradients, or "plug flow" at these locations. The velocities provided by these velocity gradients are pictured in Fig.

6. The pressure gradient is only 37% higher in the x direction than in the z direction, but it is obvious that the bowing in the x direction is far greater than the area under the curve in the z direction. This gives rise to a much higher apparent viscosity in the z direction.

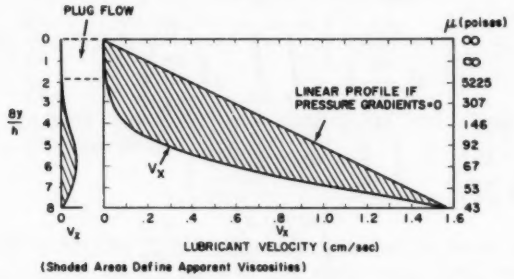

FIG. 6. Velocity profiles as a function of distance through lubricant film (Table 4 gives bearing conditions, location of point: 103.4° between quarter and mid-point, $h = .0814$ cm, $dp/dx = 23990$, $dp/dz = 17580$ dynes/cm^2/cm).

The profiles of Fig. 6 provide a physical picture of the reason for the differences. The high viscosities near one edge have a minor effect on the over-all velocities in the x direction because the velocity gradients tend to be small near this edge in any case. In the z direction the high or infinite viscosities prevent flow at just the points where the velocity gradient would be at its maximum, and so seriously decrease the flow, as shown by the drastically distorted parabola.

It is also possible to show mathematically that as the two pressure gradients both approach zero, the apparent viscosities still do not converge, even though τ_x and τ_z and, therefore, the local viscosities approach constants. Appendix I shows that in such a case μ_z approaches the local viscosity while μ_x approaches the slope of the flow curve (Fig. 7). Since for pseudoplastic fluids such as greases the slope of the flow curve is always less than or equal to the viscosity, it is apparent that μ_x must always be less than or equal to μ_z. Where the pressure gradients are not zero, the situation becomes more complicated and cannot be handled analytically, but the same results obviously carry over to some extent.

In this last respect these results are in agreement with the analysis of Milne (*7*), who considered a Bingham plastic film in an infinite width slider bearing (no side leakage). He found that the load depended primarily on the slope of the flow curve above the yield stress, which would be equivalent to μ_x above. Not having included axial flow in his analysis, he would not have encountered anything resembling μ_z. Michell (*4*) and Hersey (*5*) came to a similar conclusion.

Utility of Greases in Bearings

According to these results greases will show to best advantage in a large clearance, low speed bearing operation. As Fig. 2 shows, greases will tolerate low speeds

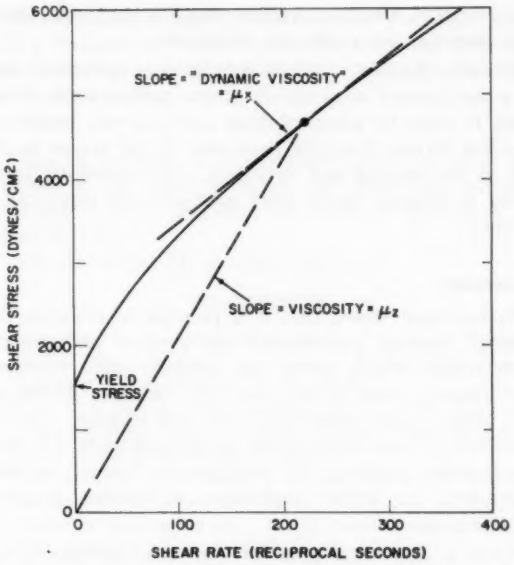

FIG. 7. Grease flow curve (Illustration of μ_x and μ_z where $dp/dx = dp/dz = 0$).

better than oils. Experience has borne this out. Also, greases react better than oils to changing conditions, as indicated by Umstatter (*8*) for "structure-viscous" materials. Figure 2 again shows that while the grease and oil carry the same safe load at 30 rpm, the safe load that the grease can carry varies much less with speed than the load oil can carry. Therefore, the grease carries three times the load of the oil at 3 rpm.

The non-Newtonianism of greases tends to raise their coefficients of friction, as also found by Milne (*7*), Hersey (*4*), Michell (*5*), and Slibar and Pasley (*9*). However, again the coefficient of friction will remain more constant with greases than with oils when the speed is increased. This can be shown from cross plots of the data in Fig. 4.

The results of these calculations are confirmed by previous workers in other respects. The flatter pressure distribution for a grease versus an oil, experimentally observed by Cohn and Oren (*6*), was calculated here.[4] This may be of practical importance where bearing metal fatigue or distortion is a problem. Secondly, the "cores" or zones of plug flow or zero velocity gradient predicted by Milne (*7*) and observed by him with the aid of aluminum paint in a transparent bearing have also been found in these calculations (Fig. 6). As the various authors who have analyzed the behavior of Bingham plastics have also shown, the presence of these "cores"

[4] It must be pointed out, however, that Cohn and Oren's observation may have been due entirely or partly to differences in eccentricity ratios, which were not measured or controlled. Lacking knowledge of the comparative viscometric properties of the oil and grease, one cannot be certain that the eccentricities were the same at the fixed loads and speeds.

has a greater effect on friction than on load, and therefore increases the coefficient of friction.

Finally, the lower rate of side leakage calculated here is a well-known attribute of grease performance. However, it must be admitted that some of this benefit in practice derives from the hardening of the grease at the rim of the bearing and, probably, the viscoelastic properties of greases, which were omitted from these calculations.

Summary

It has been shown that it is possible to calculate the journal bearing performance of greases and emerge with results which verify (or predict) their observed performance characteristics in many respects. These are (1) safety at low speeds, (2) low side leakage, (3) less sensitivity of load and friction to speed changes, (4) flatter pressure profiles, (5) existence of "cores" of plug flow, and (6) higher coefficients of friction at fixed eccentricity.

From a theoretical point of view the calculations are important in demonstrating large apparent "viscometric anisotropies," despite the fact that the viscosity at every point in the film has only one value. As explained, this is entirely due to the way the local viscosities are averaged in the calculation of the flow rates in the direction of motion and in the direction of side leakage.

These calculations can be repeated with any type of non-Newtonian fluid and any size journal bearing. The method is in the form of a digital computer program rather than a closed analytical expression from which generalizations can be drawn, but this situation is becoming more the rule today than the exception, especially in such complex problems.

Appendix I

Estimating μ_x and μ_z at Corner Points

At a "corner point" (and also at the very tip of the pressure peak) dp/dx and $dp/dz \longrightarrow 0$, there is no bowing in the velocity profiles, the shearing stress, $\tau_z \longrightarrow 0$, and τ_x becomes constant across the film.

By definition, in comparison with a Newtonian fluid:

$$\mu_x = \frac{(h^3/12)\ (dp/dx)}{(Vh/2) - Q_x} \qquad [1]$$

When $dp/dx \longrightarrow 0$ this expression becomes indeterminate, since $Q \longrightarrow Vh/2$. It must then be evaluated by L'Hospital's rule, differentiating both numerator and denominator with respect to dp/dx. The only term that offers any difficulty is $dQ_x/d(dp/dx)$. To find Q_x one must first find the local velocity $\mathbf{v}_x$.

$$\mathbf{v}_x = \int_0^y \frac{d\mathbf{v}_x}{dy}\,dy = \int_0^y \frac{\tau_x}{\mu(\tau)}\,dy = \int_0^y f(\tau_x)\,dy \qquad [2]$$

The viscosity, μ, is a function of the resultant τ $(= \sqrt{\tau_x^2 + \tau_z^2})$ but in this case, since $\tau_z \longrightarrow 0$, $\tau = \tau_x$, and the last equality of Eq. [2] is justified.

$$Q_x = \int_0^h \mathbf{v}_x\,dy = \int_0^h \int_0^y f(\tau_x)\,dy\,dy \qquad [3]$$

$$\frac{dQ_x}{d\left(\frac{dp}{dx}\right)} = \int_0^h \int_0^y \frac{df}{d\left(\frac{dp}{dx}\right)}\,dy\,dy \qquad [4]$$

$$\frac{dQ_x}{d\left(\frac{dp}{dx}\right)} = \int_0^h \int_0^y \frac{df}{d\tau_x} \cdot \frac{d\tau_x}{d\left(\frac{dp}{dx}\right)}\,dy\,dy = \int_0^h \int_0^y \frac{df}{d\tau} \cdot \frac{d\tau_x}{d\left(\frac{dp}{dx}\right)}\,dy\,dy \qquad [5]$$

$df/d\tau$ is the reciprocal of the slope of the shear stress-rate curve, which as τ_x approaches a constant can be considered a constant, "α." The relationship between τ_x and dp/dx is found from the force balance portion of the Navier-Stokes relation, upon which the whole theory of hydrodynamic lubrication is based:

$$\frac{dp}{dx} = \frac{d\tau_x}{dy} \quad \text{or} \quad \tau_x = \tau_{x0} + \frac{dp}{dx}\,y \qquad [6]$$

where τ_{x0} is the shear stress at one wall.

$$\frac{d\tau_x}{d\left(\frac{dp}{dx}\right)} = \frac{d\tau_{x0}}{d\left(\frac{dp}{dx}\right)} + y \qquad [7]$$

Inserting Eq. [7] and "α" in Eq. [5] one obtains:

$$\frac{dQ_x}{d\left(\frac{dp}{dx}\right)} = \int_0^h \int_0^y \frac{1}{\alpha}\left(\frac{d\tau_{x0}}{d\left(\frac{dp}{dx}\right)} + y\right) dy\,dy \qquad [8]$$

The dependency of the wall shear stress on the pressure gradient is fixed by the boundary condition that, no matter how dp/dx changes:

$$\mathbf{v}_{xh} = V = \int_0^h \frac{d\mathbf{v}_x}{dy}\,dy = \int_0^h f(\tau_x)\,dy \qquad [9]$$

where $\mathbf{v}_{xh}$ is the lubricant velocity at the moving surface, which equals V, the linear speed of the moving surface.

$$\frac{dV}{d\left(\frac{dp}{dx}\right)} = 0 = \int_0^h \frac{df}{d\left(\frac{dp}{dx}\right)} \qquad [10]$$

Inserting Eq. [7] and "α" in Eq. [10] one obtains

$$0 = \int_0^h \frac{1}{\alpha}\left(\frac{d\tau_{x0}}{d\left(\frac{dp}{dx}\right)} + y\right) dy = \frac{1}{\alpha}\left(\frac{d\tau_{x0}}{d\left(\frac{dp}{dx}\right)} \cdot h + \frac{h^2}{2}\right) \qquad [11]$$

or

$$\frac{d\tau_{x0}}{d\left(\frac{dp}{dx}\right)} = -\frac{h}{2} \qquad [12]$$

Inserting Eq. [12] into Eq. [8] one obtains

$$\frac{dQ_x}{d\left(\frac{dp}{dx}\right)} = \int_0^h \int_0^y \frac{1}{\alpha}\left(y - \frac{h}{2}\right) dy\, dy = \frac{h^3}{12\alpha} \qquad [13]$$

Applying L'Hospital's rule to Eq. [1] and inserting Eq. [12] one finds:

$$\mu_x = \frac{(h^3/12)}{(h^3/12\alpha)} = \alpha \qquad [14]$$

Thus, in the limit where both pressure gradients are zero, $\mu_x = \alpha$, the slope of the shear stress–shear rate curve, sometimes called the "dynamic viscosity."

For μ_z the situation is somewhat different. Again, by comparison with a Newtonian fluid, μ_z is defined by:

$$\mu_z = \frac{(h^3/12)(dp/dz)}{Q_z} \qquad [15]$$

This again becomes indeterminate as $dp/dz \longrightarrow 0$ since $Q_z \longrightarrow 0$. Again L'Hospital's rule must be applied, and the only difficult term is $dQ_z/d(dp/dx)$. One again must first find the velocities $\mathbf{v}_z$ and the flow rates Q_z:

$$\mathbf{v}_z = \int_0^y \frac{dv_z}{dy}\, dy = \int_0^y \frac{\tau_z}{\mu(\tau)}\, dy = \int_0^y f(\tau_z)\, dy \qquad [16]$$

In this case the last equality is true because μ is determined entirely by τ_x and is essentially a constant with respect to τ_z.

$$Q_z = \int_0^h \int_0^y f(\tau_z)\, dy\, dy \qquad [17]$$

$$\frac{dQ_z}{d\left(\frac{dp}{dz}\right)} = \int_0^h \int_0^y \frac{df}{d\left(\frac{dp}{dz}\right)} dy\, dy = \int_0^h \int_0^y \frac{df}{d\tau_z} \frac{d\tau_z}{d\left(\frac{dp}{dz}\right)} dy\, dy \qquad [18]$$

This time, however, since μ is a constant unaffected by τ_z

$$\frac{df}{d\tau_z} = \frac{d\left(\frac{\tau_z}{\mu}\right)}{d\tau_z} = \frac{1}{\mu} \qquad [19]$$

Again, adding the force balance relation analogous to Eq. [6], one obtains

$$\frac{dQ_z}{d\left(\frac{dp}{dz}\right)} = \int_0^h \int_0^y \frac{1}{\mu}\left(\frac{d\tau_{z0}}{d\left(\frac{dp}{dz}\right)} + y\right) dy\, dy \qquad [20]$$

This equation is exactly analogous to Eq. [8] except that μ replaces α. Furthermore, the remaining steps are exactly analogous to steps from Eqs. [9] to [14] so that one finally obtains

$$\mu_z = \mu \qquad [21]$$

Thus, in the limit of zero pressure gradients, μ_z is the quotient of the shear stress by the shear rate, whereas μ_x is the slope of the shear stress–shear rate curve, as shown in Fig. 7.

(For APPENDIX II, see page 248.)

REFERENCES

1. HOROWITZ, H. H., and STEIDLER, F. E., "Calculated Performance of Non-Newtonian Lubricants in Finite Width Journal Bearings," *ASLE Trans.* **4**, 275-281 (1961).
2. HOROWITZ, H. H., and STEIDLER, F. E., "The Calculated Journal-Bearing Performance of Polymer Thickened Lubricants," *ASLE Trans.* **3**, 124-133 (1960).
3. HOROWITZ, H. H., STEIDLER, F. E., and FORSTER, E. O., "The Bearing Performance and Elastic Properties of Polymer Thickened Lubricating Oils," *World Petrol. Congr. 5th, N. Y. 1959.* Section VI, 289-305 (1960).
4. MICHELL, A. G. M., "Progress of Fluid Film Lubrication," *Trans. ASME, M.S.P.* **51-21**, 153-163 (1929).
5. HERSEY, M. D., "Theory of Lubrication," 1st ed., p. 91. Wiley, New York, 1936.
6. COHN, G., and OREN, J. W., "Film Pressure Distribution in Grease-Lubricated Journal Bearings," *ASME Trans.* **71**, 555-559 (1949).
7. MILNE, A. A., "A Theory of Grease Lubrication of a Slider Bearing." *In* "Proceedings of the Second International Congress on Rheology" (V. G. W. Harrison, ed.) pp. 427-436. Academic Press, New York, 1954.
8. UMSTATTER, H., "On the Rheological Properties of Lubricants." *In* "Proceedings of the Second International Congress on Rheology" (V. G. W. Harrison, ed.), pp. 414-424. Academic Press, New York, 1954.
9. SLIBAR, A., and PASLEY, P. R., "On the Theory of Grease Lubricated Thrust Bearings," *ASME Trans.* **79**, 1229-1234 (1957).
10. BRADFORD, L. J., BARBER, E. M., and MUENGER, P. J., "Grease Lubrication Studies in Plain Journal Bearings," *J. Basic Eng. ASME Trans.* **81**, Section D, 153-161 (1961).
11. SISKO, A. W., "The Flow of Lubricating Greases," *Ind. Eng. Chem.* **50**, 1789-1792 (1958).
12. BAUER, W. A., FINKELSTEIN, A. P., and WIBERLEY, S. E., "Flow Properties of Lithium Stearate-Oil Model Greases as Functions of Soap Concentration and Temperature," Paper No. 59-AM-2B1, ASLE Annual Meeting, Buffalo, 1959.
13. FORSTER, E. O., "A Rheological Equation for Lubricating Greases," *National Lubricating Grease Institute Spokesman*, **24**, 462-465 (1961).
14. ZAKIN, J. L., "Comments on NLGI Paper 'A Rheological Equation for Lubricating Greases,'" Private communication to E. O. Forster, November 17, 1960.
15. SHUSTER, D. O., "Flow Properties of Modified Lithium Stearate-Oil Dispersions," Doctoral Thesis, Department of Chemistry, Renssalaer Polytechnic Institute, 1960.
16. STEIDLER, F. E., and HOROWITZ, H. H., "The Calculated Load-Carrying Ability of Non-Newtonian Lubricants in Hydrodynamic Bearings," *C.E.P. Symp. Series, No. 42*, **59**, 99-107 (1963).

APPENDIX II

Summary of Bearing Calculations

Case no.	ε	rpm	Load (mega dynes)	Coef. frict.	Apparent visc. (poises)		Oil flow (cc/sec)		% end flow	Load angle (°)	Angle max. press.	Max. press. (atm.)	Peak press. ratio	Notes[a]
					Load	Frict.	In	End						
1	.95	30	130.9	.0118	8.86	11.2	10.0	.448	4.5	24.6	171	6.50	.95	
2	.95	30	147.9	.0093	10	10	12.0	.475	4.0	19.3	172	7.75	—	Newtonian oil
3	.90	30	68.6	.0182	10.3	13.1	9.9	.965	9.7	32.8	166	2.38	.86	
4	.90	30	66.3	.0143	10	10	11.8	.930	7.9	26.5	168	2.68	—	Newtonian oil
5	.80	30	34.5	.0295	12.3	16.5	9.8	1.88	19.2	42.7	158	0.96	.88	
6	.80	30	28.0	.0220	10	10	11.5	1.80	15.6	36.2	161	0.89	—	Newtonian oil
8	.60	30	10.3	.0406	10	10	10.8	3.45	31.9	50.6	149	0.25	—	Newtonian oil
9	.95	300	795.1	.0103	5.37	5.90	111.4	4.81	4.3	21.4	172	40.3	.97	
10	.90	300	381.8	.0155	5.76	6.22	110.1	9.40	8.5	29.1	166	14.7	.95	
11	.80	300	173.5	.0251	6.19	7.04	107.6	18.3	17.0	39.4	160	5.1	.93	
12	.60	300	70.6	.0465	6.84	7.85	102.3	35.2	34.3	53.4	149	1.63	.96	
13	.95	10	65.2	.0130	13.2	16.5	2.8	.149	5.3	26.6	170	2.95	.86	
14	.90	10	35.6	.0202	16.1	22.7	2.9	.327	11.2	34.7	166	1.18	.82	
15	.80	10	18.4	.0335	19.7	30.1	3.0	.636	21.4	44.4	158	.49	.85	
17	.95	3	33.7	.0150	22.8	36.5	.74	.051	6.9	29.2	170	1.34	.76	
18	.90	3	18.8	.0243	28.4	48.1	.75	.100	13.3	37.3	164	.58	.77	
19	.80	3	9.81	.0420	35.0	61.9	.75	.194	25.8	46.6	157	.25	.81	
21	.90	300	52.6	.0498	7.16	8.29	319	28.5	8.9	30.8	166	1.94	.91	$C = 0.3$
22	.90	30	11.8	.0608	16.0	22.7	26.7	2.94	11.0	34.6	165	.39	.81	$C = 0.3$
23	.90	30	19.3	.0284	9.66	13.6	6.6	.457	6.9	28.7	166	1.59	.85	$L = 5$
24	.90	30	20.0	.0201	10	10	7.1	.443	6.2	23.6	167	1.93	—	Newt. oil; $L = 5$
25	.90	30	193.1	.0142	11.3	12.8	12.8	2.04	15.9	37.1	166	2.82	.84	$L = 20$
26	.90	30	170.2	.0126	10	10	15.0	1.94	12.9	29.5	168	2.95	—	Newt. oil; $L = 20$
27	.90	30	65.4	.0163	9.85	11.2	9.9	.950	9.6	30.2	165	2.41	.92	$n = .5$ $K = 470$
28	.90	30	63.1	.0198	9.54	13.2	9.5	.976	10.3	34.6	166	2.13	.84	$n = 1.5$ $K = 4.10^6$
29	.90	30	71.4	.0178	10.8	13.3	10.0	.962	9.6	32.2	166	2.54	.88	Bauer Eq'n.
30	.90	30	71.3	.0195	10.8	14.7	8.7	.970	11.2	33.9	165	2.42	.84	$\tau_0 = 3000$

[a] Notes: In all cases a bearing of diameter and width = 10 cm and a radial clearance of 0.1 cm was used with the grease described by the Forster equation, unless otherwise specified. The unlisted cases are ones at 0.60 ε that failed to converge. Lbs. = megadynes × 2.248. The apparent viscosity is calculated on the basis of the fact that for a Newtonian oil the load (or the friction) is directly proportional to the viscosity at a given geometry. Thus apparent μ = load (or friction)/load (or friction) of Newtonian oil × viscosity of Newtonian oil. The load angle is the angle between the load direction and the line of centers. The angle of maximum pressure is measured from the point of widest clearance. The maximum pressure is actually in megadynes/cm², very close to atmospheres. The peak pressure ratio is the ratio of the peak pressure to the load per unit projected area expressed relatively to a Newtonian oil at the same geometry.

ASLE TRANSACTIONS 6, 249-253 (1963)

A Note on the Stability of Flow in Loaded Journal Bearings

By R. C. DiPRIMA[1]

If two nonconcentric cylinders are rotating, a circumferential pressure gradient is created. The effect of this pressure gradient flow on the stability of the local velocity profiles is discussed. It is concluded that in the most critical region the flow due to the pressure gradient has a stabilizing effect.

Nomenclature

R_1, R_2 = radii of inner and outer cylinders, respectively
$\mathbf{V}_1, \mathbf{V}_2$ = velocities of inner and outer cylinders, respectively
C = radial clearance
ν = kinematic viscosity
y = radial coordinate measured from inner cylinder
ε = eccentricity ratio
h = film thickness
V = circumferential velocity distribution
μ = absolute viscosity
$\partial p/\partial\theta$ = circumferential pressure gradient
R_r = Reynolds Number based on $\mathbf{V}_1$
R_p = Reynolds Number based on $\partial p/\partial\theta$
R = Reynolds Number times a geometric factor

Introduction

In recent years the increasing use of low viscosity lubricants and the high speed operation of bearings have necessitated a study of turbulent lubricant films. Closely associated with this problem is a study of the stability of laminar lubricant films, and the transition from laminar to turbulent flow. While the stability of a viscous fluid between two *concentric* cylinders has been the subject of a large number of investigations starting with the classical paper of Taylor (*1*), very little is known about the much more difficult problem of the stability of a viscous fluid between two nonconcentric cylinders. This latter problem is one which would be of interest in journal bearing operation. In this note some of the recent work on stability of flow in concentric annuli that does not appear to be well known to lubrication engineers will briefly be discussed, and it will be shown how it is possible to draw some qualitative conclusions about the stability of flow in loaded plain cylindrical journal bearings.

Contributed to the American Society of Lubrication Engineers by the author. Manuscript received February 12, 1963.

[1] Professor of Mathematics, Rensselaer Polytechnic Institute, Troy, New York.

Taylor (*1*) showed both experimentally and theoretically that a viscous fluid between concentric rotating cylinders is unstable at a sufficiently large speed of the inner cylinder. If the outer cylinder is at rest and the gap between the cylinders is small compared to the mean radius, the critical speed is given by

$$\frac{\mathbf{V}_1 C}{\nu}\left(\frac{C}{R_1}\right)^{1/2} = 41.2 \qquad [1]$$

Here, R_1 is the radius of the inner cylinder, C is the gap between the cylinders, ν is the kinematic viscosity, and $\mathbf{V}_1$ is the velocity of the inner cylinder. The observed instability is a steady secondary laminar flow with the form of ring vortices spaced periodically in the axial direction. This new flow, while not a turbulent flow, does lead to increased frictional losses. At sufficiently high speeds of the inner cylinder the ring vortices break up and the flow becomes turbulent. According to Townsend (*2*) the sequence of flow regimes resembles that in a cylinder wake.

This type of instability, usually referred to as Taylor vortices, is caused by the action of the centrifugal force field. When the inner cylinder is rotating and the outer cylinder is stationary the fluid particles near the inner cylinder experience a higher centrifugal force which leads to a secondary motion when the radial pressure gradient and viscous forces are exceeded. Conversely, if the inner cylinder is at rest and the outer cylinder is rotating, the flow is stable to disturbances of the Taylor type. Indeed, Synge (*3*) has shown that a necessary condition (and a sufficient condition for an inviscid fluid) for the occurrence of Taylor vortices is that the square of the circulation of the mean flow decrease radially outward.

In lubrication problems the clearance between the cylinders is very small, say $C/R_1 \approx 1/1000$, and the corresponding critical value of the Reynolds number $R = \mathbf{V}_1 C/\nu$ for a Taylor type of instability is of the order of 1300–1400. For Reynolds numbers of this order of magnitude it is also possible that the flow may become turbulent, the mechanism of transition being similar to that in parallel flows. Considerable attention has been devoted to theoretical investigations of the stability of

parallel shear flow and to the stability of the flow between rotating cylinders with the inner cylinder at rest. In all of these investigations it has been concluded that the flow is stable to small disturbances.[2] On the other hand, the early experimental investigations of Taylor (*5*) and Wendt (*6*) on the stability of flow between concentric cylinders with the inner cylinder at rest showed that the flow does become turbulent at sufficiently high speeds of the outer cylinder. For a clearance ratio C/R_2 of the order 1/20 the critical Reynolds number based on the radius, R_2, and velocity, $\mathbf{V}_2$, of the outer cylinder is approximately

$$\frac{\mathbf{V}_2 R_2}{\nu} = 7 \times 10^4 \qquad [2]$$

The critical value of $\mathbf{V}_2 R_2/\nu$ depends upon C/R_2* and Taylor (*5*) has suggested that for C/R_2 very small the critical value of $\mathbf{V}_2 C/\nu$ is given by

$$\frac{\mathbf{V}_2 C}{\nu} \approx 2000 \qquad [3]$$

These results are, of course, in complete contradiction of small disturbance theory.

For this reason, Schultz-Grunow (*4*) recently carried out a series of experiments in which great care was taken to align the cylinders so that they were exactly concentric, and to free the system from any vibration. He found that with the outer cylinder rotating he could maintain laminar flow up to speeds higher by a factor of 5–8 than those previously obtained. On the other hand, when the cylinders were slightly eccentric the flow behaved in a similar manner to that found by the previous experimenters. Thus these experiments tend to confirm the theoretical investigations and at the same time suggest that from a practical point of view the flow between two "concentric" cylinders with a small gap and the inner cylinder at rest will be turbulent for $\mathbf{V}_2 C/\nu \approx 2000$.

Actually one can anticipate a similar phenomenon if the outer cylinder is at rest and the inner cylinder is rotating, provided, of course, Taylor vortices don't occur first. Thus, it can be expected that if $(\mathbf{V}_1 C/\nu)\sqrt{C/R_1}$ reaches a value of 41.2 before $\mathbf{V}_1 C/\nu$ reaches a value of 2000, Taylor vortices will appear. On the other hand, if C/R_1 is sufficiently small it is possible that turbulence may set in without the appearance of Taylor vortices. The dividing point would be a value of C/R_1 of roughly 1/2500; for smaller values turbulence may be expected as $\mathbf{V}_1 C/\nu$ is increased. For larger values Taylor vortices will occur, that is, for C/R_1 sufficiently small, curvature effects can be neglected and transition to turbulence will just depend upon the Reynolds number $R = \mathbf{V}_1 C/\nu$; for C/R_1 larger than, say, 1/2500 curvature effects cannot be neglected with the instability being of the form of Taylor vortices. For most journal bearings C/R_1, while very small, will generally be greater than 1/2500 by a factor of 2 or 3; hence it appears reasonable to anticipate that if the flow is unstable, the instability will be in the form of Taylor vortices.

[2] If the inner cylinder is at rest the flow is stable to disturbances of the Taylor type as mentioned earlier, and also appears to be stable to disturbances propagating in the stream direction. See reference (*4*).

* A graph showing this variation is given in (*4*) and also in (*7*).

The effect of eccentricity

When the cylinders are placed in an eccentric position and the inner cylinder is rotating, a circumferential pressure gradient is developed, and the laminar velocity distribution is given approximately by

$$V(y,\theta) = \mathbf{V}_1\left(1 - \frac{y}{h}\right) + \frac{1}{2\mu R_1}\frac{\partial p}{\partial \theta}(y^2 - yh) \qquad [4]$$

where $\partial p/\partial\theta$ denotes the circumferential pressure gradient; $h = C(1 + \varepsilon\cos\theta)$ is the film thickness, where ε is the eccentricity ratio; y is the distance measured from the inner cylinder, $0 < y < h$; and μ is the viscosity. The pressure distribution is determined by solving the Reynold's equation.

Visual experimental evidence for the existence of Taylor vortices for flow between nonconcentric cylinders is limited; however, Cole (*8*), using kerosene as his fluid ($\nu \approx 2.5$ centistokes) has run a series of experiments for $C/R_1 = 0.1$, and a range of eccentricities from $\varepsilon = 0$ to $\varepsilon = 0.8$ in which he observed Taylor vortices.[3] The results which are based on the average critical speed of several experiments are shown in Fig. 2. At first the critical value of $(\mathbf{V}_1 C/\nu)(C/R_1)^{1/2}$ increases slowly with increasing ε (it may even decrease slightly near $\varepsilon = 0$) but then begins to increase more rapidly as ε continues to increase. At $\varepsilon = 0.6$ the critical speed is higher by a factor of 1.3 than the critical speed at $\varepsilon = 0$. Wilcock (*9*) also noted that increased frictional torques were developed in lightly loaded bearings at speeds above a certain critical value, given approximately by the Taylor criterion—Eq. [1]. Smith and Fuller (*10*) also carried out a series of experiments on journal bearings operating at speeds above the Taylor critical speed. While their data does show several interesting results, they do not provide data for computing the critical speed as a function of ε.

A theoretical investigation of the stability of the circumferential flow between nonconcentric cylinders with the inner cylinder rotating, i.e., the velocity distribution given in Eq. [4], is particularly difficult since V depends upon both y and θ. To date, no one has investigated this problem. Recently, however, DiPrima (*11*) has considered the stability of a viscous fluid between

[3] At the higher eccentricity ratios visual observation was difficult due to the strong reversed flow in the maximum clearance space. In addition, repeatability was poor as the precise point of appearance of the Taylor vortices was difficult to determine.

rotating concentric cylindrical surfaces with a pressure gradient acting around the cylinders. When the outer cylinder is at rest, the velocity distribution is given by Eq. [4] with $h = C$ and $\partial p/\partial\theta$ constant. It is shown in Ref. (*11*) that the stability of this flow to disturbances of the Taylor type is governed by the values of the two parameters

$$R_r\sqrt{\frac{C}{R_1}} \text{ and } R_p\sqrt{\frac{C}{R_1}} \qquad [5]$$

where $R_r = V_1C/\nu$ is a Reynolds number based on the rotation of the inner cylinder, and

$$R_P = \left(\frac{-C^2}{12\mu R_1}\frac{\partial p}{\partial\theta}\right)\frac{C}{\nu} = \frac{V_pC}{\nu}$$

is a Reynolds number based on the average velocity due to the circumferential pressure gradient. The stability diagram is shown in Fig. 1. Notice that for $R_p = 0$,

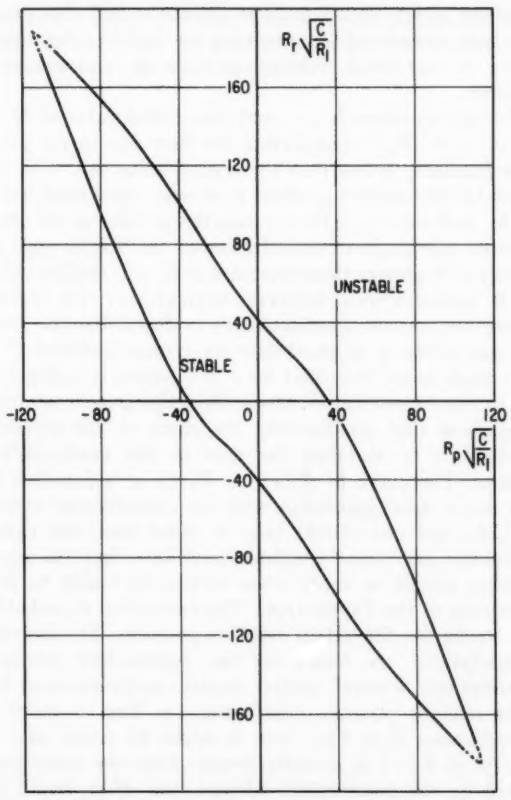

FIG. 1. A plot of the values of $R_r(C/R_1)^{1/2}$ and $R_p(C/R_1)^{1/2}$ for stable and unstable flow.

Taylor's criterion of $(R_r\sqrt{C/R_1})_{cr} = 41.2$ is obtained, and that the superposition of the flow due to the pressure gradient tends to stabilize or destabilize as it is in the opposite direction ($R_r >$ or < 0, $R_p <$ or > 0) or the same direction ($R_r >$ or < 0, $R_p >$ or < 0).

When the cylinders are nonconcentric, the velocity profile is given by Eq. [4], and once the pressure gradient $\partial p/\partial\theta$ is known, the stability of the velocity profile at a *given cross section* can be determined from Fig. 1. For the purpose of illustration we will use the Sommerfeld solution of the Reynolds equation for the infinitely long journal bearing. Then (*12*)

$$\frac{\partial p}{\partial\theta} = 6\mu V_1R_1\,(h - h_0)/h^3,\ h_0 = \left[\frac{2C(1-\varepsilon^2)}{2+\varepsilon^2}\right] \qquad [6]$$

where h_0 is the gap width at the cross section where $\partial p/\partial\theta = 0$. Using Eq. [6] and the expression of h (ε, θ), it is possible to compute local Reynolds numbers corresponding to the rotational flow (R_{rh}) and the pressure gradient flow (R_{ph}) in terms of ε and θ. The results are

$$R_{rh}\sqrt{\frac{h}{R_1}} = \frac{V_1h}{\nu}\sqrt{\frac{h}{R_1}} = R(1+\varepsilon\cos\theta)^{3/2} \qquad [7]$$

and

$$R_{ph}\sqrt{\frac{h}{R_1}} = [(-h^2)/(12\mu R_1)\ (\partial p/\partial\theta)]\frac{h}{\nu}\sqrt{\frac{h}{R_1}}$$

$$= -R\left[(1+\varepsilon\cos\theta) - \frac{2(1-\varepsilon^2)}{2+\varepsilon^2}\right]\frac{(1+\varepsilon\cos\theta)^{1/2}}{2} \qquad [8]$$

where

$$R = \frac{V_1C}{\nu}\sqrt{\frac{C}{R_1}} \qquad [9]$$

In order for the velocity profile at a given cross section (fixed θ), and for a given value of ε to be stable, it is necessary that $R_{rh}(h/R_1)^{1/2}$ and $R_{ph}(h/R_1)^{1/2}$ as determined by Eqs. [7] and [8] lie in the stable region depicted in Fig. 1. This determines a critical value of R as a function of ε and θ, say $R_\theta(\varepsilon)$. For a fixed value of ε the minimum of $R_\theta(\varepsilon)$ over θ determines a critical value $R_c(\varepsilon)$, such that for $R < R_c(\varepsilon)$ the *local* flow at each cross section will be stable. In Fig. 2, the variation of $R_\theta(\varepsilon)$ with ε is shown for several values of θ.[4] For each ε, the minimum value of $R_\theta(\varepsilon)$ occurs for $\theta = 0$. Hence the curve for $\theta = 0$ shown in Fig. 2 also gives $R_c(\varepsilon)$ as a function of ε. The value of $\theta = 0$, corresponds to the cross section of maximum width, $h = C(1+\varepsilon)$. Thus in all cases the velocity profile at this cross section is the "most unstable." It is interesting to note that while

[4] For the Sommerfeld pressure distribution the curves for other values of θ lie between the curve for $\theta = 0$ and the curve for $\theta = 180°$.

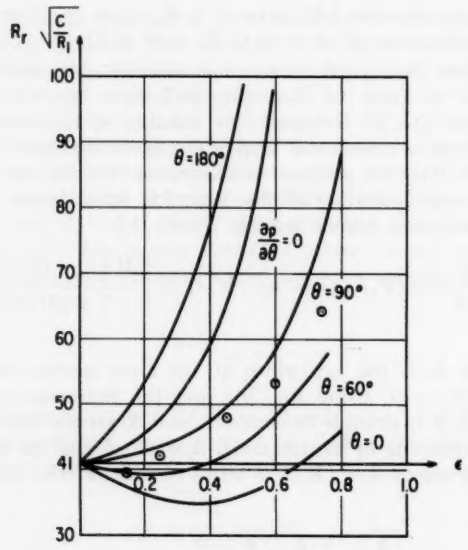

FIG. 2. The critical value of $R_r(C/R_1)^{1/2}$ as a function of ε for various values of θ. Circles indicate experimental points of Cole.

the value of $R_c(\varepsilon)$ at first decreases with increasing ε, it soon begins to increase and $R_c(\varepsilon) > R_c(\varepsilon = 0)$ for $\varepsilon > 0.67$.

To fully appreciate the effect of the flow due to the pressure gradient when the cylinders are not concentric, it is informative to consider the situation at $\theta = 0$ in more detail. Ignoring the flow due to the pressure gradient the stability criterion is

$$R_{rh}\,(h/R_1)^{1/2} = R(1 + \varepsilon \cos\theta)^{3/2} = 41.2 \qquad [10]$$

The critical values of R determined from Eq. [10] for $\theta = 0$ are shown in Table 1, where they are compared with the critical values of R taking account of the flow due to the pressure gradient. The effect of the increase in the gap width is to decrease $R_0(\varepsilon)$, while the effect of the flow due to the pressure gradient is to increase $R_0(\varepsilon)$. At a value of $\varepsilon = 0.6$ the effect of the reverse flow due to the pressure gradient almost doubles the critical value of R based on Eq. [10] alone. Corresponding results are true at the cross sections at which $(1 + \varepsilon \cos\theta) > 1$, and $R_\theta(\varepsilon)$ would be less than $R_\theta(\varepsilon = 0)$ according to the criterion given by Eq. [10]. In regions where the effect of the pressure gradient flow is to decrease the critical value of $R_\theta(\varepsilon)$, the value of h is sufficiently smaller than C so that $R_\theta(\varepsilon)$ is still much larger than $R_\theta(\varepsilon = 0)$. For example, see the curve for $\theta = 180°$ in Fig. 2.

TABLE 1
Critical Reynolds Numbers[a]

ε	R_I	R_{II}
0	41.2	41.2
0.1	35.8	37.9
0.2	31.3	36
0.3	27.7	34.9
0.4	25.0	34.9
0.5	22.3	35.7
0.6	20.2	38.7
0.7	18.4	42.3
0.8	17.0	46.2

[a] R_I indicates the critical value of R for which the flow at $\theta = 0$ will be unstable based on Taylor's criterion. R_{II} indicates the critical value of R at the same cross section with account taken of the flow due to the pressure gradient acting around the cylinders.

Discussion

Even at the thin film widths encountered in journal bearing lubrication it is reasonable to expect that the instability of the flow between two concentric cylinders with the inner cylinder rotating will occur in the form of Taylor vortices. For continuous fluid films in nonconcentric annuli, Taylor vortices can also be expected to occur as observed by Cole. In this case a pressure gradient is set up around the cylinders, and this effect has been considered by examining the stability characteristics of the local velocity profiles at various cross sections.

In regions where $h > C$ and the critical value of $R = (V_1 C/\nu)(C/R_1)^{1/2}$ (neglecting the flow due to the pressure gradient) is less than the critical value at $\varepsilon = 0$, the effect of the pressure gradient is to raise the critical value of R. And for $\varepsilon > 0.67$ the velocity profiles as *all* cross sections are stable to disturbances of the Taylor type at values of R greater than that for $\varepsilon = 0$; this critical value of R increases as ε increases beyond 0.67. In regions where the pressure gradient tends to destabilize the flow, the gap width is so small that the critical value of R is still much larger than that for $\varepsilon = 0$. While it is impossible to draw quantitative conclusions, the present analysis does show that qualitatively the effect of the pressure gradient is to stabilize the flow in the most critical regions. The curve of $R_c(\varepsilon) = R_0(\varepsilon)$ as a function of ε is not in good agreement with the experimental results of Cole, but one should bear in mind that this curve represents the worst possible condition—that the local velocity profile at *every* cross section be stable to disturbances of the Taylor type. This restriction is probably too strong for the actual stability problem. The present computations are based on the Sommerfeld pressure distribution; however, similar results can be expected for more realistic pressure distributions as long as there is a continuous fluid film. Also it might be noted that if $\partial p/\partial\theta$ at $\theta = 0$ is actually greater than the value predicted by the Sommerfeld solution, the effect would be to raise the $R_c(\varepsilon)$ curve.

Finally, it should be mentioned that in many journal bearings there is also an axial flow, and it is likely that that axial flow will also retard the occurrence of Taylor vortices. Indeed, for the flow between concentric cylinders with the inner cylinder rotating, DiPrima (*13*) has shown

that the critical value of $R = (\mathbf{V}_1 C/\nu)(C/R_1)^{1/2}$ is increased substantially by the addition of only a small axial flow. For example, for $\mathbf{W}C/\nu = 20$, where $\mathbf{W}$ is the average velocity, the critical value of R is increased by a factor of about 1.19 compared to the critical value for $\mathbf{W} = 0$. The critical value of R continues to increase with increasing $\mathbf{W}C/\nu$.

ACKNOWLEDGMENT

This work was performed at Mechanical Technology Inc., Latham, New York, under Contract Nonr-3731(00)(FBM) with the Office of Naval Research, Department of the Navy.

REFERENCES

1. Taylor, G. I., "Stability of a Viscous Liquid Contained between Two Rotating Cylinders," *Phil. Trans.* **223**, 289-343 (1923).
2. Townsend, A. A., "The Structure of Turbulent Shear Flow," pp. 292-307. Cambridge Univ. Press, London and New York, 1956.
3. Synge, J., "On the Stability of a Viscous Liquid between Rotating Coaxial Cylinders," *Proc. Roy. Soc. London, Ser. A* **167**, 250-256 (1938). See also "The Stability of Heterogeneous Liquids," *Trans. Roy. Soc. Canada* **27**, 1-18 (1933).
4. Schultz-Grunow, F. "Zur Stabiltät der Couette-Strömung," *ZAMM*, **39**, 101-110 (1959).
5. Taylor, G. I., "Fluid Friction between Rotating Cylinders," *Proc. Roy. Soc. London Ser. A***157**, 546-564 (1936).
6. Wendt, F., "Turbulente Strömung Zwischen zwei Rotierenden Koaxialen Zylindern," *Ing. Arch.* **4**, 577 (1933).
7. Schlichting, H., "Boundary Layer Theory," 4th ed., pp. 428-431, 439-444. McGraw-Hill, New York, 1960.
8. Cole, J. A., "Experiments on the Flow in Rotating Annular Clearances," Paper presented at the Conference on Lubrication and Wear, Institution of Mechanical Engineers, London, October, 1957.
9. Wilcock, D. F., "Turbulence in High-Speed Journal Bearings," *Trans. ASME* **72**, 825-834 (1950).
10. Smith, M. I., and Fuller, D. D., "Journal Bearing Operations at Superlaminar Speeds," *Trans. ASME* **78**, 469-474 (1956).
11. DiPrima, R. C., "The Stability of Viscous Flow between Rotating Concentric Cylinders with a Pressure Gradient Acting Round the Cylinders," *J. Fluid Mech.* **6**, 462-468 (1959).
12. Pinkus, O., and Sternlicht, B., "Theory of Hydrodynamic Lubrication," pp. 42-43. McGraw-Hill, New York, 1961.
13. DiPrima, R. C., "The Stability of a Viscous Fluid between Rotating Cylinders with an Axial Flow," *J. Fluid Mech.* **9**, 621-631 (1960).

CONTENTS

J. B. RITTENHOUSE, L. D. JAFFE, R. G. NAGLER, and H. E. MARTENS. Friction Measurements on a Low Earth Satellite 161

W. C. YOUNG, F. J. CLAUSS, and S. P. DRAKE. Lubrication of Ball Bearings for Space Applications 178

D. J. BOES and P. H. BOWEN. Friction-Wear Characteristics of Self-Lubricating Composites Developed for Vacuum Service 192

WILLIAM F. HADY, GORDON P. ALLEN, and ROBERT L. JOHNSON. Wear and Friction of Mechanical Carbons in Liquid Oxygen as Influenced by Transfer Films 201

W. C. CLINTON and R. L. LYON. The Effect of Adsorbed Films on the Attractive and Frictional Forces Developed in an Electrostatic Clutch 209

P. J. MAGILL, R. E. MCCURRY, and R. R. SCHAFFER. The Behavior of a Silicone-Lubricated Electrostatic Clutch 218

D. E. NEUNHERZ. Classification of Multigrade Motor Oils at 0°F 227

R. F. MCKIBBEN and D. M. FORINASH. Relating Humidity Cabinet Life of Lubricants to Their Service Life 233

H. H. HOROWITZ and F. E. STEIDLER. Calculated Performance of Greases in Journal Bearings 239

R. C. DIPRIMA. A Note on the Stability of Flow in Loaded Journal Bearings .. 249